A splitting method for semi-Lagrangian Vlasov-Poisson solvers with a strong external uniform magnetic field

Michel Mehrenberger, Anh-Tuan Vu

A splitting method for semi-Lagrangian Vlasov-Poisson solvers with a strong external uniform magnetic field

Michel MEHRENBERGER [*], Anh-Tuan VU [†]

(March 6, 2023)

Abstract

We solve numerically the Vlasov-Poisson system with a splitting method suited for strong external magnetic field. Our splitting scheme is inspired by J. Ameres [2] but uses the semi-Lagrangian solver instead of a Fourier spectral discretization solver. We show that when the magnitude of the external magnetic field becomes large while the time step is independent of the fast oscillation in time, this scheme is able to provide a consistent semi-Lagrangian discretization of the guiding-center model. In addition, we propose some numerical simulations to validate the method under the Kelvin-Helmholtz instability test case.

Keywords: Vlasov-Poisson system, Guiding-centre model, Asymptotic analysis, Splitting schemes.

Aknowledgements Centre de Calcul Intensif d'Aix-Marseille is acknowledged for granting access to its high performance computing resources. This work has been carried out within the framework of the EUROfusion Consortium, funded by the European Union via the Euratom Research and Training Programme (Grant Agreement No 101052200 EUROfusion). Views and opinions expressed are however those of the author(s) only and do not necessarily reflect those of the European Union or the European Commission. Neither the European Union nor the European Commission can be held responsible for them.

1 Introduction

We consider a plasma consisting of mass m with individual electric charge q, which is described by the Vlasov equation coupled with the Poisson to compute the self-consistent fields E in the presence of an external magnetic field $\mathbf{B}$, motivated by the magnetic confinement. The unknown $f(t,x,v)$, depending on the time t, the position x, and the velocity v, represents the distribution of particles in the phase space with $(x,v) \in \mathbb{R}^d \times \mathbb{R}^d, d = 2,3$. The Vlasov equations reads:

$$\partial_t f + v \cdot \nabla_x f + \frac{q}{m}\left(E(t,x) + v \wedge \mathbf{B}\right) \cdot \nabla_v f = 0, \quad (t,x,v) \in]0,T] \times \mathbb{R}^3 \times \mathbb{R}^3, \tag{1}$$

[*] Aix Marseille Université, CNRS, Centrale Marseille, Institut de Mathématiques de Marseille, UMR 7373, Château Gombert 39 rue F. Joliot Curie, 13453 Marseille FRANCE. E-mail : michel.MEHRENBERGER@univ-amu.fr

[†] Aix Marseille Université, CNRS, Centrale Marseille, Institut de Mathématiques de Marseille, UMR 7373, Château Gombert 39 rue F. Joliot Curie, 13453 Marseille FRANCE. E-mail : anh-tuan.vu@univ-amu.fr

To simplify, the curvature of magnetic field lines is neglected and we assume that the external magnetic field only applies in the x_3-direction

$$\mathbf{B} = (0, 0, B),$$

where B is a given constant.
In the two dimensional setting $x = (x_1, x_2)$, $v = (v_1, v_2)$ the Vlasov equation writes

$$\partial_t f + v \cdot \nabla_x f + \frac{q}{m}\left(E(t,x) + B^{\perp} v\right) \cdot \nabla_v f = 0, \ (t, x, v) \in]0, T] \times \mathbb{R}^2 \times \mathbb{R}^2, \tag{2}$$

where ${}^{\perp}v = (v_2, -v_1)$, while the Poisson equation is

$$E(t,x) = -\nabla_x \Phi(t,x), \quad -\varepsilon_0 \Delta_x \Phi = \rho(t,x) = q \int_{\mathbb{R}^2} f(t,x,v) \mathrm{d}v, \tag{3}$$

where ε_0 is the permittivity of the vacuum. We complete the above system with the initial condition

$$f(0, x, v) = f_0(x, v).$$

The well-posedness of the Vlasov-Poisson problem is well known, see [9] for the weak solution, and [10, 11, 12, 13] for the strong solution. The numerical solution of the Vlasov equation can be classically performed by Lagrangian, Eulerian, or semi-Lagrangian methods. Lagrangian particle methods like particle in cell methods (PIC) consist of approximating the plasma by a finite number of macro-particles. The trajectories of these particles are computed from the characteristic curves given by Vlasov equation, whereas self-consistent fields are computed by gathering the charge densities of the particles on a mesh of the physical space (see [14]). Eulerian methods have been used to discretize Vlasov's equation on a phase space grid instead of particles. Semi-Lagrangian methods can be viewed as a combination of Lagrangian methods and Eulerian methods which consist in computing the distribution function on a grid by following the characteristic curves, backward in time for a one-time step and interpolating the value at the feet of the characteristics using the grid point values of the distribution function at the previous time step, see [8, 15]. This method is usually coupled with a time splitting.

We are interested in the long-time behavior of particles under the regime of intense magnetic field, i.e. $T \to +\infty$ and $|B| \to +\infty$ in order to observe a drift phenomenon in the plane orthogonal to the magnetic field direction. Therefore, we first introduce a set of characteristic scales. The characteristic length scale $\bar{x}$ is the Debye length

$$\bar{x} = \lambda_D = \left(\frac{k_B \varepsilon_0 \bar{T}}{4\pi \bar{n} q^2}\right)^{1/2},$$

where k_B is the Boltzmann constant, $\bar{T}$ is the temperature scale and $\bar{n}$ is the density scale. Then, the characteristic velocity $\bar{v}$ is the thermal velocity

$$\bar{v} = v_{th} = \left(\frac{k_B \bar{T}}{m}\right)^{1/2}.$$

The characteristic magnitude of the electric field $\bar{E}$ can be expressed from $\bar{n}$ and $\bar{x}$ by

$$\bar{E} = \frac{4\pi q \bar{n} \bar{x}}{\varepsilon_0}.$$

Finally, we denote by $\bar{B}$ the characteristic magnitude of the magnetic field and $\bar{f} = \dfrac{\bar{n}}{\bar{v}^2}$ the distribution function scale. Next, we introduce various time scales that appear in the problem:

- T_0 the observation time scale,
- $T_p = w_p^{-1} = \dfrac{\bar{x}}{\bar{v}}$ the reciprocal plasma frequency,
- $T_c = w_c^{-1} = \dfrac{m}{q\bar{B}}$ the reciprocal cyclotron frequency.

The above regime i.e. $(T \to +\infty, |B| \to +\infty)$ corresponds to the following scaling assumption in [1] given by

$$\frac{T_0}{T_p} = \frac{1}{\varepsilon}, \quad \frac{T_c}{T_p} = \varepsilon. \tag{4}$$

The small parameter $\varepsilon > 0$ is related to the ratio between the reciprocal Larmor frequency and the advection time scale. Then we define the new variables and given fields by

$$x' = \frac{x}{\bar{x}},\ v' = \frac{v}{\bar{v}},\ t' = \frac{t}{T_0},\ E'(t', x') = \frac{E(t,x)}{\bar{E}},\ B' = \frac{B}{\bar{B}},$$

and the new unknown

$$f'(t', x', v') = \frac{f(t,x,v)}{\bar{f}}.$$

Inserting all these changes into (2), we obtain the dimensionless equation

$$\frac{1}{w_p T_0}\frac{\partial f'}{\partial t'} + v' \cdot \nabla_{x'} f' + \frac{q}{m}\left[E' + \frac{w_c}{w_p} B'^{\perp} v'\right] \cdot \nabla_{v'} f' = 0, \quad (t', x', v') \in]0, T'] \times \mathbb{R}^2 \times \mathbb{R}^2.$$

For the sake of clarity and simplicity, we drop the primes in the above equation. Therefore, under the scaling assumption (4), the Vlasov equation can be recast in dimensionless variables, as follows:

$$\varepsilon\frac{\partial f_\varepsilon}{\partial t} + v \cdot \nabla_x f_\varepsilon + \frac{q}{m} E_\varepsilon \cdot \nabla_v f_\varepsilon + \frac{1}{\varepsilon}\frac{qB}{m}^{\perp} v \cdot \nabla_v f_\varepsilon = 0, \quad (t, x, v) \in]0, T] \times \mathbb{R}^2 \times \mathbb{R}^2, \tag{5}$$

where the Poisson equation for the potential Φ_ε satisfies $E_\varepsilon(t,x) = -\nabla_x \Phi_\varepsilon(t,x)$ and

$$-\varepsilon_0 \Delta_x \Phi_\varepsilon(t,x) = q\rho_\varepsilon(t,x) = q\int_{\mathbb{R}^2} f_\varepsilon(t,x,v)\mathrm{d}v. \tag{6}$$

We are interested in the behavior of the Vlasov-Poisson equation (5)-(6) as $\varepsilon \to 0$. At the continuous level, following the work of L. Saint Raymond [5] or more recently of Miot [7] using the characteristic curves, it can be proved that the density particle $(\rho_\varepsilon)_{\varepsilon>0}$ converges in some ways to the solution of the guiding center model

$$\partial_t \rho(t,x) + \frac{{}^{\perp}E(t,x)}{B} \cdot \nabla_x \rho(t,x) = 0,\ (t,x) \in]0,T] \times \mathbb{R}^2, \tag{7}$$

$$E(t,x) = -\nabla_x \Phi(t,x),\ -\varepsilon_0 \Delta_x \Phi(t,x) = q\rho(t,x). \tag{8}$$

This means that when watching the dynamic of particles on a long enough time as the intensity of the magnetic field $|B|$ is large enough (i.e $\varepsilon << 1$), the density particles of the Vlasov-Poisson system (2)-(3) is approximated by the density of the system (7)-(8). Hence, the asymptotic model (7)-(8) is sufficient to describe the Vlasov-Poisson system in this regime and it only requires solving a two-dimensional problem instead of a four-dimensional problem like the Vlasov-Poisson problem, thus reducing the cost of numerical simulation. Moreover, since it does not contain any stiff term, standard numerical methods can be employed to approximate it, c.f [8] using the backward semi-Lagrangian methods. Readers can refer

to the semi-Lagrangian method for guiding center simulations on different meshes, see for example [18, 19, 20].

In this work, we perform the numerical solution of the Vlasov-Poisson equation (5)-(6) by semi-Lagrangian methods coupled with a time splitting, inspired by the splitting schemes introduced in [2]. Before describing and analyzing our numerical methods for the Vlasov-Poisson equation, we need to observe the motion of each individual charged particle in the electromagnetic field. The trajectories of particles are computed from the characteristic curves corresponding to the Vlasov equation (5) as follows:

$$\begin{aligned} \frac{\mathrm{dX}_\varepsilon(\mathrm{t})}{\mathrm{dt}} &= \frac{1}{\varepsilon} V_\varepsilon(t), & X_\varepsilon(0) &= x \in \mathbb{R}^2, \\ \frac{\mathrm{dV}_\varepsilon(\mathrm{t})}{\mathrm{dt}} &= \frac{q}{m} \frac{E_\varepsilon(t, X_\varepsilon(t))}{\varepsilon} + \frac{\omega_c}{\varepsilon^2}{}^{\perp} V_\varepsilon(t), & V_\varepsilon(0) &= v \in \mathbb{R}^2, \end{aligned}$$

whereas the electric field is computed from a discretization of the Poisson equation on a mesh of the physical space. When the electromagnetic field is constant and given, by direct computation, one sees that the trajectory of particle is described by

$$\begin{aligned} V_\varepsilon(t) &= \mathcal{R}\left(-\frac{\omega_c}{\varepsilon^2} t\right) V_\varepsilon(0) + \varepsilon \frac{{}^{\perp}E}{B}, \\ X_\varepsilon(t) &= \underbrace{\left[X_\varepsilon(0) + \varepsilon \frac{{}^{\perp}V_\varepsilon(0)}{\omega_c}\right]}_{\text{center circle}} + \underbrace{t \frac{{}^{\perp}E}{B}}_{\text{slow drift}} + \underbrace{\mathcal{R}\left(-\frac{\omega_c}{\varepsilon^2} t + \pi/2\right) \varepsilon \frac{V_\varepsilon(0)}{\omega_c}}_{\text{fast Larmor rotation}}. \end{aligned}$$

The evolution of a given particle's position is a combination of two different time movements: a slow dynamic of the center of the circle $x_g = x + \varepsilon^{\perp} v/\omega_c$, usually called guiding center, which is given by the drift velocity and a fast rotation of period about $T_c = \varepsilon^2 2\pi/\omega_c$, with a small radius $\varepsilon|v|/\omega_c$ around guiding center. Thus, the Vlasov-Poisson system is multi-scale. Due to high oscillations in time, if one wants to do accurate simulation of the Vlasov problem using classical numerical schemes, one needs small time steps, typically smaller than T_c. A way to avoid this restriction is to use the asymptotic model (7)-(8), since it does not contain fast oscillations in time, and so a very small time step is no longer required in order to simulate these oscillations. However, the aim of this work is to produce a reference solution of the Vlasov-Poisson equation for several values of the parameter ε.

From the discrete point of view, we are interested in a method which is able to capture this singularly oscillatory limit, while the numerical parameters may be kept independent with respect to ε, in particular the large time step, so that the numerical method provides a consistent discretization of the limit system as $\varepsilon \to 0$. This concept is called Asymptotic Preserving property (see [17]). The methods of passage from Vlasov-Poisson equation to the Guiding-center model, which satisfy this property have been studied by recent works within the framework of PIC method, which allow to focus on the construction of a numerical scheme in time of the characteristic equations. Readers can refer to various multi-scale techniques that have been proposed such as the exponential integrator in velocity in [16], implicit-explicit time discretizations in [4], and two-scale formulation integrator in [21].

In this paper, we propose an alternative to such methods allowing us to make direct simulations of the Vlasov-Poisson system with large time steps with respect to $\mathcal{O}(\varepsilon^2)$. This work is based on the same splitting method as [2] but the semi-Lagrangian Vlasov solver is used instead of a Fourier spectral discretization solver. Now, we start to summarize the basis of the method and the results of this paper. The time splitting that is used to approximate the solution of the Vlasov-Poisson system is based on exact computations of the following

two equations:

$$\varepsilon\partial_t f_\varepsilon + v\cdot\nabla_x f_\varepsilon + \frac{1}{\varepsilon}\frac{qB}{m}{}^{\perp}v\cdot\nabla_v f_\varepsilon = 0, \tag{9}$$

$$\varepsilon\partial_t f_\varepsilon + \frac{q}{m}E_\varepsilon(t,x)\cdot\nabla_v f_\varepsilon = 0. \tag{10}$$

The time splitting presented here for the Vlasov equation in strong magnetic field into two parts where one part includes the transport term and magnetic term, and the other part includes the electric term which has also been applied in [24] for the finite radius approximation Larmor regime. First, we consider the approximation of the characteristic curves. The exact characteristic curves of the Vlasov equation can be approximated by a composition of flows associated with the equations (9)-(10) respectively. Under the first order time splitting, the approximation of the exact characteristic curves can be written as:

$$X_\varepsilon(t) = X_\varepsilon(0) + \left[\mathcal{R}\left(-\frac{\omega_c}{\varepsilon^2}t + \pi/2\right) - \mathcal{R}(\pi/2)\right]\frac{\varepsilon}{\omega_c}V_\varepsilon(0),$$

$$V_\varepsilon(t) = \mathcal{R}\left(-\frac{\omega_c}{\varepsilon^2}t\right)V_\varepsilon(0) + \frac{q}{m\varepsilon}\int_0^t E_\varepsilon(s, X_\varepsilon(s))\mathrm{d}s,$$

(see (47) in Section 3). We now want to study formally the stability of this characteristic curves. Setting $Z_\varepsilon(t) = X_\varepsilon(t) + \varepsilon\dfrac{{}^{\perp}V_\varepsilon(t)}{\omega_c}$, the above system can be re-written for $(Z_\varepsilon, \varepsilon V_\varepsilon)$ as

$$Z_\varepsilon(t) = Z_\varepsilon(0) + \int_0^t \frac{{}^{\perp}E_\varepsilon}{B}(s, Z_\varepsilon(s) - \varepsilon\frac{{}^{\perp}V_\varepsilon(s)}{\omega_c})\mathrm{d}s,$$

$$\varepsilon V_\varepsilon(t) = \mathcal{R}\left(-\frac{\omega_c}{\varepsilon^2}t\right)\varepsilon V_\varepsilon(0) + \frac{q}{m}\int_0^t E_\varepsilon(s, Z_\varepsilon(0) - \mathcal{R}\left(-\frac{\omega_c}{\varepsilon^2}s\right)\frac{\varepsilon}{\omega_c}{}^{\perp}V_\varepsilon(0))\mathrm{d}s.$$

Under some classical smoothness assumption on the electric field E_ε and initial data $(X_\varepsilon(0), \varepsilon V_\varepsilon(0))$ we show formally when $\varepsilon \to 0$ that $Z_\varepsilon \rightharpoonup Z$ and $\varepsilon V_\varepsilon \rightharpoonup V \neq 0$ which satisfy the following system:

$$Z(t) = Z(0) + \int_0^t \frac{{}^{\perp}E}{B}(s, Z(s) - V(s))\mathrm{d}s,$$

$$V(t) = \frac{q}{m}\int_0^t \frac{1}{2\pi}\int_0^{2\pi} E(s, Z(0) - \mathcal{R}\left(-\theta\right)\frac{{}^{\perp}V(0)}{\omega_c})\mathrm{d}\theta\mathrm{d}s.$$

We see that the limit system does not coincide with the characteristic curves corresponding to the guiding center model (7), in contrast to the the result obtained in [4] where it has been shown that the velocity $\varepsilon V_\varepsilon$ tends to 0 as $\varepsilon \to 0$ which implies that the particle's position approximate the guiding center position.

Next we will study the approximation of the distribution function f_ε when using the splitting scheme (9)-(10). Since each equation can be solved exactly in time using the characteristic method when the magnetic field is uniform, the error is only due to the splitting procedure (first order for Lie spliting, second order for Strang splitting). If we use such a method, we have to guarantee the accuracy of the scheme, especially when considering the high frequency oscillations of the particles. By investigating the commutator, the global error of the p-order splitting is $\mathcal{O}(\Delta t^{p+1}/\varepsilon^{p+1})$, see Appendix for $p = 1, 2$. This error bound indicates that to obtain good results for the numerical solution of the distribution function $f_\varepsilon(t, x, v)$, the time step Δt has to be the same order of ε which would require very large CPU time cost when considering a very small ε. However, considering the numerical solution for the density particle $\rho_\varepsilon(t, x)$ obtained from the approximation of

the distribution function $f_\varepsilon(t,x,v)$, we realize that it can be performed with larger time step, and moreover it provides a consistent approximation to the guiding center model. To see the asymptotic limit as ε goes to 0, we expect that when ε becomes very small, the distribution function $f_\varepsilon(t,x,v)$ satisfies $f_\varepsilon(t,x,v) \approx f_\varepsilon(t,x-\varepsilon^\perp v/\omega_c,v)$ and so, we get that $\rho_\varepsilon(t,x) = \int_{\mathbb{R}^2} f_\varepsilon(t,x,v)\mathrm{d}v \approx \int_{\mathbb{R}^2} f_\varepsilon(t,x-\varepsilon^\perp v/\omega_c,v)\mathrm{d}v$. Following [7], we work on the gyro-coordinates $(x-{}^\perp v, v)$ and focus on the equations satisfied by the shifted distribution $f_\varepsilon(t,x-\varepsilon^\perp v/\omega_c,v)$. Performing the change variables, we get equations for $f_\varepsilon(t,x-\varepsilon^\perp v/\omega_c,v)$ that can be written as (see Proposition 3.3):

$$\begin{aligned}
\partial_t f_\varepsilon(t,x-\varepsilon\frac{{}^\perp v}{\omega_c},v) + \omega_c\frac{{}^\perp v}{\varepsilon^2}\cdot\nabla_v\left[f_\varepsilon(t,x-\varepsilon\frac{{}^\perp v}{\omega_c},v)\right] = 0,\\
\partial_t f_\varepsilon(t,x-\varepsilon\frac{{}^\perp v}{\omega_c},v) + \frac{{}^\perp E_\varepsilon}{B}(t,x-\varepsilon\frac{{}^\perp v}{\omega_c})\cdot\nabla_x f_\varepsilon(t,x-\varepsilon\frac{{}^\perp v}{\omega_c},v)\\
+\frac{1}{\varepsilon}\frac{q}{m}E_\varepsilon(t,x-\varepsilon\frac{{}^\perp v}{\omega_c})\cdot\nabla_v\left[f_\varepsilon(t,x-\varepsilon\frac{{}^\perp v}{\omega_c},v)\right] = 0.
\end{aligned}$$

After integrating these equations with respect to velocity, we get the following equations

$$\begin{aligned}
\int_{\mathbb{R}^2}\partial_t f_\varepsilon(t,x-\varepsilon\frac{{}^\perp v}{\omega_c},v)\mathrm{d}v = 0,\\
\int_{\mathbb{R}^2}\partial_t f_\varepsilon(t,x-\varepsilon\frac{{}^\perp v}{\omega_c},v)\mathrm{d}v + \int_{\mathbb{R}^2}\frac{{}^\perp E_\varepsilon}{B}(t,x-\varepsilon\frac{{}^\perp v}{\omega_c})\cdot\nabla_x f_\varepsilon(t,x-\varepsilon\frac{{}^\perp v}{\omega_c},v)\mathrm{d}v = 0,
\end{aligned}$$

which do not contain the stiff term. Formally passing to the limit as $\varepsilon\to 0$ we obtain

$$\begin{aligned}
\int_{\mathbb{R}^2}\partial_t f(t,x,v)\mathrm{d}v = 0,\\
\int_{\mathbb{R}^2}\partial_t f(t,x,v)\mathrm{d}v + \int_{\mathbb{R}^2}\frac{{}^\perp E}{B}(t,x)\cdot\nabla_x f(t,x,v)\mathrm{d}v = 0,
\end{aligned}$$

which corresponds to the guiding center approximation

$$\partial_t\rho(t,x) = 0, \quad \partial_t\rho(t,x) + \frac{{}^\perp E(t,x)}{B}\cdot\nabla_x\rho(t,x) = 0.$$

Finally, we will construct the full discretized numerical scheme for the distribution function $f_\varepsilon(t,x,v)$ from the splitting scheme (9)-(10) by using the backward semi-Lagrangian method. The first order scheme in time and second one of solutions are presented. Then we perform a formal analysis of the first order full-discretized scheme for the density particle $\rho_\varepsilon(t,x)$ to show that the numerical method provides a consistent discretization to the guiding center model. During the implementation, we have to filter out the fast rotation of velocity and then remove the fast translation of the electric field that occur in the characteristic curves by making a change of variable in the direction of the velocity.

The paper is organized as follows. In Section 2 we briefly first recall the main steps of the semi-Lagrangian method for solving the Vlasov-Poisson system, and we present then two splitting schemes: exponential Boris and Scovel's method. Section 3 is devoted to investigate the asymptotic limit for the approximation of characteristic curves and then the density of the Vlasov equation under the Scovel method. Then the full discretized numerical solution is constructed from the Scovel method using the semi-Lagrangian method in Section 4. In Section 5 we write an algorithm for the second order accuracy of the exponential Boris and the Scovel method. Finally, in Section 6 we present some numerical results for the Kelvin-Helmholtz instability test case.

2 The time-splitting problem

Now we will recall the principles of semi-Lagrangian method for the Vlasov-Poisson equation cf. [8] in two dimensions of the phase space. In this Section, we work on the unscaled Vlasov-Poisson equation (2)-(3) for the sake of simplicity in the presentation. We return to the scale system when we study the asymptotic limit in Section 3. The characteristic curves corresponding to the Vlasov equation (2) are the solutions of the following first order differential system:

$$\begin{cases} \dot{X}(t;s,x,v) = V(t;s,x,v), \\ \dot{V}(t;s,x,v) = \dfrac{qB}{m}^{\perp} V(t;s,x,v) + \dfrac{q}{m} E(t, X(t;s,x,v)), \end{cases} \tag{11}$$

with the initial conditions

$$X(s;s,x,v) = x, \quad V(s;s,x,v) = v.$$

We denote by $(X(t;s,x,v), V(t;s,x,v))$ the position in phase space at time t, of a particle which was in (x,v) at time s. Then, the solution of the Vlasov equation (2) is given by

$$f(t,x,v) = f(s, X(s;t,x,v), V(s;t,x,v)) \tag{12}$$

$$= f_0(X(0;t,x,v), V(0;t,x,v)), \ \ (x,v) \in \mathbb{R}^2 \times \mathbb{R}^2, \ \ t \geq 0. \tag{13}$$

Replacing s by t^n and t by t^{n+1} in (12), and denoting $X^n = X(t^n; t^{n+1}, x, v)$ and $V^n = V(t^n; t^{n+1}, x, v)$ we have

$$f(t^{n+1}, x, v) = f(t^n, X^n, V^n).$$

For each point of the phase space grid (x,v), the distribution function is updated thanks to the two following steps:

i. Find the starting point of the characteristic curves ending at (x,v), i.e $X^n = X(t^n; t^{n+1}, x, v)$ and $V^n = V(t^n; t^{n+1}, x, v)$ by solving (11).

ii. Compute $f(t^n, X^n, V^n)$ by the method based on Lagrange interpolation, f being known only at mesh points at time t^n.

We now perform a time discretization in the step **i.** of (11) by introducing a splitting procedure.

2.1 The exponential Boris algorithm

The characteristics of the splitting underlying the exponential Boris algorithm reads [15]:

$$\begin{cases} \dot{X}(t;s,x,v) = V(t;s,x,v), \\ \dot{V}(t;s,x,v) = 0, \end{cases} \tag{14}$$

$$\begin{cases} \dot{X}(t;s,x,v) = 0, \\ \dot{V}(t;s,x,v) = \dfrac{qB}{m}^{\perp} V(t;s,x,v), \end{cases} \tag{15}$$

$$\begin{cases} \dot{X}(t;s,x,v) = 0, \\ \dot{V}(t;s,x,v) = \dfrac{q}{m} E(t, X(t;s,x,v)), \end{cases} \tag{16}$$

which leads us to the equations associated with the first order differential systems (14), (15) and (16) respectively:

$$\partial_t f + v \cdot \nabla_x f = 0, \tag{17}$$

$$\partial_t f + \frac{qB}{m}[v_2\partial_{v_1} f - v_1\partial_{v_2} f] = 0, \tag{18}$$

$$\partial_t f + \frac{q}{m}E(t,x)\cdot\nabla_v f = 0. \tag{19}$$

We denote $\varphi_{\Delta t}^{[f]}$, $\varphi_{\Delta t}^{[B]}$ and $\varphi_{\Delta t}^{[E]}$ the exact solutions corresponding to the equations (17), (18) and (19) on one time step Δt from the initial condition $f_0(x,v)$. The solutions $\varphi_{\Delta t}^{[f]}$ and $\varphi_{\Delta t}^{[E]}$ can be computed exactly in time since the advection fields in the equations (17) and (19) do not depend on the variable to be advected. The solution $\varphi_{\Delta t}^{[B]}$ of (18) can also be solved exactly in time, since the fact that characteristic equation (15) can be computed exactly. With the two-dimensional rotation matrix

$$\mathcal{R}(\theta) = \begin{pmatrix} \cos(\theta) & -\sin(\theta) \\ \sin(\theta) & \cos(\theta) \end{pmatrix},$$

the characteristic solution to equation (15) on one time step Δt writes

$$X(\Delta t; 0, x, v) = x, \quad V(\Delta t; 0, x, v) = \mathcal{R}(-\theta)V(0), \text{ with } \theta = \frac{qB}{m}\Delta t.$$

Hence, the solution to (18) by the method characteristic (13) writes

$$\begin{aligned} \varphi_{\Delta t}^{B} &= f_0(X(0;\Delta t,x,v), V(0;\Delta t,x,v)) \\ &= f_0(x, \mathcal{R}(\theta)v), \quad \theta = \frac{qB}{m}\Delta t. \end{aligned}$$

For step **ii.**, a two-dimensional interpolation has to be performed in the variable v of $\varphi_{\Delta t}^{[B]}$ to update the numerical unknown. However, high-dimensional interpolation is known to be non conservative and it is obviously more demanding in terms of complexity and time. To remedy this difficulty, we use the method in [3] where the authors proposed a splitting strategy to reduce the problem into very simple one-dimensional linear transport equations which can be solved efficiently with a semi-Lagrangian method. The splitting is based on the fact that the two-dimensional rotation matrix $\mathcal{R}(\theta)$ is decomposed into a product of three shear matrices:

$$\mathcal{R}(\theta) = \begin{pmatrix} \cos(\theta) & -\sin(\theta) \\ \sin(\theta) & \cos(\theta) \end{pmatrix} = \begin{pmatrix} 1 & -\tan(\theta/2) \\ 0 & 1 \end{pmatrix} \begin{pmatrix} 1 & 0 \\ \sin(\theta) & 1 \end{pmatrix} \begin{pmatrix} 1 & -\tan(\theta/2) \\ 0 & 1 \end{pmatrix}, \tag{20}$$

for $\theta \neq k\pi, k \in \mathbb{Z}^\star$. This formula has been generalized to arbitrary dimension, the reader can refer to [22, 23]. As a consequence, the computation of $\varphi_{\Delta t}^{[B]}$ can be done by solving three one dimensional linear equations (in v_1, v_2 and v_1 direction successively), i.e.

$$\begin{aligned} f_0(x,v) \to f^\star(x,v) = f_0(x, v_1 - \tan(\theta/2)v_2, v_2) \to f^{\star\star}(x,v) = f^\star(x, v_1, \sin(\theta)v_1 + v_2) \\ \to \varphi_{\Delta t}^{B} = f^{\star\star}(x, v_1 - \tan(\theta/2)v_2, v_2). \end{aligned} \tag{21}$$

This factorization is very useful to compute the rotation, since, using the semi-Lagrangian methods, it requires one dimensional interpolations instead of two dimensional interpolation. Moreover, when the angle θ is small (i.e. $B\Delta t << 1$), by approximating $\sin(x) \approx x$ and $\tan(x) \approx x$, we get the approximate decomposition of rotation (20) given by

$$\mathcal{R}(\theta) = \begin{pmatrix} \cos(\theta) & -\sin(\theta) \\ \sin(\theta) & \cos(\theta) \end{pmatrix} \approx \begin{pmatrix} 1-\theta^2/2 & -\theta+\theta^3/4 \\ \theta & 1-\theta^2/2 \end{pmatrix} = \begin{pmatrix} 1 & -\theta/2 \\ 0 & 1 \end{pmatrix} \begin{pmatrix} 1 & 0 \\ \theta & 1 \end{pmatrix} \begin{pmatrix} 1 & -\theta/2 \\ 0 & 1 \end{pmatrix},$$

which correspond exactly to the computation of $\varphi_{\Delta t}^{[B]}$ by using a Strang splitting for equation (18), where the splitting steps read:

$$\partial_t f + \frac{qB}{m} v_2 \cdot \nabla_{v_1} f = 0, \ \ \Delta t/2$$
$$\partial_t f - \frac{qB}{m} v_1 \cdot \nabla_{v_2} f = 0, \ \ \Delta t$$
$$\partial_t f + \frac{qB}{m} v_2 \cdot \nabla_{v_1} f = 0, \ \ \Delta t/2.$$

Note that, contrary to the exact splitting (20), this factorization is not exact: there is remainder term which is evaluated as $\mathcal{O}(B^2\Delta t^2)$. Consequently, it is less accurate than (21) and then the time step can not be taken quite large.

Now, we want to use the splitting methods to approximate the solution f in (12) of the system (2)-(3). A first order Lie method based on the exponential Boris algorithm writes

$$\chi_{\Delta t}^{\text{Lie}} = f(\Delta t) + \mathcal{O}(\Delta t^2)$$

where

$$\chi_{\Delta t}^{\text{Lie}} = \varphi_{\Delta t}^{[f]} \circ \varphi_{\Delta t}^{[B]} \circ \varphi_{\Delta t}^{[E]},$$

and then the Strang method based on the exponential Boris algorithm writes

$$\chi_{\Delta t}^{\text{Strang}} = f(\Delta t) + \mathcal{O}(\Delta t^3)$$

(which is a second order accurate splitting method) with

$$\chi_{\Delta t}^{\text{Strang}} = \varphi_{\Delta t/2}^{[f]} \circ \varphi_{\Delta t/2}^{[B]} \circ \varphi_{\Delta t}^{[E]} \circ \varphi_{\Delta t/2}^{[B]} \circ \varphi_{\Delta t/2}^{[f]}. \tag{22}$$

To achieve the second order accurate as Strang splitting, one can consider the composition of a first-order method like Lie method with its adjoint cf. [3]. This composition method writes

$$\chi_{\Delta t}^{\text{Compo}} = \chi_{\Delta t/2}^{\text{Lie}} \circ \left(\chi_{\Delta t/2}^{\text{Lie}}\right)^{\star}, \tag{23}$$

where the adjoint method $\left(\chi_{\Delta t/2}^{\text{Lie}}\right)^{\star}$ of the Lie method $\chi_{\Delta t/2}^{\text{Lie}}$ is denoted the inverse map of the original method with reserved time step, and it writes

$$\left(\chi_{\Delta t/2}^{\text{Lie}}\right)^{\star} = \left(\chi^{\text{Lie}}\right)_{-\Delta t/2}^{-1} = \left(\varphi^{[E]}\right)_{-\Delta t/2}^{-1} \circ \left(\varphi^{[B]}\right)_{-\Delta t/2}^{-1} \circ \left(\varphi^{[f]}\right)_{-\Delta t/2}^{-1}.$$

Since $\varphi_{\Delta t/2}^{[E]}$ is the exact solution of equation (19) on the half-time step Δt with the initial data f_0, and so $\varphi_{\Delta t/2}^{[E]} = f_0(v - E_0 \cdot \Delta t/2)$ where the electric field E_0 is computed from discretization of the Poisson equation (3) at the initial time, it yields that $\left(\varphi_{\Delta t/2}^{[E]}\right)^{-1} = f_0(v + E_0 \cdot \Delta t/2)$ and hence $\left(\varphi^{[E]}\right)_{-\Delta t/2}^{-1} = f_0(v - E_0 \cdot \Delta t/2) = \varphi_{\Delta t/2}^{[E]}$. Similarly, we also have $\left(\varphi^{[f]}\right)_{-\Delta t/2}^{-1} = \varphi_{\Delta t/2}^{[f]}$. For $\left(\varphi^{[B]}\right)_{-\Delta t/2}^{-1}$, from (21), we have the inverse solution $\left(\varphi_{\Delta t/2}^{[B]}\right)^{-1}$ writes

$$f_0(x,v) \to f^{\star\star}(x,v) = f_0(x, v_1 + \tan(\theta/2)v_2, v_2) \to f^{\star}(x,v) = f^{\star\star}(x, v_1, -\sin(\theta)v_1, v_2)$$
$$\left(\varphi_{\Delta t}^{[B]}\right)^{-1} = f^{\star}(x, v_1 + \tan(\theta/2)v_2, v_2), \ \theta = \frac{qB}{m}\frac{\Delta t}{2}$$

hence it yields that $\left(\varphi^{[B]}\right)_{-\Delta t/2}^{-1} = \varphi_{\Delta t/2}^{[B]}$. Combining these computations, we deduce that the adjoint of the Lie method $\left(\chi_{\Delta t/2}^{\text{Lie}}\right)^{\star}$ writes

$$\left(\chi_{\Delta t/2}^{\text{Lie}}\right)^{\star} = \varphi_{\Delta t/2}^{[E]} \circ \varphi_{\Delta t/2}^{[B]} \circ \varphi_{\Delta t/2}^{[f]} = \chi_{\Delta t/2}^{\text{Lie}}.$$

Therefore $\chi_{\Delta t}^{\text{Compo}} = \chi_{\Delta t}^{\text{Strang}}$ is of order 2 in time.

2.2 The Scovel method

The characteristic of the splitting underlying Scovel's method reads cf. [2]:

$$\begin{cases} \dot{X}(t;s,x,v) = V(t;s,x,v), \\ \dot{V}(t;s,x,v) = \dfrac{qB}{m}^{\perp} V(t;s,x,v), \end{cases} \tag{24}$$

$$\begin{cases} \dot{X}(t;s,x,v) = 0, \\ \dot{V}(t;s,x,v) = \dfrac{q}{m} E(t, X(t;s,x,v)), \end{cases} \tag{25}$$

which leads us to the equations associated with the characteristic equations (24) and (25) respectively:

$$\partial_t f + v \cdot \nabla_x f + \frac{qB}{m}^{\perp} v \cdot \nabla_v f = 0, \tag{26}$$

$$\partial_t f + \frac{q}{m} E(t,x) \cdot \nabla_v f = 0. \tag{27}$$

Note the following properties of the rotation matrix:

$$\frac{\mathrm{d}}{\mathrm{d}\theta} \mathcal{R}(-\theta + \pi/2) = \mathcal{R}(-\theta), \tag{28}$$

since

$$\frac{\mathrm{d}}{\mathrm{d}\theta} \mathcal{R}(-\theta + \pi/2) = \left(\frac{\mathrm{d}}{\mathrm{d}\theta} \mathcal{R}(-\theta) \right) \mathcal{R}(\pi/2) = \begin{pmatrix} -\sin(\theta) & \cos(\theta) \\ -\cos(\theta) & -\sin(\theta) \end{pmatrix} \begin{pmatrix} 0 & -1 \\ 1 & 0 \end{pmatrix} = \mathcal{R}(-\theta).$$

Thanks to (28), the exact solution of the characteristic curves in the equation (24) on one time step Δt reads:

$$V(\Delta t; 0, x, v) = \mathcal{R}(-\theta) v, \;\; \theta = \frac{qB}{m} \Delta t. \tag{29}$$

$$\begin{aligned} X(\Delta t; 0, x, v) &= x + \int_0^{\Delta t} V(\tau; 0, x, v) \mathrm{d}\tau = x + \int_0^{\Delta t} \mathcal{R}(-\frac{qB}{m}\tau) v \mathrm{d}\tau \\ &= x + \frac{m}{qB} \int_0^{\Delta t} \frac{\mathrm{d}}{\mathrm{d}\tau} \mathcal{R}(-\frac{qB}{m}\tau + \pi/2) v \mathrm{d}\tau \\ &= x + \frac{m}{qB} \left[\mathcal{R}\left(-\frac{qB}{m} \Delta t + \pi/2 \right) - \mathcal{R}(\pi/2) \right] v \\ &= x + \frac{m}{qB} \begin{pmatrix} \sin(\theta) & 1 - \cos(\theta) \\ \cos(\theta) - 1 & \sin(\theta) \end{pmatrix} v, \;\; \theta = \frac{qB}{m} \Delta t. \end{aligned} \tag{30}$$

We can therefore rewrite the equations (29) and (30) in matrix form as follows:

$$\begin{pmatrix} X(\Delta t; 0, x, v) \\ V(\Delta t; 0, x, v) \end{pmatrix} = \begin{pmatrix} 1 & 0 & \frac{m}{qB}\sin(\theta) & \frac{m}{qB}(1 - \cos(\theta)) \\ 0 & 1 & \frac{m}{qB}(\cos(\theta) - 1) & \frac{m}{qB}\sin(\theta) \\ 0 & 0 & \cos(\theta) & \sin(\theta) \\ 0 & 0 & \sin(-\theta) & \cos(\theta) \end{pmatrix} \begin{pmatrix} x \\ v \end{pmatrix}, \;\; \theta = \frac{qB}{m} \Delta t. \tag{31}$$

We denote $\gamma_{\Delta t}^{[B]}$ and $\gamma_{\Delta t}^{[E]}$ the exact solutions corresponding to the equations (26) and (27) on one time step Δt from an initial condition $f_0(x,v)$. From (31), we can deduce that the exact solution of equation (26) writes

$$\gamma_{\Delta t}^{[B]} = f_0(X(0; \Delta t, x, v), V(0; \Delta t, x, v)), \tag{32}$$

where

$$\begin{pmatrix} X(0;\Delta t,x,v) \\ V(0;\Delta t,x,v) \end{pmatrix} = \begin{pmatrix} 1 & 0 & \frac{m}{qB}\sin(-\theta) & \frac{m}{qB}(1-\cos(\theta)) \\ 0 & 1 & \frac{m}{qB}(\cos(\theta)-1) & \frac{m}{qB}\sin(-\theta) \\ 0 & 0 & \cos(\theta) & \sin(-\theta) \\ 0 & 0 & \sin(\theta) & \cos(\theta) \end{pmatrix} \begin{pmatrix} x \\ v \end{pmatrix}, \quad \theta = \frac{qB}{m}\Delta t. \tag{33}$$

For step **ii.**, a four-dimensional interpolation needs to be used in order to update the function values of the numerical unknown on the phase space grid. Therefore, to avoid four-dimensional interpolation, we propose an exact splitting that allows us to reduce four-dimensional interpolation to one-dimensional interpolations. To do so, the matrix (33) can be expressed into two shears:

$$\begin{pmatrix} 1 & 0 & 0 & 0 \\ 0 & 1 & 0 & 0 \\ 0 & 0 & \cos(\theta) & \sin(-\theta) \\ 0 & 0 & \sin(\theta) & \cos(\theta) \end{pmatrix} \begin{pmatrix} 1 & 0 & \frac{m}{qB}\sin(-\theta) & \frac{m}{qB}(1-\cos(\theta)) \\ 0 & 1 & \frac{m}{qB}(\cos(\theta)-1) & \frac{m}{qB}\sin(-\theta) \\ 0 & 0 & 1 & 0 \\ 0 & 0 & 0 & 1 \end{pmatrix}, \tag{34}$$

where the first matrix is decomposed into three shears as (20) and the second one can be expressed into a product of four shear transformations:

$$\begin{pmatrix} 1 & 0 & \frac{m}{qB}\sin(-\theta) & 0 \\ 0 & 1 & 0 & 0 \\ 0 & 0 & 1 & 0 \\ 0 & 0 & 0 & 1 \end{pmatrix} \begin{pmatrix} 1 & 0 & 0 & 0 \\ 0 & 1 & \frac{m}{qB}(\cos(\theta)-1) & 0 \\ 0 & 0 & 1 & 0 \\ 0 & 0 & 0 & 1 \end{pmatrix} \begin{pmatrix} 1 & 0 & 0 & \frac{m}{qB}(1-\cos(\theta)) \\ 0 & 1 & 0 & 0 \\ 0 & 0 & 1 & 0 \\ 0 & 0 & 0 & 1 \end{pmatrix} \begin{pmatrix} 1 & 0 & 0 & 0 \\ 0 & 1 & 0 & \frac{m}{qB}\sin(-\theta) \\ 0 & 0 & 1 & 0 \\ 0 & 0 & 0 & 1 \end{pmatrix}$$

leads to an exact splitting in time. In consequence, we just have to solve shear transformations which are nothing but one-dimensional linear advections. Moreover, for the small angle θ, by approximating $\sin(x) \approx x$ and $1-\cos(x) \approx x^2/2 \approx 0$, the product of two matrices in (34) becomes

$$\begin{pmatrix} 1 & 0 & 0 & 0 \\ 0 & 1 & 0 & 0 \\ 0 & 0 & \cos(\theta) & \sin(-\theta) \\ 0 & 0 & \sin(\theta) & \cos(\theta) \end{pmatrix} \begin{pmatrix} 1 & 0 & -\Delta t & 0 \\ 0 & 1 & 0 & -\Delta t \\ 0 & 0 & 1 & 0 \\ 0 & 0 & 0 & 1 \end{pmatrix}, \quad \theta = \frac{qB}{m}\Delta t$$

which implies that

$$\gamma_{\Delta t}^{[B]} = \varphi_{\Delta t}^{[B]} \circ \varphi_{\Delta t}^{[f]}, \tag{35}$$

where $\varphi_{\Delta t}^{[f]}$ and $\varphi_{\Delta t}^{[B]}$ are exact solutions of equations (17) and (18) and this is equivalent to splitting the equation (24) into successive equations (14) and (15). We see that $\gamma_{\Delta t}^{[B]}$ does not remain the exact solution of equation (26).

We consider now the adjoint solution of $\gamma_{\Delta t}^{[B]}$. The adjoint solution $\left(\gamma_{\Delta t}^{[B]}\right)^\star$ reads

$$\left(\gamma_{\Delta t}^{[B]}\right)^\star = \left(\gamma^{[B]}\right)_{-\Delta t}^{-1} = f_0(X(-\Delta t;0,x,v), V(-\Delta t;0,x,v)),$$

because of the fact that $\binom{X(-\Delta t;0,x,v)}{V(-\Delta t;0,x,v)}$ is just the inverse of $\binom{X(0;\Delta t,x,v)}{V(0;\Delta t,x,v)}$ with the time step reversed. From (31) and (33), we get $(X,V)(-\Delta t;0,x,v) = (X,V)(0;\Delta t,x,v)$ which yields that $\left(\gamma_{\Delta t}^{[B]}\right)^\star = \gamma_{\Delta t}^{[B]}$. Hence $\left(\gamma_{\Delta t}^{[B]}\right)^\star$ is still exact solution to equation (26). Therefore, we can use the decomposition as in (34) to compute the adjoint solution. For symmetric composition

with the adjoint method, the matrix created by $\binom{X(-\Delta t;0,x,v)}{V(-\Delta t;0,x,v)}$ can be decomposed into two shears that is the inverse of the product of two matrices in (34) with the time step reversed

$$\begin{pmatrix} 1 & 0 & \frac{m}{qB}\sin(-\theta) & \frac{m}{qB}(\cos(\theta)-1) \\ 0 & 1 & \frac{m}{qB}(1-\cos(\theta)) & \frac{m}{qB}\sin(-\theta) \\ 0 & 0 & 1 & 0 \\ 0 & 0 & 0 & 1 \end{pmatrix} \begin{pmatrix} 1 & 0 & 0 & 0 \\ 0 & 1 & 0 & 0 \\ 0 & 0 & \cos(\theta) & \sin(-\theta) \\ 0 & 0 & \sin(\theta) & \cos(\theta) \end{pmatrix} \tag{36}$$

where the second matrix is decomposed into three shears as (20) and the first matrix can be decomposed into a product of four shear transformations:

$$\begin{pmatrix} 1 & 0 & 0 & 0 \\ 0 & 1 & 0 & \frac{m}{qB}\sin(-\theta) \\ 0 & 0 & 1 & 0 \\ 0 & 0 & 0 & 1 \end{pmatrix} \begin{pmatrix} 1 & 0 & 0 & \frac{m}{qB}(\cos(\theta)-1) \\ 0 & 1 & 0 & 0 \\ 0 & 0 & 1 & 0 \\ 0 & 0 & 0 & 1 \end{pmatrix} \begin{pmatrix} 1 & 0 & 0 & 0 \\ 0 & 1 & \frac{m}{qB}(1-\cos(\theta)) & 0 \\ 0 & 0 & 1 & 0 \\ 0 & 0 & 0 & 1 \end{pmatrix} \begin{pmatrix} 1 & 0 & \frac{m}{qB}\sin(-\theta) & 0 \\ 0 & 1 & 0 & 0 \\ 0 & 0 & 1 & 0 \\ 0 & 0 & 0 & 1 \end{pmatrix}$$

For the small angle θ, the product of two matrices in (36) becomes

$$\begin{pmatrix} 1 & 0 & -\Delta t & 0 \\ 0 & 1 & 0 & -\Delta t \\ 0 & 0 & 1 & 0 \\ 0 & 0 & 0 & 1 \end{pmatrix} \begin{pmatrix} 1 & 0 & 0 & 0 \\ 0 & 1 & 0 & 0 \\ 0 & 0 & \cos(\theta) & \sin(-\theta) \\ 0 & 0 & \sin(\theta) & \cos(\theta) \end{pmatrix}, \quad \theta = \frac{qB}{m}\Delta t.$$

Hence, we get

$$\left(\gamma_{\Delta t}^{[B]}\right)^{\star} = \varphi_{\Delta t}^{[f]} \circ \varphi_{\Delta t}^{[B]}. \tag{37}$$

and $\left(\gamma_{\Delta t}^{[B]}\right)^{\star}$ is not the exact solution of (26). This is equivalent to splitting the equation (24) into successive equations (15) and (14). It is clear that, in this situation i.e. θ is small, from (35) and (37) the solution $\gamma_{\Delta t}^{[B]}$ and its adjoint are different, since these solutions are not exact solutions for the equation (26).

Now, we want to use the Scovel method in combination with Strang's splitting or the composition with adjoint method to approximate the solution (13) of the system (2)-(3). The second order Strang splitting based on the Scovel method writes $\Gamma_{\Delta t}^{\text{Strang}} = f(\Delta t)+\mathcal{O}(\Delta t^3)$ with

$$\Gamma_{\Delta t}^{\text{Strang}} = \gamma_{\Delta t/2}^{[B]} \circ \gamma_{\Delta t}^{[E]} \circ \gamma_{\Delta t/2}^{[B]}. \tag{38}$$

The composition with adjoint method based on the Scovel method writes

$$\Gamma_{\Delta t}^{\text{Compo}} = \left(\gamma_{\Delta t/2}^{[E]} \circ \gamma_{\Delta t/2}^{[B]}\right)^{\star} \circ \left(\gamma_{\Delta t/2}^{[E]} \circ \gamma_{\Delta t/2}^{[B]}\right). \tag{39}$$

Since $\left(\gamma_{\Delta t/2}^{[E]}\right)^{\star} = \gamma_{\Delta t/2}^{[E]}$ and $\left(\gamma_{\Delta t/2}^{[B]}\right)^{\star} = \gamma_{\Delta t/2}^{[B]}$ we obtain

$$\begin{aligned} \Gamma_{\Delta t}^{\text{Compo}} &= \left(\gamma_{\Delta t/2}^{[B]}\right)^{\star} \circ \left(\gamma_{\Delta t/2}^{[E]}\right)^{\star} \circ \gamma_{\Delta t/2}^{[E]} \circ \gamma_{\Delta t/2}^{[B]} \\ &= \gamma_{\Delta t/2}^{[B]} \circ \gamma_{\Delta t/2}^{[E]} \circ \gamma_{\Delta t/2}^{[E]} \circ \gamma_{\Delta t/2}^{[B]} = \Gamma_{\Delta t}^{\text{Strang}}. \end{aligned}$$

Therefore the composed Scovel coincides with the Strang splitting based on the Scovel method and so it is of order 2 in time. Moreover from (35) and (37), for the small values of $B \cdot \Delta t$, it is easily seen that the method splitting based on Scovel method is same the one based on exponential Boris algorithm.

3 Consistency in the limit $\varepsilon \to 0$ of Scovel method

In this section, we consider the characteristic system of the Vlasov equation (5) given by

$$\begin{cases} \varepsilon \dot{X}_\varepsilon(t;s,x,v) = V_\varepsilon(t;s,x,v), \\ \varepsilon \dot{V}_\varepsilon(t;s,x,v) = \dfrac{qB}{m} \dfrac{{}^\perp V_\varepsilon(t;s,x,v)}{\varepsilon} + \dfrac{q}{m} E_\varepsilon(t, X_\varepsilon(t;s,x,v)), \quad (t,s) \in [0,T], \end{cases} \tag{40}$$

and the characteristic equation of the guiding-center approximation (7)-(8) given by

$$\dot{Y}(t;s,x) = \frac{{}^\perp E(t, Y(t;s,x))}{B}, \quad (t,s) \in [0,T]. \tag{41}$$

In the sequel we will denote $X_\varepsilon(t) = X_\varepsilon(t;s,x,v)$ and $V_\varepsilon(t) = V_\varepsilon(t;s,x,v)$.
We define then the following combination of the characteristics:

$$Z_\varepsilon(t) = X_\varepsilon(t) + \frac{m}{qB} \varepsilon {}^\perp V_\varepsilon(t), \tag{42}$$

which is the formula giving the Guiding center position.

Proposition 3.1 *For all $(x,v) \in \mathbb{R}^2 \times \mathbb{R}^2$, the evolution of the Guiding Center $Z_\varepsilon(t)$ satisfies:*

$$\dot{Z}_\varepsilon(t) = \frac{{}^\perp E_\varepsilon(t, X_\varepsilon(t))}{B}.$$

Proof. By direct computation and using of equations (40) we have:

$$\begin{aligned} \dot{Z}_\varepsilon(t) &= \dot{X}_\varepsilon(t) + \frac{m}{qB} \varepsilon {}^\perp \dot{V}_\varepsilon(t) \\ &= \frac{V_\varepsilon(t)}{\varepsilon} + \frac{m}{qB} {}^\perp \left(\frac{qB}{m} \frac{{}^\perp V_\varepsilon(t)}{\varepsilon} + \frac{q}{m} E_\varepsilon(t, X_\varepsilon(t)) \right) = \frac{{}^\perp E_\varepsilon(t, X_\varepsilon(t))}{B}. \end{aligned}$$

□

We consider now the Vlasov equation (5) under the Scovel method, that means the distribution function $f_\varepsilon(t,x,v)$ solves successively

$$\varepsilon \partial_t f_\varepsilon(t,x,v) + v \cdot \nabla_x f_\varepsilon + \frac{\omega_c}{\varepsilon} {}^\perp v \cdot \nabla_v f_\varepsilon = 0, \quad (t,x,v) \in]0,T] \times \mathbb{R}^2 \times \mathbb{R}^2, \tag{43}$$

and

$$\varepsilon \partial_t f_\varepsilon(t,x,v) + \frac{q}{m} E_\varepsilon(t,x) \cdot \nabla_v f_\varepsilon = 0, \quad (t,x,v) \in]0,T] \times \mathbb{R}^2 \times \mathbb{R}^2, \tag{44}$$

where the electric field E_ε is computed from the Poisson equation after performing the equation (43).

3.1 The asymptotic limit for the characteristic curves

First, we observe the approximation of the exact Guiding center position Z_ε in (42) when computing the composition of the characteristic equations associated with equations (43) and (44) respectively. Then we formally analyse the asymptotic behavior of the sequence $(Z_\varepsilon)_\varepsilon$ as ε goes to zero and compare with the position of guiding center approximation in (41). The characteristic equation associated with equation (43) is

$$\mathcal{E}^1_\varepsilon(t) : \begin{cases} \varepsilon \dot{X}_\varepsilon(t) = V_\varepsilon(t), \\ \\ \varepsilon \dot{V}_\varepsilon(t) = \dfrac{qB}{m} \dfrac{{}^\perp V_\varepsilon(t)}{\varepsilon}, \end{cases} \qquad t > 0$$

and with equation (44) being

$$\mathcal{E}_\varepsilon^2(t): \begin{cases} \varepsilon \dot{X}_\varepsilon(t) = 0, & \\ & t > 0 \\ \varepsilon \dot{V}_\varepsilon(t) = \dfrac{q}{m} E_\varepsilon(t, X_\varepsilon(t)), & \end{cases}$$

where the electric field E_ε is computed from the Poisson equation.
Using the formulae (29)-(30), the exact solution of the subflow $\mathcal{E}_\varepsilon^1(t)$ reads then

$$\begin{aligned} \varepsilon X_{\varepsilon,\star} &= \varepsilon X_\varepsilon(0) + \frac{m\varepsilon^2}{qB}\left[\mathcal{R}\left(-\frac{qB}{m}\frac{t}{\varepsilon^2} + \pi/2\right) - \mathcal{R}(\pi/2)\right] V_\varepsilon(0), \\ V_{\varepsilon,\star} &= \mathcal{R}\left(-\frac{qB}{m}\frac{t}{\varepsilon^2}\right) V_\varepsilon(0), \end{aligned} \tag{45}$$

and the exact solution of the subflow $\mathcal{E}_\varepsilon^2(t)$ with the initial condition $(X_{\varepsilon,\star}, V_{\varepsilon,\star})$ reads

$$\begin{aligned} \varepsilon X_\varepsilon(t) &= \varepsilon X_{\varepsilon,\star}, \\ \varepsilon V_\varepsilon(t) &= \varepsilon V_{\varepsilon,\star} + \frac{q}{m}\int_0^t E_\varepsilon(s, X_{\varepsilon,\star})\mathrm{d}s. \end{aligned} \tag{46}$$

Combining (45) and (46) we get the approximate characteristic curves of the Vlasov equation under the Scovel method

$$\begin{aligned} X_\varepsilon(t) &= X_\varepsilon(0) + \frac{m}{qB}\left[\mathcal{R}\left(-\frac{qB}{m}\frac{t}{\varepsilon^2} + \pi/2\right) - \mathcal{R}(\pi/2)\right] \varepsilon V_\varepsilon(0), \\ \varepsilon V_\varepsilon(t) &= \mathcal{R}\left(-\frac{qB}{m}\frac{t}{\varepsilon^2}\right) \varepsilon V_\varepsilon(0) + \frac{q}{m}\int_0^t E_\varepsilon(s, X_\varepsilon(s))\mathrm{d}s. \end{aligned} \tag{47}$$

Substituting the second equation into the first one of (47), we obtain that

$$X_\varepsilon(t) = X_\varepsilon(0) + \frac{m}{qB}\mathcal{R}(\pi/2)\varepsilon\left[V_\varepsilon(t) - V_\varepsilon(0)\right] + \frac{q}{m}\int_0^t \frac{{}^\perp E_\varepsilon(s, X_\varepsilon(s))}{B}\mathrm{d}s.$$

Then, using (42), this equation becomes:

$$Z_\varepsilon(t) = Z_\varepsilon(0) + \int_0^t \frac{{}^\perp E_\varepsilon}{B}\left(s, Z_\varepsilon(s) - \frac{m}{qB}\varepsilon^\perp V_\varepsilon(s)\right)\mathrm{d}s.$$

Therefore, the system (47) can be re-written for $(Z_\varepsilon, \varepsilon V_\varepsilon)$ as:

$$\begin{aligned} Z_\varepsilon(t) &= Z_\varepsilon(0) + \int_0^t \frac{{}^\perp E_\varepsilon}{B}\left(s, Z_\varepsilon(s) - \frac{m}{qB}\varepsilon^\perp V_\varepsilon(s)\right)\mathrm{d}s, \\ \varepsilon V_\varepsilon(t) &= \mathcal{R}\left(-\frac{q}{mB}\frac{t}{\varepsilon^2}\right)\varepsilon V_\varepsilon(0) + \frac{q}{m}\int_0^t E_\varepsilon\left(s, Z_\varepsilon(0) - \frac{m}{qB}\mathcal{R}\left(-\frac{m}{qB}\frac{s}{\varepsilon^2}\right)\varepsilon^\perp V_\varepsilon(0)\right)\mathrm{d}s. \end{aligned} \tag{48}$$

We expect that the family of trajectories $(Z_\varepsilon, \varepsilon V_\varepsilon)_{\varepsilon>0}$ is stable as the parameter ε becomes small, and we are looking for the limit trajectory $(Z, V) = \lim_{\varepsilon\to 0}(Z_\varepsilon, \varepsilon V_\varepsilon)$. Obviously, we see the appearance of two time scales, a slow time scale depending on the variable t and also a fast time scale depending on the variable $s = t/\varepsilon^2$. In order to establish the convergence of $(Z_\varepsilon, \varepsilon V_\varepsilon)_{\varepsilon>0}$, we appeal to a standard result in homogenization theory, c.f [6].

Proposition 3.2 *Let $U = U(z,t,s) : \mathcal{O}\times\mathbb{R}_+\times\mathbb{R}_+ \to \mathbb{R}$ be a function in $L^p\left(\mathcal{O}\times\mathbb{R}_+; C_\sharp(\mathbb{R}_+)\right)$, where $\mathcal{O}$ is an open set of $\mathbb{R}^N$ and $C_\sharp(\mathbb{R}_+)$ stands for the set of continuous periodic of period functions of period $L > 0$. We consider rapidly oscillating function of the form $U_\varepsilon(z,t) = U(z,t,t/\varepsilon)$. Then we have $U_\varepsilon \to < U > (z,t)$ as $\varepsilon \to 0$ weakly in $L^p(\mathcal{O}\times\mathbb{R}_+)$ for $p \in [1,\infty)$ and $\star$-weakly in $L^\infty(\mathcal{O}\times\mathbb{R}_+)$, where $< U > (z,t) = \dfrac{1}{L}\int_0^L U(z,t,s)\mathrm{d}s$ is the mean value of U with respect to s.*

Now, we formally show that the limit trajectory (Z,V) of $(Z_\varepsilon, \varepsilon V_\varepsilon)_{\varepsilon>0}$ in (48) satisfies the following equations:

$$\begin{aligned} Z(t) &= Z(0) + \int_0^t \frac{{}^\perp E}{B}\left(s, Z(s) - \frac{m}{qB}{}^\perp V(s)\right)\mathrm{d}s, \\ V(t) &= \frac{q}{m}\int_0^t \frac{1}{2\pi}\int_0^{2\pi} E\left(s, Z(0) - \frac{m}{qB}\mathcal{R}\left(-\theta\right){}^\perp V(0)\right)\mathrm{d}\theta\mathrm{d}s. \end{aligned} \tag{49}$$

Indeed, by Proposition 3.2 we have the following weak-$\star$ convergences in $L^\infty(R^2)^2$

$$\mathcal{R}\left(-\frac{q}{mB}\frac{t}{\varepsilon^2}\right)\varepsilon V_\varepsilon(0) \rightharpoonup \frac{1}{2\pi}\int_0^{2\pi}\mathcal{R}(-\theta)\mathrm{d}\theta V(0) = 0,$$

and

$$\begin{aligned} &\frac{q}{m}\int_0^t E_\varepsilon\left(s, Z_\varepsilon(s) - \frac{m}{qB}\mathcal{R}\left(-\frac{m}{qB}\frac{s}{\varepsilon^2}\right)\varepsilon^\perp V_\varepsilon(0)\right)\mathrm{d}s \\ \rightharpoonup\ &\frac{q}{m}\int_0^t \frac{1}{2\pi}\int_0^{2\pi} E\left(s, Z(s) - \frac{m}{qB}\mathcal{R}\left(-\theta\right){}^\perp V(0)\right)\mathrm{d}\theta\mathrm{d}s \text{ as } \varepsilon \to 0. \end{aligned}$$

Substituting these approximations into the first equation of (48) and then passing to the limit, when ε goes to 0, leads to (Z,V) satisfies equation (49).
We see that from the first equation in the system (49) the time evolution of particle's position $Z(t)$ is not compatible with the characteristic position (41) of the guiding center model. Thus when $\varepsilon \to 0$, the guiding center position Z_ε does not approach the correct trajectory.

3.2 The asymptotic limit for the density particle

We will use the splitting scheme (43)-(44) to approximate the distribution function $f_\varepsilon(t,x,v)$ and then compute the density particle $\rho_\varepsilon(t,x)$. We show formally that the limit $\rho(t,x)$ of the sequence $(\rho_\varepsilon)_\varepsilon$ when ε goes to 0 is consistent with the guiding center equation, based on the work of Miot in [7]. Motivated by the computation in the Proposition 3.1, we introduce the change of coordinates $(x,v) \to (\bar{x},v)$ and consider the gyro-coordinates given by

$$\bar{x} = x + \varepsilon\frac{{}^\perp v}{\omega_c}, \quad v = v, \ \ \omega_c = \frac{qB}{m}.$$

At any time $t \in [0,T]$, we introduce the new distribution of particles $\bar{f}_\varepsilon(t)$ in the new coordinates $(\bar{x},v)$, that is

$$\bar{f}_\varepsilon(t,\bar{x},v) = f_\varepsilon(t,x,v), \ \ x = \bar{x} - \varepsilon\frac{{}^\perp v}{\omega_c}.$$

Performing the above change of coordinates allow us transform the equations (43)-(44) of presence density f_ε into equations of $\bar{f}_\varepsilon$ which give respectively by:

Proposition 3.3 *We have*

$$\partial_t \bar{f}_\varepsilon(t,\bar{x},v) + \omega_c \frac{{}^\perp v}{\varepsilon^2} \cdot \nabla_v \bar{f}_\varepsilon = 0, \ \ (t,\bar{x},v) \in [0,T] \times \mathbb{R}^2 \times \mathbb{R}^2, \tag{50}$$

and

$$\partial_t \bar{f}_\varepsilon + \frac{{}^\perp E_\varepsilon}{B}\left(t,\bar{x} - \varepsilon \frac{{}^\perp v}{\omega_c}\right) \cdot \nabla_{\bar{x}} \bar{f}_\varepsilon + \frac{q}{m}\frac{E_\varepsilon}{\varepsilon}\left(t,\bar{x} - \varepsilon \frac{{}^\perp v}{\omega_c}\right) \cdot \nabla_v \bar{f}_\varepsilon = 0, \ (t,\bar{x},v) \in [0,T] \times \mathbb{R}^2 \times \mathbb{R}^2. \tag{51}$$

Proof. We compute:

$$\partial_t f_\varepsilon = \partial_t \bar{f}_\varepsilon, \quad \nabla_x f_\varepsilon = \nabla_{\bar{x}} \bar{f}_\varepsilon,$$

and

$$\nabla_v f_\varepsilon = {}^t(\partial_v \bar{x}) \nabla_{\bar{x}} \bar{f}_\varepsilon + \nabla_v \bar{f}_\varepsilon = {}^t\left(\frac{\varepsilon}{\omega_c}\mathcal{R}(-\pi/2)\right) \nabla_{\bar{x}} \bar{f}_\varepsilon + \nabla_v \bar{f}_\varepsilon = \frac{\varepsilon}{\omega_c}\mathcal{R}(\pi/2)\nabla_{\bar{x}} \bar{f}_\varepsilon + \nabla_v \bar{f}_\varepsilon.$$

Combining the above computations we obtain that

$$\begin{aligned}
\varepsilon \partial_t f_\varepsilon + v \cdot \nabla_x f_\varepsilon + \frac{\omega_c}{\varepsilon}{}^\perp v \cdot \nabla_v f_\varepsilon &= \varepsilon \partial_t \bar{f}_\varepsilon + v \cdot \nabla_{\bar{x}} \bar{f}_\varepsilon + \frac{\omega_c}{\varepsilon}{}^\perp v \cdot \left[\frac{\varepsilon}{\omega_c}\mathcal{R}(\pi/2)\nabla_{\bar{x}} \bar{f}_\varepsilon + \nabla_v \bar{f}_\varepsilon\right] \\
&= \varepsilon \partial_t \bar{f}_\varepsilon + v \cdot \nabla_{\bar{x}} \bar{f}_\varepsilon - v \cdot \nabla_{\bar{x}} \bar{f}_\varepsilon + \frac{\omega_c}{\varepsilon}{}^\perp v \cdot \nabla_v \bar{f}_\varepsilon \\
&= \varepsilon \partial_t \bar{f}_\varepsilon + \frac{\omega_c}{\varepsilon}{}^\perp v \cdot \nabla_v \bar{f}_\varepsilon,
\end{aligned}$$

and we also have

$$\begin{aligned}
\varepsilon \partial_t f_\varepsilon + \frac{q}{m} E(t,x) \cdot \nabla_v f_\varepsilon &= \varepsilon \partial_t \bar{f}_\varepsilon + \frac{q}{m} E_\varepsilon(t,x) \cdot \left[\frac{\varepsilon}{\omega_c}\mathcal{R}(\pi/2)\nabla_{\bar{x}} \bar{f}_\varepsilon + \nabla_v \bar{f}_\varepsilon\right] \\
&= \varepsilon \partial_t \bar{f}_\varepsilon + \varepsilon \frac{{}^\perp E_\varepsilon}{B}\left(t,\bar{x} - \varepsilon \frac{{}^\perp v}{\omega_c}\right) \cdot \nabla_{\bar{x}} \bar{f}_\varepsilon + \frac{q}{m} E_\varepsilon\left(t,\bar{x} - \varepsilon \frac{{}^\perp v}{\omega_c}\right) \cdot \nabla_v \bar{f}_\varepsilon,
\end{aligned}$$

which yield the result. □

We then consider the macroscopic density in the gyro-coordinates $\bar{x}$, that is

$$\bar{\rho}_\varepsilon(t,\bar{x}) = \int_{\mathbb{R}^2} \bar{f}_\varepsilon(t,\bar{x},v)\mathrm{d}v = \int_{\mathbb{R}^2} f_\varepsilon(t,\bar{x} - \varepsilon \frac{{}^\perp v}{\omega_c}, v)\mathrm{d}v.$$

After integrating into the equations in Proposition 3.3 with respect to the velocity v, the density $\bar{\rho}_\varepsilon$ solves successively the following equations:

Proposition 3.4 *We have*

$$\partial_t \bar{\rho}_\varepsilon(t,\bar{x}) = 0, \ \ (t,\bar{x}) \in [0,T] \times \mathbb{R}^2, \tag{52}$$

and

$$\partial_t \bar{\rho}_\varepsilon(t,\bar{x}) + \mathrm{div}_{\bar{x}}\left[\int_{\mathbb{R}^2} \frac{{}^\perp E_\varepsilon}{B}\left(t,\bar{x} - \varepsilon \frac{{}^\perp v}{\omega_c}\right) \bar{f}_\varepsilon \mathrm{d}v\right] = 0, \quad (t,\bar{x}) \in [0,T] \times \mathbb{R}^2. \tag{53}$$

Proof. The first equation is obvious since

$$\int_{\mathbb{R}^2} {}^\perp v \cdot \nabla_v \bar{f}_\varepsilon \mathrm{d}v = 0.$$

For the second equation we have to show that

$$\int_{\mathbb{R}^2} E_\varepsilon\left(t,\bar{x}-\varepsilon\frac{{}^\perp v}{\omega_c}\right)\cdot\nabla_v\bar{f}_\varepsilon \mathrm{d}v = 0.$$

After using the integration by partial w.r.t the variable v, we have to compute the divergence of the following term

$$\begin{aligned}
\mathrm{div}_v\left[E_\varepsilon\left(t,\bar{x}-\varepsilon\frac{{}^\perp v}{\omega_c}\right)\right] &= \partial_{v_1}E^1_\varepsilon\left(t,\bar{x}-\varepsilon\frac{{}^\perp v}{\omega_c}\right)+\partial_{v_2}E^2_\varepsilon\left(t,\bar{x}-\varepsilon\frac{{}^\perp v}{\omega_c}\right)\\
&= \frac{\varepsilon}{\omega_c}\left(\partial_{x_2}E^1_\varepsilon\right)\left(t,\bar{x}-\varepsilon\frac{{}^\perp v}{\omega_c}\right)-\frac{\varepsilon}{\omega_c}\left(\partial_{x_1}E^2_\varepsilon\right)\left(t,\bar{x}-\varepsilon\frac{{}^\perp v}{\omega_c}\right)\\
&= 0,
\end{aligned}$$

where we used $E_\varepsilon = (E^1_\varepsilon, E^2_\varepsilon) = -(\partial_{x_1}\Phi_\varepsilon, \partial_{x_2}\Phi_\varepsilon)$, hence the second equation of Proposition 3.5 follows. □

Remark 3.1 *We see that the evolution of the density particle from the equations* (52)-(53) *does not contain the fast scale, so a very small time step is no longer required to simulate well. Then we compare it with the exponential Boris algorithm presented in Section 2 when applying the above procedure. In this procedure splitting, the simulation of density particle will be affected by the time step. Indeed, we appeal the exponential Boris algorithm for the Vlasov equation as*

$$\begin{aligned}
\varepsilon\partial_t f_\varepsilon(t,x,v)+v\cdot\nabla_x f_\varepsilon &= 0,\\
\varepsilon\partial_t f_\varepsilon(t,x,v)+\frac{\omega_c}{\varepsilon}{}^\perp v\cdot\nabla_v f_\varepsilon &= 0,\\
\varepsilon\partial_t f_\varepsilon(t,x,v)+\frac{q}{m}E_\varepsilon(t,x)\cdot\nabla_v f_\varepsilon &= 0.
\end{aligned}$$

When we apply the above change of coordinates, the above equations becomes:

$$\begin{aligned}
\varepsilon\partial_t\bar{f}_\varepsilon(t,\bar{x},v)+v\cdot\nabla_{\bar{x}}\bar{f}_\varepsilon &= 0,\\
\varepsilon\partial_t\bar{f}_\varepsilon(t,\bar{x},v)-v\cdot\nabla_{\bar{x}}\bar{f}_\varepsilon+\frac{\omega_c}{\varepsilon}{}^\perp v\cdot\nabla_v\bar{f}_\varepsilon &= 0,\\
\partial_t\bar{f}_\varepsilon(t)+\frac{{}^\perp E_\varepsilon}{B}\left(t,\bar{x}-\varepsilon\frac{{}^\perp v}{\omega_c}\right)\cdot\nabla_{\bar{x}}\bar{f}_\varepsilon+\frac{q}{m}\frac{E_\varepsilon}{\varepsilon}\left(t,\bar{x}-\varepsilon\frac{{}^\perp v}{\omega_c}\right)\cdot\nabla_v\bar{f}_\varepsilon &= 0.
\end{aligned}$$

Integrating these equations w.r.t the variable v, we obtain

$$\begin{aligned}
\varepsilon\partial_t\bar{\rho}_\varepsilon(t)+\nabla_{\bar{x}}\cdot\int_{\mathbb{R}^2}v\bar{f}_\varepsilon\mathrm{d}v &= 0,\\
\varepsilon\partial_t\bar{\rho}_\varepsilon(t)-\nabla_{\bar{x}}\cdot\int_{\mathbb{R}^2}v\bar{f}_\varepsilon\mathrm{d}v &= 0,\\
\partial_t\bar{\rho}_\varepsilon(t,\bar{x})+\mathrm{div}_{\bar{x}}\left[\int_{\mathbb{R}^2}\frac{{}^\perp E_\varepsilon}{B}\left(t,\bar{x}-\varepsilon\frac{{}^\perp v}{\omega_c}\right)\bar{f}_\varepsilon\mathrm{d}v\right] &= 0.
\end{aligned}$$

We see that the stiff term is still present in the above system. Therefore, in order to obtain good results with this method, the time step Δt has to be the same order of ε which penalizes the method in terms of CPU time cost when we consider a very small ε.

Finally, we will formally check the asymptotic behavior of the sequence of density particle $(\rho_\varepsilon)_\varepsilon$. Passing formal to the limit as $\varepsilon \to 0$ in the equations of Proposition 3.4 yield

$$\partial_t \rho(t,x) = 0, \quad \partial_t \rho(t,x) + \mathrm{div}_x \left[\int_{\mathbb{R}^2} \frac{{}^\perp E(t,x)}{B} f(t,x,v) \mathrm{d}v \right] = 0.$$

Therefore we get the density limit ρ solves successively the following equations:

$$\partial_t \rho(t,x) = 0, \quad \partial_t \rho(t,x) + \frac{{}^\perp E(t,x)}{B} \cdot \nabla_x \rho(t,x) = 0.$$

Proposition 3.5 ***(formal)*** *Assume that the family $(E_\varepsilon)_{\varepsilon>0}$ is uniformly bounded in $L^\infty(\mathbb{R}_+ \times \mathbb{R}^2)$ and the sequences $(\bar{\rho}_\varepsilon)_{\varepsilon>0}$ satisfy the equations in Proposition 3.4, with the initial data $(f_{\varepsilon,0})_{\varepsilon>0}$ be a non negative presence density satisfying*

$$\sup_{\varepsilon>0} \int_{\mathbb{R}^2} \int_{\mathbb{R}^2} f_{\varepsilon,0}(\bar{x},v) \mathrm{d}\bar{x}\mathrm{d}v < +\infty.$$

Then, there is a sequence $(\varepsilon_k)_k$ such that $\rho_{\varepsilon_k} \to \rho$, $E_{\varepsilon_k} \to E$ as $\varepsilon_k \to 0$ and the limit (ρ, E) solves successively the following equations:

$$\begin{aligned} \partial_t \rho(t,\bar{x}) &= 0, \\ \partial_t \rho(t,\bar{x}) + \frac{{}^\perp E}{B}(t,\bar{x}) \cdot \nabla_{\bar{x}} \rho(t,\bar{x}) &= 0, \end{aligned} \tag{54}$$

in the sense of distribution.

Proof. The uniform boundedness w.r.t $\varepsilon > 0$ of the total mass $\int_{\mathbb{R}^2} \int_{\mathbb{R}^2} f_\varepsilon(t) \mathrm{d}x\mathrm{d}v$ and the electric field E_ε implies that there exists $\rho \in L^\infty([0,T], \mathcal{M}^+(\mathbb{R}^2))$ and $E \in L^\infty([0,T] \times \mathbb{R}^2)$, such that up to extraction of a subsequence $(\rho_{\varepsilon_k})_k$, the following convergences hold as $k \to +\infty$

$$\begin{aligned} \rho_{\varepsilon_k} \to \rho \text{ in } L^\infty([0,T], \mathcal{M}^+(\mathbb{R}^2)) \text{ weak} - \star, \\ E_{\varepsilon_k} \to E \text{ in } L^\infty([0,T] \times \mathbb{R}^2) \text{ weak} - \star. \end{aligned}$$

Let $\Psi \in C_0^\infty((0,T) \times \mathbb{R}^2)$, from the equation (53) we have

$$\begin{aligned} &\frac{\mathrm{d}}{\mathrm{dt}} \int_{\mathbb{R}^2} \bar{\rho}_{\varepsilon_k}(t,\bar{x}) \Psi(t,\bar{x}) \mathrm{d}\bar{x} = \int_{\mathbb{R}^2} \bar{\rho}_{\varepsilon_k}(t,\bar{x}) \partial_t \Psi(t,\bar{x}) \mathrm{d}\bar{x} \\ &+ \int_{\mathbb{R}^2} \nabla_{\bar{x}} \Psi(t,\bar{x}) \cdot \left(\int_{\mathbb{R}^2} \frac{{}^\perp E_{\varepsilon_k}}{B} \left(t, \bar{x} - \varepsilon_k \frac{{}^\perp v}{\omega_c} \right) \bar{f}_{\varepsilon_k}(t,\bar{x},v) \mathrm{d}v \right) \mathrm{d}\bar{x}. \end{aligned}$$

Observing the first term in the above expression we get

$$\begin{aligned} \int_{\mathbb{R}^2} \bar{\rho}_{\varepsilon_k}(t,\bar{x}) \partial_t \Psi(t,\bar{x}) \mathrm{d}\bar{x} &= \int_{\mathbb{R}^2} \int_{\mathbb{R}^2} \bar{f}_{\varepsilon_k}(t,\bar{x},v) \partial_t \Psi(t,\bar{x}) \mathrm{d}\bar{x}\mathrm{d}v \\ &= \int_{\mathbb{R}^2} \int_{\mathbb{R}^2} f_{\varepsilon_k} \left(t, \bar{x} - \varepsilon_k \frac{{}^\perp v}{\omega_c}, v \right) \partial_t \Psi(t,\bar{x}) \mathrm{d}\bar{x}\mathrm{d}v \\ &= \int_{\mathbb{R}^2} \int_{\mathbb{R}^2} f_{\varepsilon_k}(t,\bar{x},v) \, \partial_t \Psi(t, \bar{x} + \varepsilon_k \frac{{}^\perp v}{\omega_c}) \mathrm{d}\bar{x}\mathrm{d}v. \end{aligned}$$

Similarly for the second term,

$$\int_{\mathbb{R}^2} \nabla_{\bar{x}}\Psi(t,\bar{x}) \cdot \left(\int_{\mathbb{R}^2} \frac{{}^{\perp}E_{\varepsilon_k}}{B}\left(t, \bar{x} - \varepsilon_k \frac{{}^{\perp}v}{\omega_c}\right) \bar{f}_{\varepsilon_k}(t,\bar{x},v)\mathrm{d}v \right) \mathrm{d}\bar{x}$$
$$= \int_{\mathbb{R}^2}\int_{\mathbb{R}^2} \nabla_{\bar{x}}\Psi(t,\bar{x}+\varepsilon_k\frac{{}^{\perp}v}{\omega_c}) \cdot \frac{{}^{\perp}E_{\varepsilon_k}}{B}(t,\bar{x})\, f_{\varepsilon_k}(t,\bar{x},v)\mathrm{d}v\mathrm{d}\bar{x}.$$

Finally, we obtain

$$\frac{\mathrm{d}}{\mathrm{dt}}\int_{\mathbb{R}^2} \bar{\rho}_{\varepsilon_k}(t,\bar{x})\Psi(t,\bar{x})\mathrm{d}\bar{x} = \int_{\mathbb{R}^2}\int_{\mathbb{R}^2} f_{\varepsilon_k}(t,\bar{x},v)\,\partial_t\Psi(t,\bar{x}+\varepsilon_k\frac{{}^{\perp}v}{\omega_c})\mathrm{d}\bar{x}\mathrm{d}v$$
$$+ \int_{\mathbb{R}^2}\int_{\mathbb{R}^2} \nabla_{\bar{x}}\Psi(t,\bar{x}+\varepsilon_k\frac{{}^{\perp}v}{\omega_c}) \cdot \frac{{}^{\perp}E_{\varepsilon_k}}{B}(t,\bar{x})\, f_{\varepsilon_k}(t,\bar{x},v)\mathrm{d}v\mathrm{d}\bar{x}.$$

The expression on the right of this equality can be rewritten as

$$\int_{\mathbb{R}^2} \rho_{\varepsilon_k}(t,\bar{x})\,\partial_t\Psi(t,\bar{x})\mathrm{d}\bar{x} + \int_{\mathbb{R}^2} \nabla_{\bar{x}}\Psi(t,\bar{x}) \cdot \frac{{}^{\perp}E_{\varepsilon_k}}{B}(t,\bar{x})\,\rho_{\varepsilon_k}(t,\bar{x})\mathrm{d}\bar{x}$$
$$+ \int_{\mathbb{R}^2}\int_{\mathbb{R}^2} f_{\varepsilon_k}(t,\bar{x},v)\left[\partial_t\Psi(t,\bar{x}+\varepsilon_k\frac{{}^{\perp}v}{\omega_c}) - \partial_t\Psi(t,\bar{x})\right]\mathrm{d}\bar{x}\mathrm{d}v$$
$$+ \int_{\mathbb{R}^2}\int_{\mathbb{R}^2} \left[\nabla_{\bar{x}}\Psi(t,\bar{x}+\varepsilon_k\frac{{}^{\perp}v}{\omega_c}) - \nabla_{\bar{x}}\Psi(t,\bar{x})\right] \cdot \frac{{}^{\perp}E_{\varepsilon_k}}{B}(t,\bar{x})\, f_{\varepsilon_k}(t,\bar{x},v)\mathrm{d}v\mathrm{d}\bar{x}.$$

By using Lebesgue's dominated convergence theorem and the fact that we assumed that the uniform boundedness of electric field $E_{\varepsilon_k} \in L^\infty$, as $\varepsilon_k \to 0$, we deduce, for any $\Psi \in C_0^\infty((0,T)\times\mathbb{R}^2)$, that

$$\frac{\mathrm{d}}{\mathrm{dt}}\int_{\mathbb{R}^2} \rho(t,\bar{x})\Psi(t,\bar{x})\mathrm{d}\bar{x} = \int_{\mathbb{R}^2} \rho(t,\bar{x})\,\partial_t\Psi(t,\bar{x})\mathrm{d}\bar{x} + \int_{\mathbb{R}^2} \nabla_{\bar{x}}\Psi(t,\bar{x}) \cdot \frac{{}^{\perp}E}{B}(t,\bar{x})\,\rho(t,\bar{x})\mathrm{d}\bar{x},$$

which yields the equation (54) after integrating w.r.t the variable time t. □

4 Numerical scheme

This Section will be devoted to the construction of a numerical scheme for the splitting scheme (43)-(44) using the semi-Lagrangian method. We will perform the analysis of the first order numerical scheme: we check formally that this numerical scheme provides a consistent discretization.

Let $\Delta t > 0$ be the time step and denote $t_n = n\Delta t$ for $n \geq 0$ as the discretisation of the t-variables. Then denoting $f_{\varepsilon,n}(x,v)$ with the approximation of $f_\varepsilon(t_n,x,v)$, $\rho_{\varepsilon,n}(x)$ with the approximation of $\rho_\varepsilon(t_n,x)$ and $E_{\varepsilon,n}(x)$ with the approximation of $E_\varepsilon(t_n,x)$. We define $(X_{\varepsilon,n},V_{\varepsilon,n}) = (X_\varepsilon,V_\varepsilon)(t_n;t_{n-1},X_{\varepsilon,n-1},V_{\varepsilon,n-1})$.

4.1 The first order numerical scheme

The numerical scheme of the forward trajectory of particles $(X_\varepsilon(t),V_\varepsilon(t))$
Now we give a time discretizations for equations (45)-(46) based on the explicit Euler scheme. The discretization in time of the equation (45) on a time step Δt can thus be written as follows:

$$\begin{cases} \varepsilon X_\varepsilon(t_{n+1/2};t_n,X_{\varepsilon,n},V_{\varepsilon,n}) = \varepsilon X_{\varepsilon,n} + \dfrac{m\varepsilon^2}{qB}\left[\mathcal{R}\left(-\dfrac{qB}{m}\dfrac{\Delta t}{\varepsilon^2}+\pi/2\right) - \mathcal{R}(\pi/2)\right]V_{\varepsilon,n}, \\ V_\varepsilon(t_{n+1/2};t_n,X_{\varepsilon,n},V_{\varepsilon,n}) = \mathcal{R}\left(-\dfrac{qB}{m}\dfrac{\Delta t}{\varepsilon^2}\right)V_{\varepsilon,n}, \end{cases}$$

and we evaluate the distribution function at time t_n at the foot of the characteristics starting (x, v) at time $t_{n+1/2}$ as

$$f_{\varepsilon,\star}(x,v) = f_{\varepsilon,n}(X_\varepsilon(t_n; t_{n+1/2}, x, v), V_\varepsilon(t_n; t_{n+1/2}, x, v)).$$

Then we compute the electric field E_ε at time t_{n+1} by substituting $f_{\varepsilon,\star}$ in the Poisson equation. Hence the discretization in time of the equation (46) on the time step Δt becomes

$$\begin{cases} \varepsilon X_{\varepsilon,n+1} = \varepsilon X_\varepsilon(t_{n+1/2}; t_n, X_{\varepsilon,n}, V_{\varepsilon,n}), \\ \varepsilon V_{\varepsilon,n+1} = \varepsilon V_\varepsilon(t_{n+1/2}; t_n, X_{\varepsilon,n}, V_{\varepsilon,n}) + \dfrac{q}{m}\Delta t E_{\varepsilon,n+1}(X_\varepsilon(t_{n+1/2}; t_n, X_{\varepsilon,n}, V_{\varepsilon,n})). \end{cases}$$

Therefore the numerical solution at the time t_{n+1} for trajectory particles is

$$\begin{cases} X_{\varepsilon,n+1} = X_{\varepsilon,n} + \dfrac{m}{qB}\left[\mathcal{R}\left(-\dfrac{qB}{m}\dfrac{\Delta t}{\varepsilon^2} + \pi/2\right) - \mathcal{R}(\pi/2)\right]\varepsilon V_{\varepsilon,n}, \\ \varepsilon V_{\varepsilon,n+1} = \mathcal{R}\left(-\dfrac{qB}{m}\dfrac{\Delta t}{\varepsilon^2}\right)\varepsilon V_{\varepsilon,n} + \dfrac{q}{m}\Delta t E_{\varepsilon,n+1}(X_{\varepsilon,n+1}). \end{cases} \tag{55}$$

We now study the position of the guiding center by substituting the second equation in the first one of (55)

$$X_{\varepsilon,n+1} = X_{\varepsilon,n} + \frac{m}{qB}\mathcal{R}(\pi/2)\varepsilon\left[V_{\varepsilon,n+1} - V_{\varepsilon,n}\right] + \Delta t\frac{{}^\perp E_{\varepsilon,n+1}(X_{\varepsilon,n+1})}{B}.$$

Using then the formula (42), we can rewrite this equation as

$$Z_{\varepsilon,n+1} - Z_{\varepsilon,n} = \Delta t\frac{{}^\perp E_{\varepsilon,n+1}(X_{\varepsilon,n+1})}{B}.$$

Finally, the system (55) can be re-written for $(Z_{\varepsilon,n}, \varepsilon V_{\varepsilon,n})$ as

$$\begin{aligned} \frac{Z_{\varepsilon,n+1} - Z_{\varepsilon,n}}{\Delta t} &= \frac{{}^\perp E_{\varepsilon,n+1}}{B}\left(Z_{\varepsilon,n+1} - \frac{m}{qB}\varepsilon^\perp V_{\varepsilon,n+1}\right), \\ \varepsilon V_{\varepsilon,n+1} - \mathcal{R}\left(-\frac{qB}{m}\frac{\Delta t}{\varepsilon^2}\right)\varepsilon V_{\varepsilon,n} &= \frac{q}{m}\Delta t E_{\varepsilon,n+1}\left(Z_{\varepsilon,n} - \frac{m}{qB}\mathcal{R}\left(-\frac{qB}{m}\frac{\Delta t}{\varepsilon^2}\right)\varepsilon^\perp V_{\varepsilon,n}\right), \end{aligned} \tag{56}$$

with the initial data $(Z_{\varepsilon,0}, V_{\varepsilon,0}) = \left(X_{\varepsilon,0} + \dfrac{m}{qB}\varepsilon^\perp V_{\varepsilon,0}, V_{\varepsilon,0}\right)$.

Proposition 4.1 ***(formal)*** *Assume that $(E_{\varepsilon,n})_{\varepsilon>0}$ is uniformly bounded in $L^\infty([0,T]\times\mathbb{R}^2)$ and consider a time step $\Delta t > 0$, a final time $T > 0$ and set $N_T = [T/\Delta t]$. Assume that the sequences $(X_{\varepsilon,n}, V_{\varepsilon,n})_{\varepsilon>0}$ and $(Z_{\varepsilon,n})_{\varepsilon>0}$ given by (55) and (56) respectively, for all $1 \le n \le N_T$, and the initial data $(X_{\varepsilon,0}, \varepsilon V_{\varepsilon,0})_{\varepsilon>0}$ is uniformly bounded in $L^\infty(\mathbb{R}^2)^4$ with respect to $\varepsilon > 0$. Then, for $1 \le n \le N_T$, $Z_{\varepsilon,n} \rightharpoonup Z_n$ and $\varepsilon V_{\varepsilon,n} \rightharpoonup V_n$ weak-$\star$ in $L^\infty(\mathbb{R}^2)^2$, as $\varepsilon \to 0$ and the limit $(Z_n, V_n)_{0\le n\le N_T-1}$ satisfies the following equations:*

$$\begin{aligned} \frac{Z_{n+1} - Z_n}{\Delta t} &= \frac{{}^\perp E_{n+1}}{B}\left(Z_{n+1} - \frac{m}{qB}{}^\perp V_{n+1}\right), \\ V_{n+1} &= \Delta t\frac{1}{2\pi}\int_0^{2\pi}\frac{q}{m}E_{n+1}\left(Z_n - \frac{m}{qB}\mathcal{R}\left(-\theta\right)^\perp V_n\right)\mathrm{d}\theta. \end{aligned} \tag{57}$$

Proof. For all $1 \le n \le N_T$, we consider $(Z_{\varepsilon,n}, \varepsilon V_{\varepsilon,n})$ the solution to (56) now labeled w.r.t $\varepsilon > 0$. Since the family of electric field $(E_{\varepsilon,n})_{\varepsilon>0}$ and the initial sequence $(X_{\varepsilon,0}, \varepsilon V_{\varepsilon,0})$ are

uniformly bounded in $L^\infty(\mathbb{R}^2)^4$ w.r.t $\varepsilon > 0$, hence the sequence $(Z_{\varepsilon,n}, \varepsilon V_{\varepsilon,n})$ is too. Therefore, we can extract a subsequence labeled by ε_k and find some (Z_n, V_n) such that

$$Z_{\varepsilon_k,n} \to Z_n, \quad \varepsilon V_{\varepsilon_k,n} \to V_n \ \text{ weak} - \star \text{ in } \ L^\infty(\mathbb{R}^2)^2 \text{ as } \varepsilon_k \to 0.$$

Thanks to the Proposition 3.2 we get the following weak-$\star$ convergence in $L^\infty(\mathbb{R}^2)^2$

$$\mathcal{R}\left(-\frac{m}{qB}\frac{\Delta t}{\varepsilon_k^2}\right)\varepsilon V_{\varepsilon_k,n} \rightharpoonup \frac{1}{2\pi}\int_0^{2\pi}\mathcal{R}(-\theta)\mathrm{d}\theta V_n = 0,$$

and

$$E_{\varepsilon_k,n+1}\left(Z_{\varepsilon_k,n} - \frac{m}{qB}\mathcal{R}\left(-\frac{qB}{m}\frac{\Delta t}{\varepsilon_k^2}\right)\varepsilon_k{}^{\perp}V_{\varepsilon_k,n}\right) \rightharpoonup \frac{1}{2\pi}\int_0^{2\pi} E_{n+1}\left(Z_n - \frac{m}{qB}\mathcal{R}\left(-\theta\right)^{\perp}V_n\right)\mathrm{d}\theta.$$

Substituting these limits in the equations of (56) and passing to the limit as $\varepsilon_k \to 0$, we obtain that the limit (Z_n, V_n) satisfying (57). We are done if we show that the limit point (Z_n, V_n) is uniquely determined. The uniqueness of the limit point V_n can be easily seen by the second equation of (57) and that of the limit point Z_n by observing that the first equation of (55) can be written as

$$Z_{\varepsilon,n+1} = Z_{\varepsilon,n} - \frac{m}{qB}\mathcal{R}\left(-\frac{qB}{m}\frac{\Delta t}{\varepsilon^2}\right)\varepsilon^{\perp}V_{\varepsilon,n} + \frac{m}{qB}\varepsilon^{\perp}V_{\varepsilon,n+1}.$$

□

The full-discretized numerical scheme for the distribution function $f_{\varepsilon,n}(x,v)$
First of all, we assume that the initial distribution $f_0 \in C_c^1(\mathbb{R}^2\times\mathbb{R}^2)$ whose support is included in some $\Omega = [-R,R]^2\times[-v_R,v_R]^2 \subset \mathbb{R}^2\times\mathbb{R}^2$ for $R > 0$, $v_R > 0$ large enough and we introduce the finite uniform mesh points $(x_{i,j}, v_{k,l})$ whose coordinates are denoted by

$$x_{i,j} = (x_i, x_j),\ (i,j) \in 0,1,2,...,N_x - 1 \ \text{ and } \ v_{k,l} = (v_k, v_l),\ (k,l) \in 0,1,2,...,N_v - 1$$

to discretize the phase-space computional domain $(x,v) \in \Omega$ where $\Delta x_1, \Delta x_2$ are the sizes of one cell in x_i, x_j directions and $\Delta v_1, \Delta v_2$ are the sizes of one cell in v_k, v_l directions. Then, we give the value of distribution function f_ε at the mesh points $(x_{i,j}, v_{k,l})$ at any given time t_n. Therefore, the numerical scheme which allow us go to from time t_n to t_{n+1} and compute $f_{\varepsilon,n+1}(x_{i,j}, v_{k,l})$ using the characteristics backward in time can be described as follow:
(A1) Computing the distribution function at time $t_{n+1/2}$ at the foot of the characteristic subflow $\mathcal{E}_\varepsilon^1$ starting $(x_{i,j}, v_{k,l})$ at time t_{n+1} using the Lagrange interpolation operator. This action is given by the operator $\tilde{\mathcal{T}}_1$ as follow:

$$\tilde{\mathcal{T}}_1 f_{\varepsilon,n}(x_{i,j}, v_{k,l}) = \Pi\mathcal{T}_1 f_{\varepsilon,n}(x_{i,j}, v_{k,l}),$$

where Π is the Lagrange interpolation operator with

$$\mathcal{T}_1 f_{\varepsilon,n}(x_{i,j}, v_{k,l}) = f_{\varepsilon,n}(X_\varepsilon(t_{n+1/2}; t_{n+1}, x_{i,j}, v_{k,l}), V_\varepsilon(t_{n+1/2}; t_{n+1}, x_{i,j}, v_{k,l})),$$

and

$$\begin{cases} X_\varepsilon(t_{n+1/2}; t_{n+1}, x_{i,j}, v_{k,l}) = x_{i,j} + \left[\mathcal{R}\left(\dfrac{qB}{m}\dfrac{\Delta t}{\varepsilon^2} + \pi/2\right) - \mathcal{R}(\pi/2)\right]\varepsilon\dfrac{v_{k,l}}{\omega_c}, \\ V_\varepsilon(t_{n+1/2}; t_{n+1}, x_{i,j}, v_{k,l}) = \mathcal{R}\left(\dfrac{qB}{m}\dfrac{\Delta t}{\varepsilon^2}\right)v_{k,l}. \end{cases}$$

The output from above is integrated with respect to velocity to provide an approximation for the density at time t_{n+1},

$$\rho[\tilde{\mathcal{T}}_1 f_{\varepsilon,n}](t_{n+1}, x_{i,j}) = \int_{\mathbb{R}^2} \tilde{\mathcal{T}}_1 f_{\varepsilon,n}(x_{i,j}, v)\mathrm{d}v,$$

which is then substituted into the Poisson equation to compute the approximation of the electric field at time t_{n+1}, that is

$$E_{\varepsilon,n+1}(x_{i,j}) = -\nabla_x \Phi_{\varepsilon,n+1}(x_{i,j}), \quad -\epsilon_0 \Delta_x \Phi_{\varepsilon,n+1}(x_{i,j}) = q \int_{\mathbb{R}^2} \tilde{\mathcal{T}}_1 f_{\varepsilon,n}(x_{i,j}, v)\mathrm{d}v.$$

(A2) The result obtained from **(A1)** is computed the distribution function at time t_n at the foot of the characteristic subflow $\mathcal{E}_\varepsilon^2$ starting $(X_\varepsilon(t_{n+1/2}; t_{n+1}, x_{i,j}, v_{k,l}), V_\varepsilon(t_{n+1/2}; t_{n+1}, x_{i,j}, v_{k,l}))$ at time $t_{n+1/2}$ with the electric field $E_{\varepsilon,n+1}$ using the Lagrange interpolation operator. This action is described by the operator $\tilde{\mathcal{T}}_2$ as follow:

$$\tilde{\mathcal{T}}_2 f_{\varepsilon,n}(x_{i,j}, v_{k,l}) = \Pi \mathcal{T}_2 f_{\varepsilon,n}(x_{i,j}, v_{k,l}),$$

with

$$\mathcal{T}_2 f_{\varepsilon,n}(x_{i,j}, v_{k,l}) = f_{\varepsilon,n}(X_\varepsilon(t_n; t_{n+1/2}, x_{i,j}, v_{k,l}), V_\varepsilon(t_n; t_{n+1/2}, x_{i,j}, v_{k,l})),$$

where

$$\begin{cases} X_\varepsilon(t_n; t_{n+1/2}, x_{i,j}, v_{k,l}) = x_{i,j}, \\ V_\varepsilon(t_n; t_{n+1/2}, x_{i,j}, v_{k,l}) = v_{k,l} - \dfrac{q}{m}\dfrac{\Delta t}{\varepsilon} E_{\varepsilon,n+1}(x_{i,j}). \end{cases}$$

If we use such a method, due to the $\frac{1}{\varepsilon}$-frequency oscillations of the electric field, we have to guarantee the accurate simulation of the scheme using the semi-Lagrangian solvers. Therefore, the time step Δt must satisfy the following condition:

$$\Delta t < \mathcal{O}(\varepsilon |v_R|), \tag{58}$$

where v_R denotes the maximum value in the velocity grid.
Finally, the full-discretized numerical scheme can be written as:

$$f_{\varepsilon,n+1}(x_{i,j}, v_{k,l}) = \tilde{\mathcal{T}}_2 \circ \tilde{\mathcal{T}}_1 f_{\varepsilon,n}(x_{i,j}, v_{k,l}), \tag{59}$$

and then we compute the density $\rho_{\varepsilon,n+1}$ given by

$$\rho_{\varepsilon,n+1}(x_{i,j}) = \Delta v_1 \Delta v_2 \sum_{k,l=0}^{N_v-1} f_{\varepsilon,n+1}(x_{i,j}, v_{k,l}).$$

The asymptotic limit of full discretization for density $(\rho_{\varepsilon,n})_{\varepsilon>0}$
In the Section 3.2, we have been analysed the asymptotic limit of the semi-discretization in time for density particle ρ_ε. Now, we want to study the asymptotic limit property of the full discretized density $\rho_{\varepsilon,n+1}(x_{i,j})$, as $\varepsilon \to 0$. To do this, we rewrite the formula of the distribution function $f_{\varepsilon,n+1}$ in (59) as:

$$\Pi\mathcal{T}_2 \circ \Pi\mathcal{T}_1 f_{\varepsilon,n}(x_{i,j}, v_{k,l}) = \Pi[\mathcal{T}_2 \circ \mathcal{T}_1] f_{\varepsilon,n}(x_{i,j}, v_{k,l}) + \mathcal{O}((\Delta x_1)^p (\Delta x_2)^p) + \mathcal{O}((\Delta v_1)^p (\Delta v_2)^p),$$

where p denotes the degree of the Lagrange interpolation operator. Hence, considering the fine phase space mesh, we can expect that

$$\Pi\mathcal{T}_2 \circ \Pi\mathcal{T}_1 f_{\varepsilon,n}(x_{i,j}, v_{k,l}) \approx \Pi f_{\varepsilon,n}(X_\varepsilon(t_n; t_{n+1}, x_{i,j}, v_{k,l}), V_\varepsilon(t_n; t_{n+1}, x_{i,j}, v_{k,l})),$$

where $[\mathcal{T}_2 \circ \mathcal{T}_1] f_{\varepsilon,n}(x_{i,j}, v_{k,l}) = f_{\varepsilon,n}(X_\varepsilon(t_n; t_{n+1}, x_{i,j}, v_{k,l}), V_\varepsilon(t_n; t_{n+1}, x_{i,j}, v_{k,l}))$ with

$$\begin{cases} X_\varepsilon(t_n; t_{n+1}, x_{i,j}, v_{k,l}) = x_{i,j} + \left[\mathcal{R}\left(\dfrac{qB}{m}\dfrac{\Delta t}{\varepsilon^2} + \pi/2\right) - \mathcal{R}(\pi/2)\right] \varepsilon \dfrac{v_{k,l}}{\omega_c}, \\ V_\varepsilon(t_n; t_{n+1}, x_{i,j}, v_{k,l}) = \mathcal{R}\left(\dfrac{qB}{m}\dfrac{\Delta t}{\varepsilon^2}\right) v_{k,l} - \dfrac{q}{m}\dfrac{\Delta t}{\varepsilon} E_{\varepsilon,n+1}(x_{i,j}). \end{cases}$$

We now give a formal proof that the density $\rho_{\varepsilon,n}$ obtained from $f_{\varepsilon,n}$

$$\rho_{\varepsilon,n+1}(x_{i,j}) \approx \Delta v_1 \Delta v_2 \sum_{k,l=0}^{N_v-1} \Pi f_{\varepsilon,n}(X_\varepsilon(t_n; t_{n+1}, x_{i,j}, v_{k,l}), V_\varepsilon(t_n; t_{n+1}, x_{i,j}, v_{k,l})) \tag{60}$$

is a consistent first order approximation w.r.t Δt of the guiding center model, that is

$$\rho_{\varepsilon,n} \to \rho_n, \quad \text{as } \varepsilon \to 0,$$

and the limit $(\rho_n)_n$ is a first order numerical solution w.r.t Δt of the guiding center equation provided by the semi-Lagrangian method. Before passing to the limit, we need the following Lemma:

Lemma 4.1 *Let us consider a time step $\Delta t > 0$, a final time $T > 0$ and set $N_T = [T/\Delta t]$. Assuming that the initial distribution function $f_0(x, v)$ whose support is included in $\Omega = [-R, R]^2 \times [-v_R, v_R]^2$ and $(f_{\varepsilon,n})_{0 \le n \le N_T - 1}$ is the numerical solution of the Vlasov-Poisson system, computed by the numerical scheme in* (59)*. Then, for $1 \le n \le N_T$, we have*

$$\mathcal{T}_1 f_{\varepsilon,n}(x_{i,j}, v_{k,l}) = \mathcal{T}_1 f_{\varepsilon,n}(x_{i,j} - \varepsilon \frac{{}^\perp v_{k,l}}{\omega_c}, v_{k,l}) + \mathcal{O}(\varepsilon).$$

Consequently, we get

$$\begin{aligned} &\mathcal{T}_2 \circ \mathcal{T}_1 f_{\varepsilon,n}(x_{i,j}, v_{k,l}) = \\ &\quad f_{\varepsilon,n}(x_{i,j} + \mathcal{R}\left(\frac{qB}{m}\frac{\Delta t}{\varepsilon^2} + \pi/2\right) \varepsilon \frac{v_{k,l}}{\omega_c}, \mathcal{R}\left(\frac{qB}{m}\frac{\Delta t}{\varepsilon^2}\right) v_{k,l} - \frac{q}{m}\frac{\Delta t}{\varepsilon} E_{\varepsilon,n+1}(x_{i,j})) + \mathcal{O}(\varepsilon). \end{aligned}$$

Proof. Since

$$\begin{aligned} \mathcal{T}_1 f_{\varepsilon,n}(x_{i,j}, v_{k,l}) &= f_\varepsilon(t_n, X_\varepsilon(t_n; t_{n+1/2}, x_{i,j}, v_{k,l}), V_\varepsilon(t_n; t_{n+1/2}, x_{i,j}, v_{k,l})) \\ &= f_\varepsilon(t_n, x_{i,j} + \left[\mathcal{R}\left(\frac{qB}{m}\frac{\Delta t}{\varepsilon^2} + \pi/2\right) - \mathcal{R}(\pi/2)\right] \varepsilon \frac{v_{k,l}}{\omega_c}, \mathcal{R}\left(\frac{qB}{m}\frac{\Delta t}{\varepsilon^2}\right) v_{k,l}), \end{aligned}$$

we get

$$\begin{aligned} &\mathcal{T}_1 f_{\varepsilon,n}(x_{i,j} - \varepsilon \frac{{}^\perp v_{k,l}}{\omega_c}, v_{k,l}) \\ &= f_\varepsilon(t_n, x_{i,j} - \varepsilon \frac{{}^\perp v_{k,l}}{\omega_c} + \left[\mathcal{R}\left(\frac{qB}{m}\frac{\Delta t}{\varepsilon^2} + \pi/2\right) - \mathcal{R}(\pi/2)\right] \varepsilon \frac{v_{k,l}}{\omega_c}, \mathcal{R}\left(\frac{qB}{m}\frac{\Delta t}{\varepsilon^2}\right) v_{k,l}) \\ &= f_\varepsilon(t_n, x_{i,j} + \mathcal{R}\left(\frac{qB}{m}\frac{\Delta t}{\varepsilon^2} + \pi/2\right) \varepsilon \frac{v_{k,l}}{\omega_c}, \mathcal{R}\left(\frac{qB}{m}\frac{\Delta t}{\varepsilon^2}\right) v_{k,l}). \end{aligned}$$

Hence we deduce by the mean-value theorem that

$$|\mathcal{T}_1 f_{\varepsilon,n}(x_{i,j}, v_{k,l}) - \mathcal{T}_1 f_{\varepsilon,n}(x_{i,j} - \varepsilon \frac{{}^\perp v_{k,l}}{\omega_c}, v_{k,l})| \le \frac{\varepsilon}{\omega_c} \|\nabla f_\varepsilon(t_n)\|_\infty |v_{k,l}| \le C\varepsilon,$$

where $C = C(\omega_c, f_0, v_R)$ and then it implies that

$$\mathcal{T}_1 f_{\varepsilon,n}(x_{i,j}, v_{k,l}) = \mathcal{T}_1 f_{\varepsilon,n}(x_{i,j} - \varepsilon \frac{^\perp v_{k,l}}{\omega_c}, v_{k,l}) + \mathcal{O}(\varepsilon). \tag{61}$$

Finally, we apply the operator $\mathcal{T}_2$ to (61) and we obtain

$$\begin{aligned}
\mathcal{T}_2 \circ \mathcal{T}_1 f_{\varepsilon,n}(x_{i,j}, v_{k,l}) &= \mathcal{T}_2 \circ \left[\mathcal{T}_1 f_{\varepsilon,n}(x_{i,j} - \varepsilon \frac{^\perp v_{k,l}}{\omega_c}, v_{k,l}) \right] + \mathcal{O}(\varepsilon) \\
&= f_{\varepsilon,n}(x_{i,j} + \mathcal{R}\left(\frac{qB}{m}\frac{\Delta t}{\varepsilon^2} + \pi/2\right)\frac{v_{k,l}}{\omega_c}, \mathcal{R}\left(\frac{qB}{m}\frac{\Delta t}{\varepsilon^2}\right) v_{k,l} - \frac{q}{m}\frac{\Delta t}{\varepsilon} E_{\varepsilon,n+1}(x_{i,j})) + \mathcal{O}(\varepsilon),
\end{aligned}$$

since the operator $\mathcal{T}_2$ is linear. □

Thanks to the Lemma 3.1 we have that

$$\begin{aligned}
&\Delta v_1 \Delta v_2 \sum_{k,l=0}^{N_v-1} \Pi \mathcal{T}_2 \circ \mathcal{T}_1 f_{\varepsilon,n}(x_{i,j}, v_{k,l}) \\
&= \Delta v_1 \Delta v_2 \sum_{k,l=0}^{N_v-1} \Pi f_{\varepsilon,n}(x_{i,j} - \varepsilon \mathcal{R}\left(\frac{qB}{m}\frac{\Delta t}{\varepsilon^2}\right)\frac{^\perp v_{k,l}}{\omega_c}, \mathcal{R}\left(\frac{qB}{m}\frac{\Delta t}{\varepsilon^2}\right) v_{k,l} - \frac{q}{m}\frac{\Delta t}{\varepsilon} E_{\varepsilon,n+1}(x_{i,j})) + \mathcal{O}(\varepsilon) \\
&= \Delta v_1 \Delta v_2 \sum_{k,l=0}^{N_v-1} \Pi f_{\varepsilon,n}(x_{i,j} - \varepsilon \frac{^\perp v_{k,l}}{\omega_c}, v_{k,l} - \frac{q}{m}\frac{\Delta t}{\varepsilon} E_{\varepsilon,n+1}(x_{i,j})) + \mathcal{O}(\Delta v_1 \Delta v_2) + \mathcal{O}(\varepsilon),
\end{aligned}$$

where we used the change of variable $v_{k,l} \mapsto \mathcal{R}(-\frac{qB}{m}\frac{\Delta t}{\varepsilon^2}) v_{k,l}$ to filter the fast rotation in velocity. The error $\mathcal{O}(\Delta v_1 \Delta v_2)$ comes from the fact that the discrete integral over the velocity variable is not conserved by a rotation. Performing then the translation $v_{k,l} \mapsto v_{k,l} + \frac{q}{m}\frac{\Delta t}{\varepsilon} E_{\varepsilon,n+1}(x_{i,j})$ to remove the stiff term, with the condition (58) to ensure that this change of variable is well defined in the velocity grid. If we consider a fine mesh in the direction of velocity, we can expect that the density $\rho_{\varepsilon,n+1}$ in (60) can be approximated by

$$\begin{aligned}
\rho_{\varepsilon,n+1} &\approx \Delta v_1 \Delta v_2 \sum_{k,l=0}^{N_v-1} \Pi [\mathcal{T}_2 \circ \mathcal{T}_1] f_{\varepsilon,n}(x_{i,j}, v_{k,l}) \\
&\approx \Delta v_1 \Delta v_2 \sum_{k,l=0}^{N_v-1} \Pi f_{\varepsilon,n}(x_{i,j} - \frac{\Delta t}{B}{}^\perp E_{\varepsilon,n+1}(x_{i,j}) - \varepsilon \frac{^\perp v_{k,l}}{\omega_c}, v_{k,l}) + \mathcal{O}(\varepsilon).
\end{aligned} \tag{62}$$

Formally passing to the limit as $\varepsilon \to 0$ in (62), we obtain that

$$\begin{aligned}
\rho_{n+1}(x_{i,j}) &\approx \Delta v_1 \Delta v_2 \sum_{k,l=0}^{N_v-1} \Pi f_n(x_{i,j} - \frac{\Delta t}{B}{}^\perp E_{n+1}(x_{i,j}), v_{k,l}) \\
&= \sum_{k,l=0}^{N_v-1} \Pi \rho_n(x_{i,j} - \frac{\Delta t}{B}{}^\perp E_{n+1}(x_{i,j})),
\end{aligned}$$

which is a consistent first order approximation with respect to Δt of the guiding center model provided by the semi-Lagrangian method.

4.2 The first order adjoint scheme

Now we consider the first order which is an adjoint of Lie method in Section 4.1

$$\mathcal{E}_\varepsilon^1(t): \begin{cases} \varepsilon \dot{X}_\varepsilon(t) = 0, & \\ & \text{over } \Delta t > 0 \\ \varepsilon \dot{V}_\varepsilon(t) = \dfrac{q}{m} E_\varepsilon(t, X_\varepsilon(t)), & \end{cases}$$

$$\mathcal{E}_\varepsilon^2(t): \begin{cases} \varepsilon \dot{X}_\varepsilon(t) = V_\varepsilon(t), & \\ & \text{over } \Delta t > 0 \\ \varepsilon \dot{V}_\varepsilon(t) = \dfrac{qB}{m} \dfrac{{}^\perp V_\varepsilon(t)}{\varepsilon}. & \end{cases}$$

We give a time discretization for these equations based on explicit Euler scheme. The discretization in time of the equation $\mathcal{E}_\varepsilon^1(t)$ on a time step Δt can thus be written as follows:

$$\begin{cases} \varepsilon X_{\varepsilon,\star} = \varepsilon X_{\varepsilon,n}, \\ \varepsilon V_{\varepsilon,\star} = \varepsilon V_{\varepsilon,n} + \dfrac{q}{m} \Delta t E_{\varepsilon,n}(X_{\varepsilon,n}), \end{cases}$$

and the equation $\mathcal{E}_\varepsilon^2(t)$ with the initial condition $(X_{\varepsilon,n}, V_{\varepsilon,n})$ given by

$$\begin{cases} X_{\varepsilon,n+1} = X_{\varepsilon,\star} + \dfrac{m}{qB} \left[\mathcal{R}\left(-\dfrac{qB}{m\varepsilon^2} \Delta t + \pi/2 \right) - \mathcal{R}(\pi/2) \right] \varepsilon V_\varepsilon(t_{n+1/2}; t_n, X_{\varepsilon,n}, V_{\varepsilon,n}), \\ V_{\varepsilon,n+1} = \mathcal{R}\left(-\dfrac{qB}{m\varepsilon^2} \Delta t \right) V_{\varepsilon,\star}. \end{cases}$$

Therefore, the numerical solution at time t_{n+1} for the trajectory particles reads:

$$\begin{cases} X_{\varepsilon,n+1} = X_{\varepsilon,n} + \dfrac{m}{qB} \left[\mathcal{R}\left(-\dfrac{qB}{m\varepsilon^2} \Delta t + \pi/2 \right) - \mathcal{R}(\pi/2) \right] \left(\varepsilon V_{\varepsilon,n} + \dfrac{q}{m} \Delta t E_{\varepsilon,n}(X_{\varepsilon,n}) \right), \\ \varepsilon V_{\varepsilon,n+1} = \mathcal{R}\left(-\dfrac{qB}{m\varepsilon^2} \Delta t \right) \left(\varepsilon V_{\varepsilon,n} + \dfrac{q}{m} \Delta t E_{\varepsilon,n}(X_{\varepsilon,n}) \right). \end{cases} \tag{63}$$

We then evaluate the distribution function at time t_n at the foot of the characteristic curves starting (x, v) at time t_{n+1}

$$f_{\varepsilon,n+1}(x, v) = f_{\varepsilon,n}(X_\varepsilon(t_n; t_{n+1}, x, v), V_\varepsilon(t_n; t_{n+1}, x, v)),$$

which is substituted into the Poisson equation to compute the approximation of the electric field at time t_{n+1}.
In order to study the guiding center position, we substitute the second equation into the first one of (63) to get

$$X_{\varepsilon,n+1} = X_{\varepsilon,n} + \frac{m}{qB} \mathcal{R}(\pi/2) \varepsilon [V_{\varepsilon,n+1} - V_{\varepsilon,n}] + \Delta t \frac{{}^\perp E_{\varepsilon,n}(X_{\varepsilon,n})}{B}.$$

Using then the formula (42), we can write this equation for $Z_{\varepsilon,n}$ as

$$\frac{Z_{\varepsilon,n+1} - Z_{\varepsilon,n}}{\Delta t} = \frac{{}^\perp E_{\varepsilon,n}(X_{\varepsilon,n})}{B}.$$

Finally, the equation (63) can be rewritten for $(Z_{\varepsilon,n}, V_{\varepsilon,n})$ as

$$\begin{aligned} \frac{Z_{\varepsilon,n+1} - Z_{\varepsilon,n}}{\Delta t} &= \frac{{}^\perp E_{\varepsilon,n}}{B} (Z_{\varepsilon,n} - \frac{m}{qB} \varepsilon^\perp V_{\varepsilon,n}), \\ \mathcal{R}\left(\frac{qB}{m\varepsilon^2} \Delta t \right) \varepsilon V_{\varepsilon,n+1} &= \varepsilon V_{\varepsilon,n} + \frac{q}{m} \Delta t E_{\varepsilon,n}(Z_{\varepsilon,n} - \frac{m}{qB} \varepsilon^\perp V_{\varepsilon,n}). \end{aligned} \tag{64}$$

Proposition 4.2 *Assume that $(E_{\varepsilon,n})_{\varepsilon>0}$ is uniformly bounded in $L^\infty(\mathbb{R}^2)^2$ and consider a time step $\Delta t > 0$, a final time $T > 0$ and set $N_T = [T/\Delta t]$. Assume that the sequences $(X_{\varepsilon,n}, V_{\varepsilon,n})_{0\le n\le N_T}$ and $(Z_{\varepsilon,n})_{\varepsilon>0}$ given by (63) and (64) respectively, for all $1 \le n \le N_T$, and the initial data $(X_{\varepsilon,0}, \varepsilon V_{\varepsilon,0})_{\varepsilon>0}$ is uniformly bounded in $L^\infty(\mathbb{R}^2)^2$ with respect to $\varepsilon > 0$. Then, for $1 \le n \le N_T$, $Z_{\varepsilon,n} \rightharpoonup Z_n$ and $\varepsilon V_{\varepsilon,n} \rightharpoonup V_n$ weak-$\star$ in $L^\infty(\mathbb{R}^2)^2$, as $\varepsilon \to 0$ and the limit $(Z_n, V_n)_{0\le n\le N_T-1}$ satisfies the following equations:*

$$\frac{Z_{n+1} - Z_n}{\Delta t} = \frac{{}^\perp E_n}{B}\left(Z_n - \frac{m}{qB}{}^\perp V_n\right),$$
$$V_n = -\frac{q}{m}\Delta t E_n(Z_n - \frac{m}{qB}{}^\perp V_n). \tag{65}$$

The full discretized numerical scheme for the distribution function $f_{\varepsilon,n}(x,v)$
(A1) Computing the distribution function at time $t_{n+1/2}$ at the foot of the characteristic subflow $\mathcal{E}^1_\varepsilon$ starting $(x_{i,j}, v_{k,l})$ at time t_{n+1} using the Lagrange interpolation operator. This action is described by:

$$\tilde{\mathcal{T}}_1 f_{\varepsilon,n}(x_{i,j}, v_{k,l}) = \Pi \mathcal{T}_1 f_{\varepsilon,n}(x_{i,j}, v_{k,l}),$$

where

$$\mathcal{T}_1 f_{\varepsilon,n}(x_{i,j}, v_{k,l}) = f_{\varepsilon,n}(X_\varepsilon(t_{n+1/2}; t_{n+1}, x_{i,j}, v_{k,l}), V_\varepsilon(t_{n+1/2}; t_{n+1}, x_{i,j}, v_{k,l})),$$

with

$$X_\varepsilon(t_{n+1/2}; t_{n+1}, x_{i,j}, v_{k,l}) = x_{i,j},$$
$$V_\varepsilon(t_{n+1/2}; t_{n+1}, x_{i,j}, v_{k,l}) = v_{k,l} - \frac{q}{m}\frac{\Delta t}{\varepsilon}E_{\varepsilon,n}(x_{i,j}).$$

(A2) The result obtained from **(A1)** is evaluated at time t_n at the foot of the characteristic subflow $\mathcal{E}^2_\varepsilon$ starting $(X_\varepsilon(t_{n+1/2}; t_{n+1}, x_{i,j}, v_{k,l}), V_\varepsilon(t_{n+1/2}; t_{n+1}, x_{i,j}, v_{k,l}))$ at time $t_{n+1/2}$ using the Lagrange interpolation operator. This action is given by:

$$\tilde{\mathcal{T}}_2 f_{\varepsilon,n}(x_{i,j}, v_{k,l}) = \Pi \mathcal{T}_2 f_{\varepsilon,n}(x_{i,j}, v_{k,l}),$$

with

$$\mathcal{T}_2 f_{\varepsilon,n}(x_{i,j}, v_{k,l}) = f_{\varepsilon,n}(X_\varepsilon(t_n; t_{n+1/2}, x_{i,j}, v_{k,l}), V_\varepsilon(t_n; t_{n+1/2}, x_{i,j}, v_{k,l})),$$

where

$$X_\varepsilon(t_n; t_{n+1/2}, x_{i,j}, v_{k,l}) = x_{i,j} + \frac{m}{qB}\left[\mathcal{R}\left(\frac{qB}{m}\frac{\Delta t}{\varepsilon^2} + \pi/2\right) - \mathcal{R}(\pi/2)\right]\varepsilon v_{k,l},$$
$$V_\varepsilon(t_n; t_{n+1/2}, x_{i,j}, v_{k,l}) = \mathcal{R}\left(\frac{qB}{m}\frac{\Delta t}{\varepsilon^2}\right)\varepsilon v_{k,l}.$$

Finally, the numerical scheme can be written as:

$$f_{\varepsilon,n+1}(x_{i,j}, v_{k,l}) = \tilde{\mathcal{T}}_2 \circ \tilde{\mathcal{T}}_1 f_{\varepsilon,n}(x_{i,j}, v_{k,l}).$$

Then we compute the density $\rho_{\varepsilon,n+1}$

$$\rho_{\varepsilon,n+1}(x_{i,j}) = \Delta v_1 \Delta v_2 \sum_{k,l=0}^{N_v-1} f_{\varepsilon,n+1}(x_{i,j}, v_{k,l}),$$

and then solve the Poisson equation at time t_{n+1} to get $E_{\varepsilon,n+1}$.
The asymptotic limit of full discretization for the density $(\rho_{\varepsilon,n})_{\varepsilon>0}$

In the same way as the proof in the subsection 4.1, we can conclude that the limit of particle density $\rho_{\varepsilon,n+1}(x_{i,j})$ approximates $\rho_{n+1}(x_{i,j})$ when ε goes to zero which satisfies the following equation

$$\rho_{n+1}(x_{i,j}) \approx \Pi\rho_n(x_{i,j} - \frac{\Delta t}{B}{}^{\perp}E_n(x_{i,j})),$$

which is a consistent first order approximation with respect to Δt of the guiding center model.

4.3 The second order scheme

We will now consider the second order scheme (39) which is the composition of Lie method (55) and its adjoint (63) over the time step $\Delta t/2$. Therefore, the first stage corresponds to

$$\mathcal{E}_\varepsilon^1 : \begin{cases} X_{\varepsilon,n+1/2} = X_{\varepsilon,n} + \dfrac{m}{qB}\left[\mathcal{R}\left(-\dfrac{qB}{m\varepsilon^2}\dfrac{\Delta t}{2} + \pi/2\right) - \mathcal{R}(\pi/2)\right]\varepsilon V_{\varepsilon,n}, \\ \varepsilon V_{\varepsilon,n+1/2} = \mathcal{R}\left(-\dfrac{qB}{m\varepsilon^2}\dfrac{\Delta t}{2}\right)\varepsilon V_{\varepsilon,n} + \dfrac{q}{m}\dfrac{\Delta t}{2}E_{\varepsilon,n+1/2}(X_{\varepsilon,n+1/2}), \end{cases}$$

where the electric field E_ε at time $t_{n+1/2}$ is computed thanks to the resolution of the Poisson equation with the distribution function

$$f_{\varepsilon,\star}(x,v) = f_{\varepsilon,n}(X_{\varepsilon,\star}, V_{\varepsilon,\star}),$$

where the characteristic curves $(X_{\varepsilon,\star}, V_{\varepsilon,\star})$ are given by

$$\begin{aligned} X_{\varepsilon,\star} &= x + \frac{m}{qB}\left[\mathcal{R}\left(\frac{qB}{m}\frac{\Delta t}{2\varepsilon^2} + \pi/2\right) - \mathcal{R}(\pi/2)\right]\varepsilon v, \\ V_{\varepsilon,\star} &= \mathcal{R}\left(\frac{qB}{m}\frac{\Delta t}{2\varepsilon^2}\right)v. \end{aligned}$$

Then, the second stage is given by

$$\mathcal{E}_\varepsilon^2 : \begin{cases} X_{\varepsilon,n+1} = X_{\varepsilon,n+1/2} \\ \qquad + \dfrac{m}{qB}\left[\mathcal{R}\left(-\dfrac{qB}{m}\dfrac{\Delta t}{2\varepsilon^2} + \pi/2\right) - \mathcal{R}(\pi/2)\right]\left(\varepsilon V_{\varepsilon,n+1/2} + \dfrac{q}{m}\dfrac{\Delta t}{2}E_{\varepsilon,n+1/2}(X_{\varepsilon,n+1/2})\right) \\ \varepsilon V_{\varepsilon,n+1} = \mathcal{R}\left(-\dfrac{qB}{m}\dfrac{\Delta t}{2\varepsilon^2}\right)\left(\varepsilon V_{\varepsilon,n+1/2} + \dfrac{q}{m}\dfrac{\Delta t}{2}E_{\varepsilon,n+1/2}(X_{\varepsilon,n+1/2})\right). \end{cases}$$

Finally, the numerical solution of trajectory particles at the time step t_{n+1} is given by

$$\begin{cases} \varepsilon V_{\varepsilon,n+1} = \mathcal{R}\left(-\dfrac{qB}{m}\dfrac{\Delta t}{\varepsilon^2}\right)\varepsilon V_{\varepsilon,n} + \dfrac{q}{m}\Delta t\mathcal{R}\left(-\dfrac{qB}{m}\dfrac{\Delta t}{2\varepsilon^2}\right)E_{\varepsilon,n+1/2}(X_{\varepsilon,n+1/2}), \\ X_{\varepsilon,n+1} = X_{\varepsilon,n} + \dfrac{m}{qB}\left[\mathcal{R}\left(-\dfrac{qB}{m}\dfrac{\Delta t}{\varepsilon^2} + \pi/2\right) - \mathcal{R}(\pi/2)\right]\varepsilon V_{\varepsilon,n} \\ \qquad + \Delta t\left[\mathcal{R}\left(-\dfrac{qB}{m}\dfrac{\Delta t}{2\varepsilon^2} + \pi/2\right) - \mathcal{R}(\pi/2)\right]\dfrac{E_{\varepsilon,n+1/2}}{B}(X_{\varepsilon,n+1/2}). \end{cases} \tag{66}$$

In order to study the guiding center position, we substitute the first equation in the second one of (66) to obtain

$$X_{\varepsilon,n+1} = X_{\varepsilon,n} + \frac{m}{qB}\mathcal{R}(\pi/2)\varepsilon[V_{\varepsilon,n+1} - V_{\varepsilon,n}] + \Delta t\frac{{}^{\perp}E_{\varepsilon,n+1/2}}{B}(X_{\varepsilon,n+1/2}).$$

Using then the formula (42), this equation can be written for $Z_{\varepsilon,n}$ as

$$\frac{Z_{\varepsilon,n+1}-Z_{\varepsilon,n}}{\Delta t}=\frac{{}^{\perp}E_{\varepsilon,n+1/2}}{B}(X_{\varepsilon,n+1/2}), \tag{67}$$

Finally the equation (66) can be re-written for $(Z_{\varepsilon,n},\varepsilon V_{\varepsilon,n})$ as

$$\begin{aligned}\frac{Z_{\varepsilon,n+1}-Z_{\varepsilon,n}}{\Delta t}&=\frac{{}^{\perp}E_{\varepsilon,n+1/2}}{B}(\bar{X}_{\varepsilon,n}-\mathcal{R}\left(-\frac{qB}{m\varepsilon^2}\frac{\Delta t}{2}\right)\frac{m}{qB}\varepsilon^{\perp}V_{\varepsilon,n}),\\ \varepsilon V_{\varepsilon,n+1}&=\mathcal{R}\left(-\frac{qB}{m\varepsilon^2}\Delta t\right)\varepsilon V_{\varepsilon,n}\\ &\quad+\frac{q}{m}\Delta t\mathcal{R}\left(-\frac{qB}{m\varepsilon^2}\frac{\Delta t}{2}\right)E_{\varepsilon,n+1/2}(Z_{\varepsilon,n}-\mathcal{R}\left(-\frac{qB}{m\varepsilon^2}\frac{\Delta t}{2}\right)\frac{m}{qB}\varepsilon^{\perp}V_{\varepsilon,n}).\end{aligned}$$

Passing formally to the limit as $\varepsilon\to 0$, we get

$$\begin{aligned}\frac{Z_{n+1}-Z_n}{\Delta t}&=\frac{1}{2\pi}\int_0^{2\pi}\frac{{}^{\perp}E_{n+1/2}}{B}(Z_n-\mathcal{R}(-\theta)\frac{m}{qB}{}^{\perp}V_n)\mathrm{d}\theta,\\ V_{n+1}&=\frac{q}{m}\Delta t\int_0^{2\pi}\mathcal{R}(-\theta)E_{n+1/2}(Z_n-\mathcal{R}(-\theta)\frac{m}{qB}{}^{\perp}V_n)\mathrm{d}\theta.\end{aligned}$$

The full discretized numerical scheme for the distribution function $f_{\varepsilon,n}$
(A1) Computing the distribution function at time $t_{n,\star\star}$ intermediate between $t_{n+1/2}$ and t_{n+1} at the foot of the characteristic subflow $\mathcal{E}_\varepsilon^1$ starting $(x_{i,j},v_{k,l})$ at time t_{n+1} using the Lagrange interpolation operator. This action is described by:

$$\tilde{\mathcal{T}}_1 f_{\varepsilon,n}(x_{i,j},v_{k,l})=\Pi\mathcal{T}_1 f_{\varepsilon,n}(x_{i,j},v_{k,l})$$

where

$$\mathcal{T}_1 f_{\varepsilon,n}(x_{i,j},v_{k,l})=f_{\varepsilon,n}(X_\varepsilon(t_{n,\star\star};t_{n+1},x_{i,j},v_{k,l}),V_\varepsilon(t_{n,\star\star};t_{n+1},x_{i,j},v_{k,l}))$$

with

$$\begin{cases}X_\varepsilon(t_{n,\star\star};t_{n+1},x_{i,j},v_{k,l})=x_{i,j}+\dfrac{m}{qB}\left[\mathcal{R}\left(\dfrac{qB}{m}\dfrac{\Delta t}{2\varepsilon^2}+\pi/2\right)-\mathcal{R}(\pi/2)\right]\varepsilon v_{k,l}\\ V_\varepsilon(t_{n,\star\star};t_{n+1},x_{i,j},v_{k,l})=\mathcal{R}\left(\dfrac{qB}{m}\dfrac{\Delta t}{2\varepsilon^2}\right)v_{k,l}.\end{cases}$$

The output from above is integrated with respect to velocity to obtain an approximation for the density at time $t_{n+1/2}$, which is then substituted into the Poisson equation to compute the approximation of the electric field at time $t_{n+1/2}$, that is

$$E(t_{n+1/2},x_{i,j})=-\nabla_x\Phi(t_{n+1/2},x_{i,j}),\quad -\epsilon_0\Delta_x\Phi(t_{n+1/2},x_{i,j})=q\int_{\mathbb{R}^2}\tilde{\mathcal{T}}_1 f_{\varepsilon,n}(x_{i,j},v)\mathrm{d}v.$$

(A2) The result obtained from **(A1)** is computed at time $t_{n+1/2}$ at the foot of the characteristic subflow $\mathcal{E}_\varepsilon^2$ starting $(x_{i,j},v_{k,l})$ at time $t_{n,\star\star}$ with the electric field $E(t_{n+1/2})$ using the Lagrange interpolation operator. This action is described by:

$$\tilde{\mathcal{T}}_2 f_{\varepsilon,n}(x_{i,j},v_{k,l})=\Pi\mathcal{T}_2 f_{\varepsilon,n}(x_{i,j},v_{k,l}),$$

where

$$\mathcal{T}_2 f_{\varepsilon,n}(x_{i,j},v_{k,l})=f_{\varepsilon,n}(X_\varepsilon(t_{n+1/2};t_{n,\star\star},x_{i,j},v_{k,l}),V_\varepsilon(t_{n+1/2};t_{n,\star\star},x_{i,j},v_{k,l})),$$

with

$$X_\varepsilon(t_{n,\star};t_{n+1/2},x_{i,j},v_{k,l}) = x_{i,j},$$
$$V_\varepsilon(t_{n,\star};t_{n+1/2},x_{i,j},v_{k,l}) = v_{k,l} - \frac{q}{m}\frac{\Delta t}{2\varepsilon}E_{\varepsilon,n+1/2}(x_{i,j}).$$

(A3) The result obtained from **(A2)** is evaluated at time $t_{n,\star}$ intermediate between t_n and $t_{n+1/2}$ at the foot of the characteristic subfow $\mathcal{E}_\varepsilon^2$ starting $(x_{i,j},v_{k,l})$ at time $t_{n+1/2}$ with the electric field $E_{n+1/2}$ using the Lagrange interpolation operator. This action is described by:

$$\tilde{\mathcal{T}}_2 f_{\varepsilon_n}(x_{i,j},v_{k,l}) = \Pi\mathcal{T}_2 f_{\varepsilon,n}(x_{i,j},v_{k,l}),$$

where

$$\mathcal{T}_2 f_{\varepsilon,n}(x_{i,j},v_{k,l}) = f_{\varepsilon,n}(X_\varepsilon(t_{n,\star};t_{n+1/2},x_{i,j},v_{k,l}),V_\varepsilon(t_{n,\star};t_{n+1/2},x_{i,j},v_{k,l})$$

with

$$X_\varepsilon(t_{n,\star};t_{n+1/2},x_{i,j},v_{k,l}) = x_{i,j},$$
$$V_\varepsilon(t_{n,\star};t_{n+1/2},x_{i,j},v_{k,l}) = v_{k,l} - \frac{q}{m}\frac{\Delta t}{2\varepsilon}E_{\varepsilon,n+1/2}(x_{i,j}).$$

(A4) The result obtained from **(A3)** is computed at time t_n at the foot of the characteristic subflow $\mathcal{E}_\varepsilon^1$ starting $(x_{i,j},v_{k,l})$ at time $t_{n,\star}$ using the Lagrange interpolation operator. This action is described by

$$\tilde{\mathcal{T}}_1 f_{\varepsilon,n}(x_{i,j},v_{k,l}) = \Pi\mathcal{T}_1 f_{\varepsilon,n}(x_{i,j},v_{k,l}),$$

where

$$\mathcal{T}_1 f_{\varepsilon,n}(x_{i,j},v_{k,l}) = f_{\varepsilon,n}(X_\varepsilon(t_n;t_{n,\star},x_{i,j},v_{k,l}),X_\varepsilon(t_n;t_{n,\star},x_{i,j},v_{k,l})),$$

with

$$\begin{cases} X_\varepsilon(t_n;t_{n,\star},x_{i,j},v_{k,l}) = x_{i,j} + \dfrac{m}{qB}\left[\mathcal{R}\left(\dfrac{qB}{m\varepsilon^2}\dfrac{\Delta t}{2}+\pi/2\right)-\mathcal{R}(\pi/2)\right]\varepsilon v_{k,l}, \\ V_\varepsilon(t_n;t_{n,\star},x_{i,j},v_{k,l}) = \mathcal{R}\left(\dfrac{qB}{m\varepsilon^2}\dfrac{\Delta t}{2}\right)v_{k,l}. \end{cases}$$

Finally, the second order numerical scheme is given by

$$f_{\varepsilon,n+1}(x_{i,j},v_{k,l}) = \tilde{\mathcal{T}}_1\circ\tilde{\mathcal{T}}_2\circ\tilde{\mathcal{T}}_2\circ\tilde{\mathcal{T}}_1 f_{\varepsilon,n}(x_{i,j},v_{k,l}),$$

then we compute the density $\rho_{\varepsilon,n+1}$

$$\rho_{\varepsilon,n+1} = \Delta v_1\Delta v_2\sum_{k,l=0}^{N_v-1} f_{\varepsilon,n+1}(x_{i,j},v_{l,k}).$$

The asymptotic limit of full discretization for the density $(\rho_{\varepsilon,n})_{\varepsilon>0}$
In the same way as the proof in the subsection 4.1, we can conclude that the limit of density $\rho_{\varepsilon,n+1}(x_{i,j})$ approximates $\rho_{n+1}(x_{i,j})$ when ε goes to zero which satisfies the following equation

$$\rho_{n+1}(x_{i,j}) \approx \Pi\rho_n(x_{i,j} - \frac{\Delta t}{B}^\perp E_{n+1/2}(x_{i,j}))$$

which is a consistent second order approximation with respect to Δt of the guiding center model provided by the semi-Lagrangian method.

5 The Algorithm

In this Section, we review the main steps of the splitting methods which are presented in the Subsections 2.1 and 2.2 in the case of directional splitting with constant advection.
Initialization: $f_0(x,v)$ is given. We then can compute $\rho(0,x) = q\int_{\mathbb{R}^2} f_0(x,v)dv$ and compute the electric field E by solving the Poisson equation. Update from t_n to $t_{n+1} = t_n + \Delta t$ with f^n is known at all grid points (x,v) and E^n is known at x.

Algorithm for Strang-Boris method

1. Perform along the v_1-axis $f^{[1]}(x,v) = f^n(x, v_1 - \tan(\frac{qB}{m}\Delta t/4), v_2)$
2. Perform along the v_2-axis $f^{[2]}(x,v) = f^{[1]}(x, v_1, \sin(\frac{qB}{m}\Delta t/2)v_1 + v_2)$
3. Perform along the v_1-axis $f^{[3]}(x,v) = f^{[2]}(x, v_1 - \tan(\frac{qB}{m}\Delta t/4), v_2)$
4. Perform along the x_1-axis $f^{[4]}(x,v) = f^{[3]}(x_1 - \Delta t/2v_1, x_2, v)$
5. Perform along the x_2-axis $f^{[5]}(x,v) = f^{[4]}(x_1, x_2 - \Delta t/2v_2, v)$
6. Computation the charge density and the electric field at time t_{n+1} by substituting $f^{[5]}$ in the Poisson equation
7. Perform along the v-axis $f^{[6]} = f^{[5]}(x, v - E(t_{n+1}, x)\Delta t)$
8. Perform along the v_1-axis $f^{[7]}(x,v) = f^{[6]}(x, v_1 - \tan(\frac{qB}{m}\Delta t/4), v_2)$
9. Perform along the v_2-axis $f^{[8]}(x,v) = f^{[7]}(x, v_1, \sin(\frac{qB}{m}\Delta t/2)v_1 + v_2)$
10. Perform along the v_1-axis $f^{[9]}(x,v) = f^{[8]}(x, v_1 - \tan(\frac{qB}{m}\Delta t/4), v_2)$
11. Perform along the x_1-axis $f^{[10]}(x,v) = f^{[9]}(x_1 - \Delta t/2v_1, x_2, v)$
12. Perform along the x_2-axis $f^{n+1}(x,v) = f^{[10]}(x_1, x_2 - \Delta t/2v_2, v)$

Algorithm for Strang-Scovel method

1. Perform along the v_1-axis $f^{[1]}(x,v) = f^n(x, v_1 - \tan(\frac{qB}{m}\Delta t/4), v_2)$
2. Perform along the v_2-axis $f^{[2]}(x,v) = f^{[1]}(x, v_1, \sin(\frac{qB}{m}\Delta t/2)v_1 + v_2)$
3. Perform along the v_1-axis $f^{[3]}(x,v) = f^{[2]}(x, v_1 - \tan(\frac{qB}{m}\Delta t/4), v_2)$
4. Perform along the x_1-axis $f^{[4]}(x,v) = f^{[3]}(x_1 - \frac{m}{qB}\sin(\frac{qB}{m}\Delta t/2)v_1, x_2, v)$
5. Perform along the x_1-axis $f^{[5]}(x,v) = f^{[4]}(x_1 + \frac{m}{qB}(1 - \cos(\frac{qB}{m}\Delta t/2))v_1, x_2, v)$
6. Perform along the x_2-axis $f^{[6]}(x,v) = f^{[5]}(x_1, x_2 + \frac{m}{qB}(\cos(\frac{qB}{m}\Delta t/2) - 1)v_1, v)$
7. Perform along the x_2-axis $f^{[7]}(x,v) = f^{[6]}(x_1, x_2 - \frac{m}{qB}\sin(\frac{qB}{m}\Delta t/2)v_2, v)$
8. Computation the charge density and the electric field at time t_{n+1} by substituting $f^{[7]}$ in the Poisson equation
9. Perform along the v-axis $f^{[8]} = f^{[7]}(x, v - E(t_{n+1}, x)\Delta t)$
10. Perform along the v_1-axis $f^{[9]}(x,v) = f^{[8]}(x, v_1 - \tan(\frac{qB}{m}\Delta t/4), v_2)$

11. Perform along the v_2-axis $f^{[10]}(x,v) = f^{[9]}(x, v_1, \sin(\frac{qB}{m}\Delta t/2)v_1 + v_2)$
12. Perform along the v_1-axis $f^{[11]}(x,v) = f^{[10]}(x, v_1 - \tan(\frac{qB}{m}\Delta t/4), v_2)$
13. Perform along the x_1-axis $f^{[12]}(x,v) = f^{[11]}(x_1 - \frac{m}{qB}\sin(\frac{qB}{m}\Delta t/2)v_1, x_2, v)$
14. Perform along the x_1-axis $f^{[13]}(x,v) = f^{[12]}(x_1 + \frac{m}{qB}(1 - \cos(\frac{qB}{m}\Delta t/2))v_1, x_2, v)$
15. Perform along the x_2-axis $f^{[14]}(x,v) = f^{[13]}(x_1, x_2 + \frac{m}{qB}(\cos(\frac{qB}{m}\Delta t/2) - 1)v_1, v)$
16. Perform along the x_2-axis $f^{n+1}(x,v) = f^{[14]}(x_1, x_2 - \frac{m}{qB}\sin(\frac{qB}{m}\Delta t/2)v_2, v)$

Algorithm for Composition with adjoint method

1. Perform along the v_1-axis $f^{[1]}(x,v) = f^{n}(x, v_1 - \tan(\frac{qB}{m}\Delta t/4), v_2)$
2. Perform along the v_2-axis $f^{[2]}(x,v) = f^{[1]}(x, v_1, \sin(\frac{qB}{m}\Delta t/2)v_1 + v_2)$
3. Perform along the v_1-axis $f^{[3]}(x,v) = f^{[2]}(x, v_1 - \tan(\frac{qB}{m}\Delta t/4), v_2)$
4. Perform along the x_1-axis $f^{[4]}(x,v) = f^{[3]}(x_1 - \frac{m}{qB}\sin(\frac{qB}{m}\Delta t/2)v_1, x_2, v)$
5. Perform along the x_1-axis $f^{[5]}(x,v) = f^{[4]}(x_1 + \frac{m}{qB}(1 - \cos(\frac{qB}{m}\Delta t/2))v_1, x_2, v)$
6. Perform along the x_2-axis $f^{[6]}(x,v) = f^{[5]}(x_1, x_2 + \frac{m}{qB}(\cos(\frac{qB}{m}\Delta t/2) - 1)v_1, v)$
7. Perform along the x_2-axis $f^{[7]}(x,v) = f^{[6]}(x_1, x_2 - \frac{m}{qB}\sin(\frac{qB}{m}\Delta t/2)v_2, v)$
8. Computation the charge density and the electric field at time $t_{n+1/2}$ by substituting $f^{[7]}$ in the Poisson equation
9. Perform along the v-axis $f^{[8]} = f^{[7]}(x, v - E(t_{n+1/2}, x)\Delta t/2)$
10. Perform along the v-axis $f^{[9]} = f^{[8]}(x, v - E(t_{n+1/2}, x)\Delta t/2)$
11. Perform along the x_2-axis $f^{[10]}(x,v) = f^{[9]}(x_1, x_2 - \frac{m}{qB}\sin(\frac{qB}{m}\Delta t/2)v_2, v)$
12. Perform along the x_2-axis $f^{[11]}(x,v) = f^{[10]}(x_1, x_2 + \frac{m}{qB}(1 - \cos(\frac{qB}{m}\Delta t/2))v_1, x_2, v)$
13. Perform along the x_1-axis $f^{[12]}(x,v) = f^{[11]}(x_1 + \frac{m}{qB}(\cos(\frac{qB}{m}\Delta t/2) - 1)v_1, x_2, v)$
14. Perform along the x_1-axis $f^{[13]}(x,v) = f^{[12]}(x_1 - \frac{m}{qB}\sin(\frac{qB}{m}\Delta t/2)v_1, x_2, v)$
15. Perform along the v_1-axis $f^{[14]}(x,v) = f^{[13]}(x, v_1 - \tan(\frac{qB}{m}\Delta t/4), v_2)$
16. Perform along the v_2-axis $f^{[15]}(x,v) = f^{[14]}(x, v_1, \sin(\frac{qB}{m}\Delta t/2)v_1 + v_2)$
17. Perform along the v_1-axis $f^{[16]}(x,v) = f^{[15]}(x, v_1 - \tan(\frac{qB}{m}\Delta t/4), v_2)$
18. Computation the charge density and the electric field at time t_{n+1} by substituting $f^{[16]}$ in the Poisson equation.

6 Numerical Simulation

This section is devoted to numerical illustrations of the numerical schemes introduced above. We consider the Vlasov-Poisson system (5)-(6) with the Kelvin-Helmholtz instability type initial data

$$f_0(x,v) = (1+\sin(k_2x_2)+\nu\cos(k_1x_1))\frac{1}{2\pi}\exp\left(-\frac{{v_1}^2+{v_2}^2}{2}\right), \tag{68}$$

defined in $\Omega_x \times \Omega_v$, where $\Omega_x = [0, L_1] \times [0, L_2]$ is the periodic domain with the lengths $L_d = 2\pi/k_d$, $d = 1, 2$, $k_d = (k_1, k_2) = (0.4, 1)$, the amplitude $\nu = 0.015$ and $\Omega_v = [-v_{\max}, v_{\max}]^2$, $v_{\max} = 8$. Then the initial density of the guiding-center approximation (7)-(8) writes:

$$\rho_0(x) = 1+\sin(k_2x_2)+\nu\cos(k_1x_1), \tag{69}$$

defined in Ω_x. The numerical parameters are Nx points in space, Nv points per velocity direction.

We perform numerical simulation using the splitting schemes coupled with the semi-Lagrangian method described in Section 2 for the Vlasov-Poisson equation (5)-(6). On the orther hand, we compute an approximation of the guiding center model (7)-(8) using a backward semi-Lagrangian method developed in [8] with Lagrangian interpolation. This reference will be used to compare our results obtained from Vlasov-Poisson system with a large magnetic field for a long time.

First of all, we are interested in the time evolution of the electrostatic energy in the first dimension $\frac{1}{2}\|E_1\|_2^2$. We focus our comparisons on the different methods presented in Section 2: the Strang splitting based on the exponential Boris algorithm, the Strang spliting and the composition with the adjoint of Scovel method from weak to strong magnetic field whilst holding the actual number of time steps constant. In Figure 1, we plot the time evolution of the electrostatic energy in the first dimension with several values of ε going from 1 to 1/132. We also compare the numerical results obtained with these schemes to a numerical solution for the Guiding center model. The run is performed up to a final time $T = 50$ with the value of the time step $\Delta t = 0.01$. For $\varepsilon = 1, 1/2, 1/4$ and $1/8$ all integrators show the same performance, but in the case of the parameter ε becomes smaller, the Scovel method is clearly better. For $\varepsilon = 1/16, 1/32, 1/64$ and $1/132$ the Strang splitting based on the exponential Boris algorithm fail entirely whereas the Strang splitting and the composition with adjoint based on Scovel's method remain unaffected, confirm the convergence of Vlasov-Poisson system (5)-(6) towards the asymptotic model (7)-(8).

Then we investigate numerically the effect of condition (58) to the convergence of the Vlasov-Poisson system (5)-(6) to its limit model (7)-(8). In Figure 2, we plot the time evolution of the electrostatic energy in the first dimension for different values ε when fixing the numerical parameters as follows: $\Delta t = 0.01, Nx = 128$ and the ratio $Nv/v_{\max} = 4$ which is denoted the number of points per cell in the velocity grid. As we can see in Figure 2 that when the parameter ε becomes smaller, we need to choose a large value of $v_{\max}$ to obtain good results. For $\varepsilon = 1/132$, we take $v_{\max} = 8$ as enough value to produce a good simulation, and then for $\varepsilon = 1/400$ and $1/1000$, this value of $v_{\max}$ is not sufficient, it gives bad result, but the value $v_{\max} = 16$ give better result. For $\varepsilon = 1/1600$, we need to choose $v_{\max} = 32$.

In the following, we will do numerical comparisons between the density particle obtained from the discretized Vlasov-Poisson system with the semi-Lagrangian method and the one corresponding to the discretized guiding center model. More precisely, we represent in the physical space the contours of the particle densities at several values of final fluid time $T \in \{10, 18, 25, 58, 98, 120\}$. First, we observe the time evolution of the density particle for the guiding center model by using Lagrangian interpolation in Figure 3. For the densities given

by Vlasov-Poisson system, first we consider the case where $\varepsilon = 1$. In this weak case, the plasma is not well confined. The lack of confinement appears to introduce diffusion like effects and does not develop the instability phenomena, see Figure 4. Then, we take with several values of $\varepsilon \in \{1/32, 1/64, 1/132\}$, and for this case, the figures in Fig. 5, 6 and 7 show the development of the instability of the density and it is obeyed to the same evolution as the density of the guiding center model in above Figure 3 for final time T going from 10 to 58, but in the case of the long final time $T = 98$ and 120 there is no longer obeyed because of the error in time.

On Fig. 8 and Fig. 9, we plot the time evolution of L^2 and L^1 for the Vlasov-Poisson system with several values of $\varepsilon \in \{1/2, 1/4, 1/8, 1/16, 1/32, 1/64, 1/132\}$ and several of number of points in the position grid $Nx = Ny \in \{32, 64, 128, 256\}$ and compare these results with the guiding center model.

On Figs. 10 and 11, we investigate the kinetic effects in the case of weak and strong magnetic fields. These figures indicate that kinetic effects are only present in the weak case. Due to the lack of confinement the distribution does not clearly display Maxwellian. For the strong field the distribution ressembles a sharp Maxwellian.

7 Conclusion

In this paper, we have used the semi-Lagrangian method to solve the four-dimensional Vlasov-Poisson system with a strong external uniform magnetic field. The splitting schemes for the Vlasov equation are presented based on the exponential Boris algorithm and Scovel method. The exponential Boris algorithm works badly. The Scovel method presented here performs independently of the strength of the magnetic field very well, we can choose the time step Δt much larger than $\mathcal{O}(\varepsilon^2)$. However, due to the high oscillation in the electric field by the Scovel method, the time step Δt is imposed to the condition (58) within the semi-Lagrangian method. As the parameter ε becomes smaller we need to take the larger value of $v_{\max}$ and then increase the number of points in the direction of velocity to produce good results. Since the semi-Lagrangian schemes are based on interpolation on a phase space mesh, we have to pay attention to the number of point in the velocity grid as $v_{\max}$ is larger. Therefore, for an intermediate value of ε, the Scovel method is an appropriate method to the Vlasov-Poisson model, but for a very small value of ε, the fluid model is an appropriate approximation to the kinetic model because it contains all the relevant dynamics and will be much cheaper. Moreover, we have shown numerically that the Scovel method provides a consistent discretization with respect to the limiting guiding center model.

8 Appendix: A priori estimate

In this Appendix, we will give the global error of the p-order Scovel method ($p = 1, 2$) presented in Section 4. We want to evaluate the global error at time t_{n+1}:

$$
\begin{aligned}
e_1 &= \|f_\varepsilon(t_{n+1}, x, v) - \mathcal{T}_2 \circ \mathcal{T}_1 f_\varepsilon(t_n, x, v)\|_{L^\infty}, \\
\tilde{e}_1 &= \|f_\varepsilon(t_{n+1}, x, v) - \mathcal{T}_1 \circ \mathcal{T}_2 f_\varepsilon(t_n, x, v)\|_{L^\infty}, \\
e_2 &= \|f_\varepsilon(t_{n+1}, x, v) - \mathcal{T}_1 \circ \mathcal{T}_2 \circ \mathcal{T}_1 f_\varepsilon(t_n, x, v)\|_{L^\infty},
\end{aligned}
$$

where the transport operators $\mathcal{T}_i$, $i = 1, 2$ are given by

$$
\begin{aligned}
\mathcal{T}_1 f_\varepsilon(t_n, x, v) &= f_\varepsilon(t_n, x + \left[\mathcal{R}\left(\frac{\omega_c}{\varepsilon^2}\Delta t + \pi/2\right) - \mathcal{R}(\pi/2)\right] \varepsilon \frac{v}{\omega_c}, \mathcal{R}\left(\frac{\omega_c}{\varepsilon^2}\Delta t\right) v), \\
\mathcal{T}_2 f_\varepsilon(t_n, x, v) &= f_\varepsilon(t_n, x, v - \frac{q}{m}\frac{\Delta t}{\varepsilon} E_\varepsilon(t, x)).
\end{aligned}
$$

Lemma 8.1 *Assume that $f_\varepsilon \in C^1_b(0,T;C^1(\mathbb{R}^2\times\mathbb{R}^2))$ and $E_\varepsilon \in C^1_b(0,T;C^1(\mathbb{R}^2))$, then there exists a constant C such that*

$$\begin{aligned}
e_1 &\le C(\|f_\varepsilon\|_{C^1_b},\|E_\varepsilon\|_{C^1_b})\left[(\Delta t/\varepsilon)^2+(\Delta t/\varepsilon)^3\right],\\
\tilde{e}_1 &\le C(\|f_\varepsilon\|_{C^1_b},\|E_\varepsilon\|_{C^1_b})(\Delta t/\varepsilon)^2,\\
e_2 &\le C(\|f_\varepsilon\|_{C^1_b},\|E_\varepsilon\|_{C^1_b})(\Delta t/\varepsilon)^3.
\end{aligned}$$

Proof. As f_ε is constant along the characteristic curves, we have

$$f_\varepsilon(t_{n+1},x,v)=f_\varepsilon(t_n,X_\varepsilon(t_n;t_{n+1},x,v),V_\varepsilon(t_n;t_{n+1},x,v)),$$

where $(X_\varepsilon,V_\varepsilon)$ are the characteristic solutions of $\frac{d}{dt}X_\varepsilon(t)=\frac{1}{\varepsilon}V_\varepsilon(t)$ and $\frac{d}{dt}V_\varepsilon(t)=\frac{q}{m}\frac{1}{\varepsilon}E_\varepsilon(t,X_\varepsilon(t))+\frac{\omega_c}{\varepsilon^2}{}^\perp V_\varepsilon(t)$. We therefore have by integrating these equations between t and t_{n+1}

$$X_\varepsilon(t;t_{n+1},x,v)=x-\frac{1}{\varepsilon}\int_t^{t_{n+1}}V_\varepsilon(s;t_{n+1},x,v)\mathrm{d}s, \tag{70}$$

$$V_\varepsilon(t;t_{n+1},x,v)=\mathcal{R}\left(\frac{\omega_c}{\varepsilon^2}(t_{n+1}-t)\right)v-\frac{q}{m\varepsilon}\int_t^{t_{n+1}}\mathcal{R}\left(\frac{\omega_c}{\varepsilon^2}(s-t)\right)E_\varepsilon(s,X_\varepsilon(s;t_{n+1},x,v))\mathrm{d}s. \tag{71}$$

We will first estimate $\tilde{e}_1=\|f_\varepsilon(t_{n+1},x,v)-\mathcal{T}_2\circ\mathcal{T}_1 f_\varepsilon(t_n,x,v)\|_{L^\infty}$.
We have

$$\mathcal{T}_1\circ\mathcal{T}_2 f_\varepsilon(t_n,x,v)=f_\varepsilon(t_n,\bar{X}_\varepsilon(t_n;t_{n+1},x,v),\bar{V}_\varepsilon(t_n;t_{n+1},x,v)),$$

where

$$\begin{aligned}
\bar{X}_\varepsilon(t_n;t_{n+1},x,v)&=x+\left[\mathcal{R}\left(\frac{\omega_c}{\varepsilon^2}\Delta t+\pi/2\right)-\mathcal{R}(\pi/2)\right]\frac{\varepsilon}{\omega_c}\left(v-\frac{q}{m}\frac{\Delta t}{\varepsilon}E_\varepsilon(t_n,x)\right),\\
\bar{V}_\varepsilon(t_n;t_{n+1},x,v)&=\mathcal{R}\left(\frac{\omega_c}{\varepsilon^2}\Delta t\right)\left(v-\frac{q}{m}\frac{\Delta t}{\varepsilon}E_\varepsilon(t_n,x)\right).
\end{aligned}$$

Now using the right rectangle rule to approximate the integral in (71) we obtain

$$V_\varepsilon(t;t_{n+1},x,v)=\mathcal{R}\left(\frac{\omega_c}{\varepsilon^2}(t_{n+1}-t)\right)v-\frac{q}{m\varepsilon}\left[(t_{n+1}-t)\mathcal{R}\left(\frac{\omega_c}{\varepsilon^2}(t_{n+1}-t)\right)E_\varepsilon(t_{n+1},x)+\mathcal{O}(\Delta t^2)\right], \tag{72}$$

then using (72) for $t=t_n$ we get

$$V_\varepsilon(t_n;t_{n+1},x,v)=\mathcal{R}\left(\frac{\omega_c}{\varepsilon^2}\Delta t\right)v-\frac{q}{m\varepsilon}\left[\Delta t\mathcal{R}\left(\frac{\omega_c}{\varepsilon^2}\Delta t\right)E_\varepsilon(t_{n+1},x)+\mathcal{O}(\Delta t^2)\right].$$

Hence, we deduce that

$$\begin{aligned}
V_\varepsilon(t_n;t_{n+1},x,v)-\bar{V}_\varepsilon(t_n;t_{n+1},x,v)&=\mathcal{O}(\Delta t/\varepsilon)(E_\varepsilon(t_n,x)-E_\varepsilon(t_{n+1},x))+\mathcal{O}(\Delta t^2/\varepsilon)\\
&=\mathcal{O}(\Delta t^2/\varepsilon).
\end{aligned} \tag{73}$$

Substituting the equality (72) into the equation (70) to get

$$\begin{aligned}
X_\varepsilon(t_n;t_{n+1},x,v)=x&+\left[\mathcal{R}\left(\frac{\omega_c}{\varepsilon^2}\Delta t+\pi/2\right)-\mathcal{R}(\pi/2)\right]\frac{\varepsilon}{\omega_c}v+\mathcal{O}(\Delta t^3/\varepsilon^2)\\
&+\left[-\Delta t\mathcal{R}\left(\frac{\omega_c}{\varepsilon^2}\Delta t+\pi/2\right)+\Delta t\mathcal{R}(\pi/2)+\mathcal{O}(\Delta t^2)\right]\frac{E_\varepsilon(t_{n+1},x)}{B},
\end{aligned}$$

where we used the formula $\dfrac{\mathrm{d}}{\mathrm{d}\theta}\mathcal{R}(-\theta+\pi/2)=\mathcal{R}(-\theta)$ and hence

$$\begin{aligned}&X_\varepsilon(t_n;t_{n+1},x,v)-\bar{X}_\varepsilon(t_n;t_{n+1},x,v)\\&=\mathcal{O}(\Delta t)\left(E_\varepsilon(t_n,x)-E_\varepsilon(t_{n+1},x)\right)+\mathcal{O}(\Delta t^3/\varepsilon^2)+\mathcal{O}(\Delta t^2)=\mathcal{O}(\Delta t^3/\varepsilon^2)+\mathcal{O}(\Delta t^2).\end{aligned}\tag{74}$$

Finally, using (73) and (74) we obtain

$$\tilde{e}_1=\|f_\varepsilon(t_{n+1},x,v)-\mathcal{T}_1\circ\mathcal{T}_2 f_\varepsilon(t_n,x,v)\|_{L^\infty}\le C(\|f_\varepsilon\|_{C_b^2},\|E_\varepsilon\|_{C_b^1})\mathcal{O}(\Delta t^2/\varepsilon^2).$$

Next, we will estimate $e_1=\|f_\varepsilon(t_{n+1},x,v)-\mathcal{T}_2\circ\mathcal{T}_1 f_\varepsilon(t_n,x,v)\|_{L^\infty}$.
We have

$$\mathcal{T}_2\circ\mathcal{T}_1 f_\varepsilon(t_n,x,v)=f_\varepsilon(t_n,\bar{X}_\varepsilon(t_n;t_{n+1},x,v),\bar{V}_\varepsilon(t_n;t_{n+1},x,v)),$$

where

$$\begin{aligned}\bar{X}_\varepsilon(t_n;t_{n+1},x,v)&=x+\left[\mathcal{R}\left(\frac{\omega_c}{\varepsilon^2}\Delta t+\pi/2\right)-\mathcal{R}(\pi/2)\right]\frac{\varepsilon}{\omega_c}v,\\\bar{V}_\varepsilon(t_n;t_{n+1},x,v)&=\mathcal{R}\left(\frac{\omega_c}{\varepsilon^2}\Delta t\right)v-\frac{q}{m}\frac{\Delta t}{\varepsilon}E_\varepsilon(t_{n+1},\bar{X}_\varepsilon(t_n;t_{n+1},x,v)).\end{aligned}$$

Using now the left rectangle rule to approximate the integral in (71) we obtain

$$V_\varepsilon(t)=\mathcal{R}\left(\frac{\omega_c}{\varepsilon^2}(t_{n+1}-t)\right)v-\frac{q}{m\varepsilon}\left[(t_{n+1}-t)E_\varepsilon(t,X_\varepsilon(t;t_{n+1},x,v))+\mathcal{O}(\Delta t^2)\right],\tag{75}$$

which implies for $t=t_n$ that

$$V_\varepsilon(t_n;t_{n+1},x,v)=\mathcal{R}\left(\frac{\omega_c}{\varepsilon^2}\Delta t\right)v-\frac{q}{m\varepsilon}\left[\Delta t E_\varepsilon(t_n,X_\varepsilon(t_n;t_{n+1},x,v))+\mathcal{O}(\Delta t^2)\right].$$

Substituting the equality (75) into the equation (70) and re-use the left rectangle rule to get

$$X_\varepsilon(t_n)=x+\left[\mathcal{R}\left(\frac{\omega_c}{\varepsilon^2}\Delta t+\pi/2\right)-\mathcal{R}(\pi/2)\right]\frac{\varepsilon}{\omega_c}v-\frac{q}{m}\frac{\Delta t^2}{\varepsilon^2}E_\varepsilon(t_n,X_\varepsilon(t_n))+\mathcal{O}(\Delta t^3/\varepsilon^2).$$

Hence we deduce that

$$X_\varepsilon(t_n;t_{n+1},x,v)-\bar{X}_\varepsilon(t_n;t_{n+1},x,v)=\mathcal{O}(\Delta t^2/\varepsilon^2)+\mathcal{O}(\Delta t^3/\varepsilon^2),\tag{76}$$

and, as a consequence

$$\begin{aligned}&V_\varepsilon(t_n)-\bar{V}_\varepsilon(t_n)=\frac{q}{m}\frac{\Delta t}{\varepsilon}\left[E_\varepsilon(t_{n+1},\bar{X}_\varepsilon(t_n))-E_\varepsilon(t_n,X_\varepsilon(t_n))\right]+\mathcal{O}(\Delta t^2/\varepsilon)\\&=\mathcal{O}(\Delta t/\varepsilon)\left[\Delta t+|\bar{X}_\varepsilon(t_n;t_{n+1},x,v)-X_\varepsilon(t_n;t_{n+1},x,v)|\right]+\mathcal{O}(\Delta t^2/\varepsilon)\\&=\mathcal{O}(\Delta t^2/\varepsilon)+\mathcal{O}(\Delta t^3/\varepsilon^3)+\mathcal{O}(\Delta t^5/\varepsilon^3)+\mathcal{O}(\Delta t^2/\varepsilon).\end{aligned}\tag{77}$$

Thus from (76) and (77) we obtain

$$e_1=\|f_\varepsilon(t_{n+1},x,v)-\mathcal{T}_2\circ\mathcal{T}_1 f_\varepsilon(t_n,x,v)\|_{L^\infty}\le C(\|f_\varepsilon\|_{C_b^1},\|E_\varepsilon\|_{C_b^1})(\mathcal{O}(\Delta t^2/\varepsilon^2)+\mathcal{O}(\Delta t^3/\varepsilon^3)).$$

Finally, we estimate $e_2=\|f_\varepsilon(t_{n+1},x,v)-\mathcal{T}_1\circ\mathcal{T}_2\circ\mathcal{T}_1 f_\varepsilon(t_n,x,v)\|_{L^\infty}$.
We have

$$\mathcal{T}_1\circ\mathcal{T}_2\circ\mathcal{T}_1 f_\varepsilon(t_n,x,v)=f_\varepsilon(t_n,\bar{X}_\varepsilon(t_n;t_{n+1},x,v),\bar{V}_\varepsilon(t_n;t_{n+1},x,v))$$

where

$$\bar{X}_\varepsilon(t_n;t_{n+1},x,v) = x + \left[\mathcal{R}\left(\frac{qB}{m\varepsilon^2}\Delta t + \pi/2\right) - \mathcal{R}(\pi/2)\right]\varepsilon\frac{v}{\omega_c} \\ - \Delta t\left[\mathcal{R}\left(\frac{qB}{m\varepsilon^2}\frac{\Delta t}{2} + \pi/2\right) - \mathcal{R}(\pi/2)\right]\frac{E_\varepsilon}{B}(t_{n+1/2}, \bar{X}_\varepsilon(t_n;t_{n+1/2},x,v)),$$

$$\bar{V}_\varepsilon(t_n;t_{n+1},x,v) = \mathcal{R}\left(\frac{qB}{m\varepsilon^2}\Delta t\right)v - \frac{q}{m}\frac{\Delta t}{\varepsilon}\mathcal{R}\left(\frac{qB}{m\varepsilon^2}\frac{\Delta t}{2}\right)E_\varepsilon(t_{n+1/2}, \bar{X}_\varepsilon(t_n;t_{n+1/2},x,v)),$$

with $\bar{X}_\varepsilon(t_n;t_{n+1/2},x,v) = x + \left[\mathcal{R}\left(\frac{qB}{m\varepsilon^2}\frac{\Delta t}{2} + \pi/2\right) - \mathcal{R}(\pi/2)\right]\varepsilon\frac{v}{\omega_c}$.
Using now the midpoint rectangle rule to approximate the integral in (71) we obtain

$$V_\varepsilon(t;t_{n+1},x,v) = \mathcal{R}\left(\frac{\omega_c}{\varepsilon^2}(t_{n+1}-t)\right)v \\ - \frac{q}{m\varepsilon}\left[(t_{n+1}-t)\mathcal{R}\left(\frac{\omega_c}{\varepsilon^2}(t_{n+1/2}-t)\right)E(t_{n+1/2}, X_\varepsilon(t_{n+1/2};t_{n+1},x,v)) + \mathcal{O}(\Delta t^3)\right], \tag{78}$$

which implies for $t = t_n$ that

$$V_\varepsilon(t_n) = \mathcal{R}\left(\frac{\omega_c}{\varepsilon^2}\Delta t\right)v - \frac{q}{m\varepsilon}\left[\Delta t\mathcal{R}\left(\frac{\omega_c}{\varepsilon^2}\frac{\Delta t}{2}\right)E_\varepsilon(t_{n+1/2}, X_\varepsilon(t_{n+1/2};t_{n+1},x,v)) + \mathcal{O}(\Delta t^3)\right].$$

Substituting the equality (78) into the equation (70) for $t = t_{n+1/2}$ and using the left rectangle rule to get

$$X_\varepsilon(t_{n+1/2}) = x + \left[\mathcal{R}\left(\frac{qB}{m\varepsilon^2}\frac{\Delta t}{2} + \pi/2\right) - \mathcal{R}(\pi/2)\right]\varepsilon\frac{v}{\omega_c} \\ + \mathcal{O}(\Delta t^4/\varepsilon) + \frac{q}{m\varepsilon^2}\frac{\Delta t^2}{4}E(t_{n+1/2}, X_\varepsilon(t_{n+1/2})) + \mathcal{O}(\Delta t^2/\varepsilon^2),$$

and hence we deduce that

$$X_\varepsilon(t_{n+1/2}) - \bar{X}_\varepsilon(t_n;t_{n+1/2},x,v) = \mathcal{O}(\Delta t^4/\varepsilon) + \mathcal{O}(\Delta t^2/\varepsilon^2) + (\Delta t^2/\varepsilon^2) = \mathcal{O}(\Delta t^2/\varepsilon^2). \tag{79}$$

Do it again for $t = t_n$ we have

$$X_\varepsilon(t_n) = x + \left[\mathcal{R}\left(\frac{qB}{m}\frac{\Delta t}{\varepsilon^2} + \pi/2\right) - \mathcal{R}(\pi/2)\right]\varepsilon\frac{v}{\omega_c} + \mathcal{O}(\Delta t^4/\varepsilon) \\ - \frac{\Delta t}{B}\left[\mathcal{R}\left(\frac{qB}{m}\frac{\Delta t}{2\varepsilon^2} + \pi/2\right) - \mathcal{R}(\pi/2)\right]E_\varepsilon(t_{n+1/2}, X_\varepsilon(t_{n+1/2};t_{n+1},x,v)) + \mathcal{O}(\Delta t^3). \tag{80}$$

where we computed the integral

$$\int_{t_n}^{t_{n+1}}(t_{n+1}-s)\mathcal{R}\left(\frac{qB}{m}\frac{t_{n+1/2}-s}{\varepsilon^2}\right)\mathrm{d}s = \frac{\varepsilon^2}{\omega_c}\int_{t_n}^{t_{n+1}}(t_{n+1}-s)\frac{d}{ds}\mathcal{R}\left(\frac{qB}{m}\frac{t_{n+1/2}-s}{\varepsilon^2} + \pi/2\right)\mathrm{d}s \\ = \frac{\varepsilon^2}{\omega_c}\left[-\Delta t\mathcal{R}\left(\frac{qB}{m}\frac{\Delta t}{2\varepsilon^2} + \pi/2\right) + \int_{t_n}^{t_{n+1}}\mathcal{R}\left(\frac{qB}{m}\frac{t_{n+1/2}-s}{\varepsilon^2} + \pi/2\right)\mathrm{d}s\right] \\ = \frac{\varepsilon^2}{\omega_c}\left[-\Delta t\mathcal{R}\left(\frac{qB}{m}\frac{\Delta t}{2\varepsilon^2} + \pi/2\right) + \Delta t\mathcal{R}\left(\frac{qB}{m}\frac{t_{n+1/2}-t_{n+1/2}}{\varepsilon^2} + \pi/2\right) + \mathcal{O}(\Delta t^3)\right] \\ = -\frac{\varepsilon^2}{\omega_c}\Delta t\left[\mathcal{R}\left(\frac{qB}{m}\frac{\Delta t}{2\varepsilon^2} + \pi/2\right) - \mathcal{R}(\pi/2)\right] + \varepsilon^2\mathcal{O}(\Delta t^3).$$

Using (79) and (80) we have

$$X_\varepsilon(t_n;t_{n+1},x,v)-\bar{X}_\varepsilon(t_n;t_{n+1},x,v)=\mathcal{O}(\Delta t^3/\varepsilon^3),$$
$$V_\varepsilon(t_n;t_{n+1},x,v)-\bar{V}_\varepsilon(t_n;t_{n+1},x,v)=\mathcal{O}(\Delta t^3/\varepsilon^3).$$

Finally we get

$$e_2=\|f_\varepsilon(t_{n+1},x,v)-\mathcal{T}_2\circ\mathcal{T}_1\circ\mathcal{T}_1 f_\varepsilon(t_n,x,v)\|_{L^\infty}\leq C(\|f_\varepsilon\|_{C_b^1},\|E_\varepsilon\|_{C_b^1})\mathcal{O}(\Delta t^3/\varepsilon^3).$$

□

References

[1] Pierre Degond and Francis Filbet, On the asymptotic limit of the three dimensional Vlasov-Poisson system for large magnetic field: Formal derivation, Journal of Statistical Physics volume 165, pages 765–784 (2016).

[2] Jakob Ameres, Splitting methods for Fourier spectral discretizations of the strongly magnetized Vlasov-Poisson and the Vlasov-Maxwell system, arXiv:1907.05319.

[3] Joackim Bernier, Fernando Casas, Nicolas Crouseilles, Splitting methods for rotation: application to Vlasov equations, SIAM Journal on Scientific Computing Vol. 42, Iss. 2 (2020).

[4] Francis Filbet, Luis Miguel Rodrigues, Asymptotically Stable Particle-In-Cell Methods for the Vlasov–Poisson System with a Strong External Magnetic Field, SIAM Journal on Numerical Analysis Vol. 54, No. 2 (2016), pp. 1120-1146.

[5] L.Saint-Raymond, Control of large velocities in the two-dimensional gyrokinetic approximation, J. Math. Pures Appl. 81 (2002) 379–399.

[6] Andrey A.Amosov, Weakly convergence for a class of rapidly oscillating functions. January 1997 Mathematical Notes 62(1):122-126.

[7] Evelyne Miot, On the gyrokinetic limit for the two-dimensional Vlasov-Poisson system, arXiv- 1603.04502 (2016).

[8] Eric Sonnendrücker, Jean Roche, Pierre Bertrand and Alain Ghizzo, The semi-Lagrangian method for the numerical resolution of the Vlasov equation, J. Comput. Physics 149, 201-220 (1999).

[9] A.A. Arsen'ev, Global existence of weak solution of Vlasov's system of equations,28 Z. Vychisl. Mat. Fiz. 15(1975) 136-147.

[10] J. Batt, Global symmetric solutions of the initial value problem in stellar dynamics,30 J. Differential Equations 25(1977) 342-364.

[11] M.Bostan, Asymptotic behavior for the Vlasov-Poisson equations with strong external magnetic field. Straight magnetic field lines, SIAM Journal on Mathematical AnalysisVol. 51, Iss. 3 (2019).

[12] T. Ukai, S. Okabe, On the classical solution in the large time of the two dimensional Vlasov equations, Osaka J. Math. 5(1978) 245-261.

[13] P.-L. Lions, B. Perthame, Propagation of moments and regularity for the 3-36 dimensional Vlasov-Poisson system, Invent. Math. 105(1991) 415-430.

[14] C.K. Birdsall, A.B. Langdon, Plasma Physics Via Computer Simulation, McGraw-Hill, New York, 1985.

[15] Nicolas Crouseilles, Lukas Einkemmer, Erwan Faou Hamiltonian splitting for the Vlasov–Maxwell equations, Journal of Computational Physics 283 (2015) 224–240.

[16] Emmanuel Frenod, Sever Adrian Hirstoaga, MathieuLutz, Eric Sonnendrücker Long Time Behaviour of an Exponential Integrator for a Vlasov-Poisson System with Strong Magnetic Field, Communications in Computational Physics, vol. 18, issue 02, pp. 263-296.

[17] J. Hu, S. Jin† and Q. Li, Asymptotic-Preserving Schemes for Multiscale Hyperbolic and Kinetic Equations, Handbook of Numerical Analysis, Volume 18, 2017, 103-129.

[18] Adnane Hamiaz, Michel Mehrenberger, Hocine Sellama and Eric Sonnendrücker, The semi-Lagrangian method on curvilinear grids, Communications in Applied and Industrial Mathematics, Volume 7 (2016) - Issue 3 (September 2016), 99 - 137.

[19] Adnane Hamiaz, Michel Mehrenberger, Aurore Back and Pierre Navaro, Guiding center simulations on curvilinear grids, ESAIM: PROCEEDINGS AND SURVEYS, March 2016, Vol. 53, 99-119.

[20] Michel Mehrenberger1, Laura S. Mendoza, Charles Prouveur and Eric Sonnendrücker, Solving the guiding-center model on a regular hexagonal mesh, ESAIM: PROCEEDINGS AND SURVEYS, March 2016, Vol. 53, p. 149-176.

[21] Nicolas Crouseilles, Mohammed Lemou, Florian Méhats, Xiaofei Zhao, Uniformly accurate Particle-in-Cell method for the long time solution of the two-dimensional Vlasov–Poisson equation with uniform strong magnetic field, Journal of Computational Physics Volume 346, 1 October 2017, Pages 172-190.

[22] Joackim Bernier, Exact splitting methods for semigroups generated by inhomogeneous quadratic differential operators, Foundations of Computational Mathematics volume 21, pages 1401–1439 (2021).

[23] Joackim Bernier, Nicolas Crouseilles, and Yingzhe Li, Exact splitting methods for kinetic and Schrödinger equations, Journal of Scientific Computing volume 86, Article number: 10 (2021).

[24] Philippe Chartier, Nicolas Crouseilles, Xiaofei Zhao, Numerical methods for the two-dimensional Vlasov-Poisson equation in the finite Larmor radius approximation regime, Journal of Computational Physics, Volume 375, 15 December 2018, Pages 619-640.

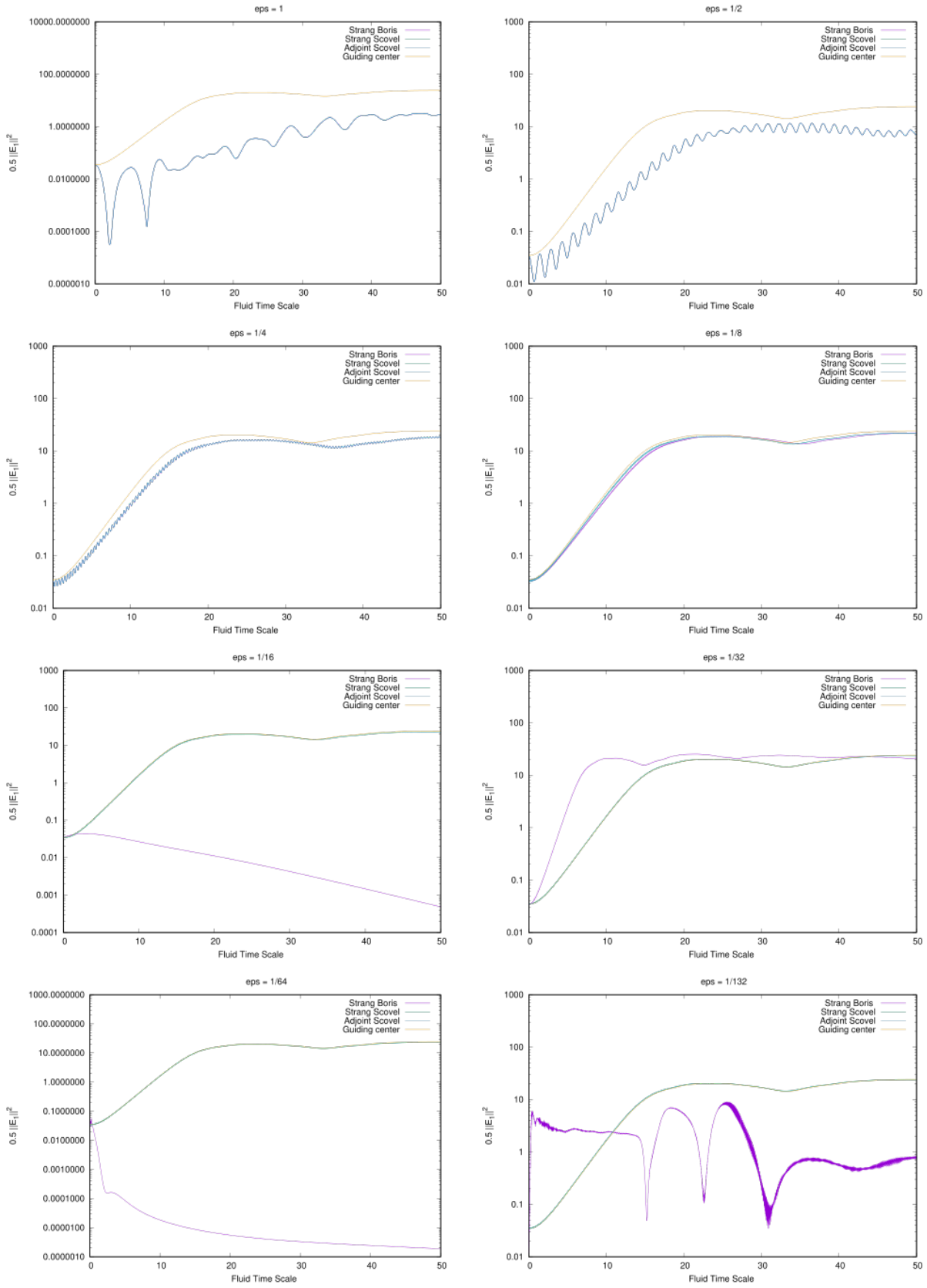

Figure 1: Comparison between the time evolution of electrostatic energy in first dimension from Vlasov-Poisson system and the guiding center model. $Nx = 128, Nv = 64, v_{\max} = 8, \Delta t = 0.01$. The number of time steps stays constant $N = 5000$.

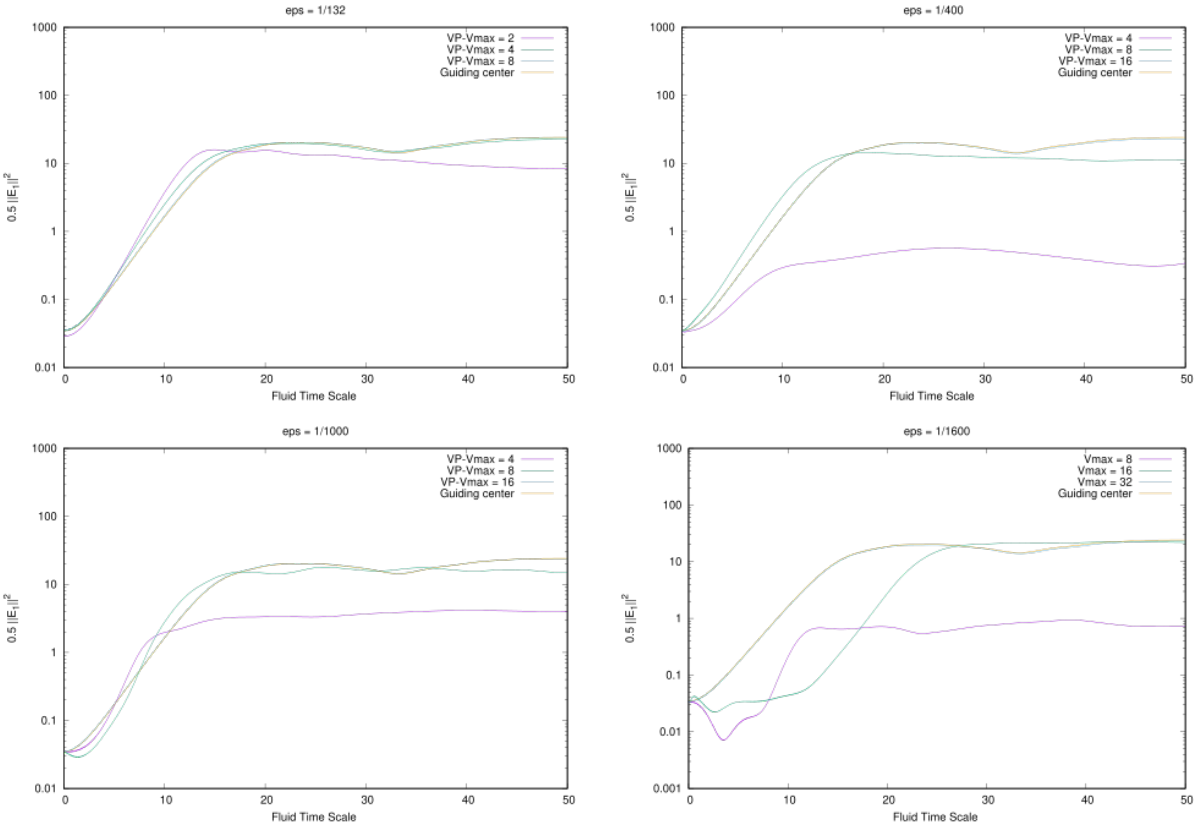

Figure 2: The time evolution of electrostatic energy in first dimension under strong magnetic field with Scovel's splitting. $Nx = 128, \Delta t = 0.01$.

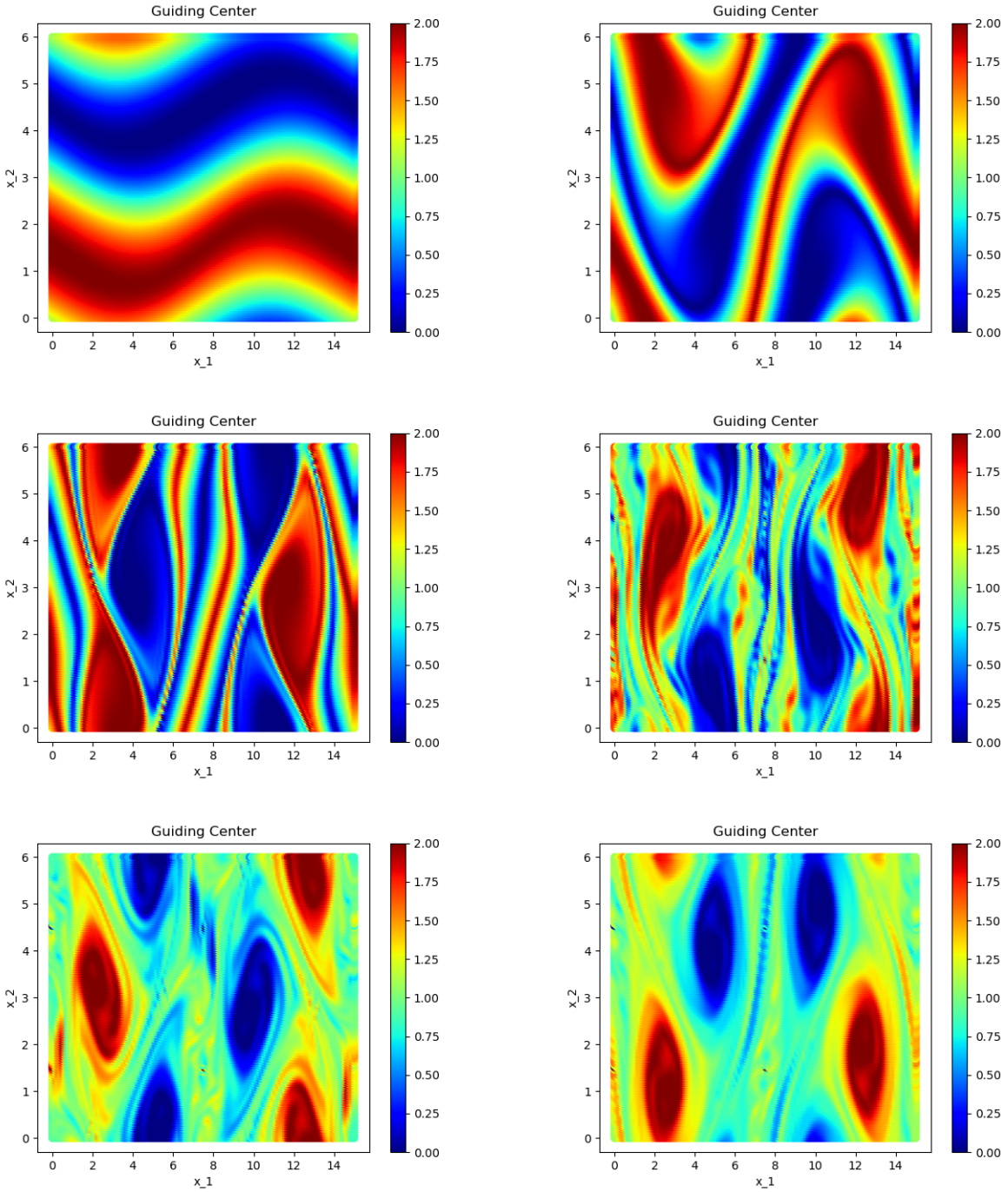

Figure 3: Simulation for time evolution of the density of Guiding center model using the Lagrangian interpolation. $Nx = Ny = 128, \Delta t = 0.01$. From left to right we present the densities's contours at fluid times scale $T = 10$, $T = 18$, $T = 25$, $T = 58$, $T = 98$ and $T = 120$.

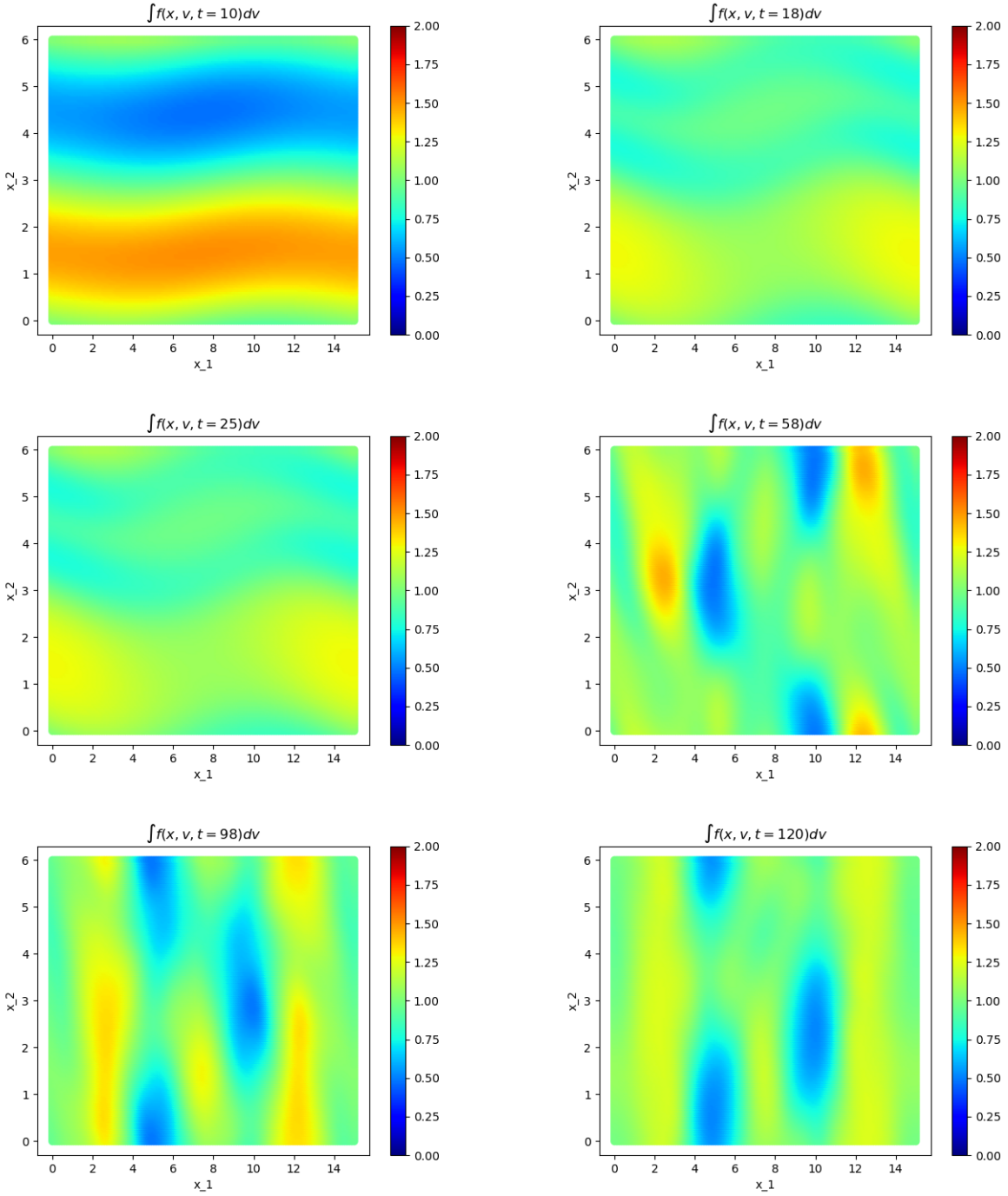

Figure 4: Simulation for time evolution of the density of Vlasov-Poisson system with $\varepsilon = 1$. $Nx = 128, Ny = 128, Nvx = 64, Nvy = 64, \Delta t = 0.01$.

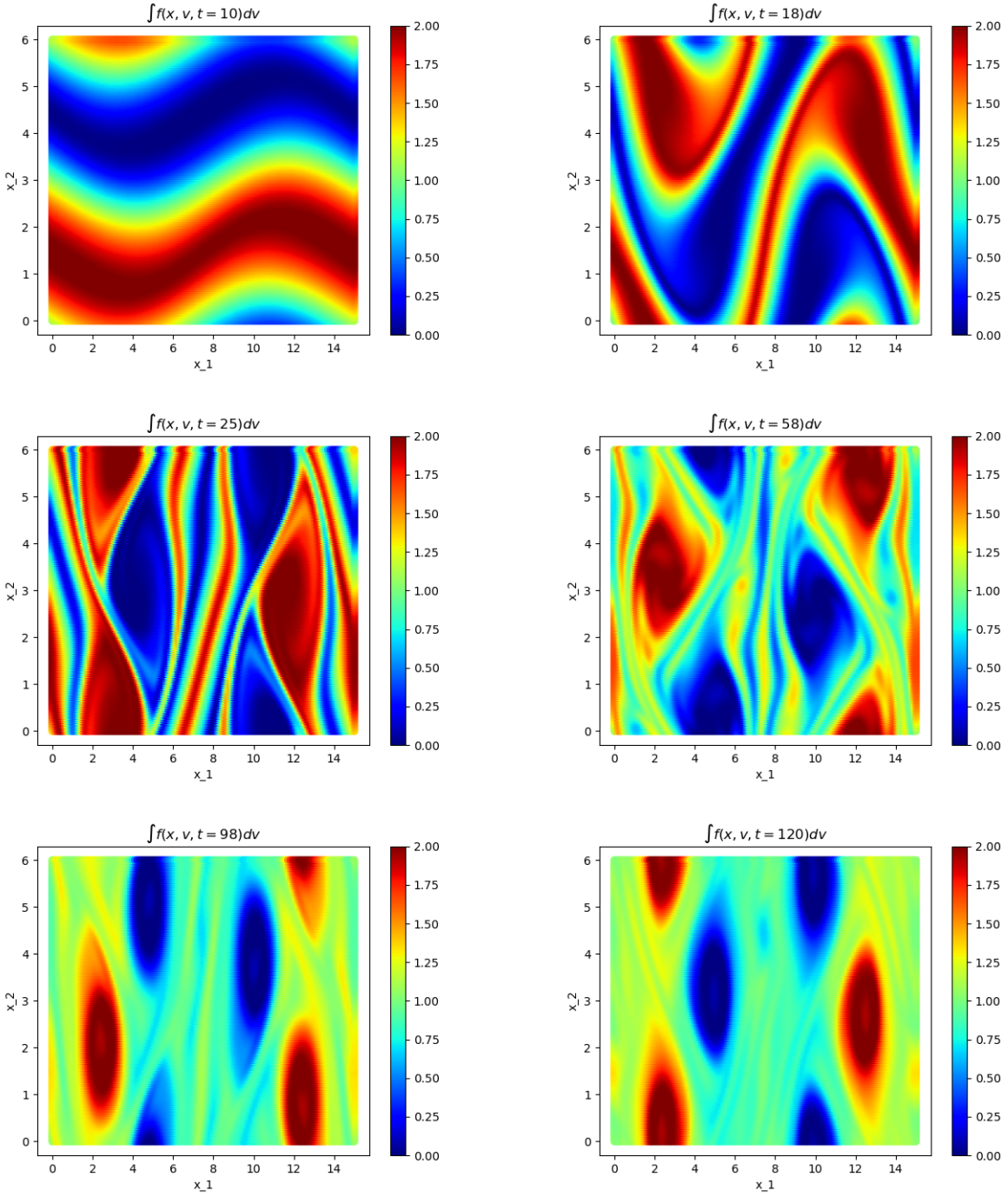

Figure 5: Simulation for time evolution of the density of Vlasov-Poisson system with $\varepsilon = 1/32$. $Nx = 128, Ny = 128, Nvx = 64, Nvy = 64, \Delta t = 0.01$.

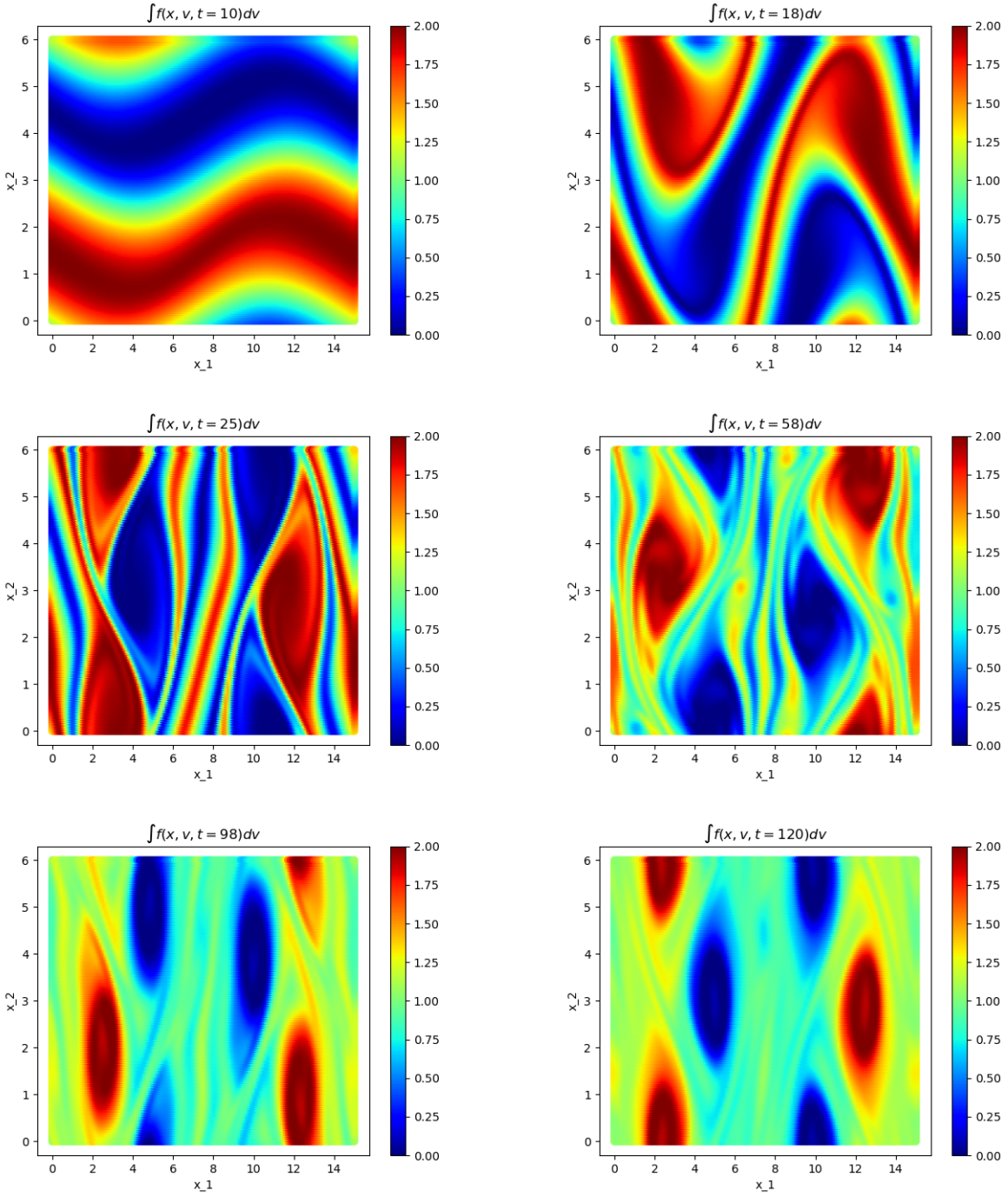

Figure 6: Simulation for time evolution of the density of Vlasov-Poisson system with $\varepsilon = 1/64$. $Nx = 128, Ny = 128, Nvx = 64, Nvy = 64, \Delta t = 0.01$.

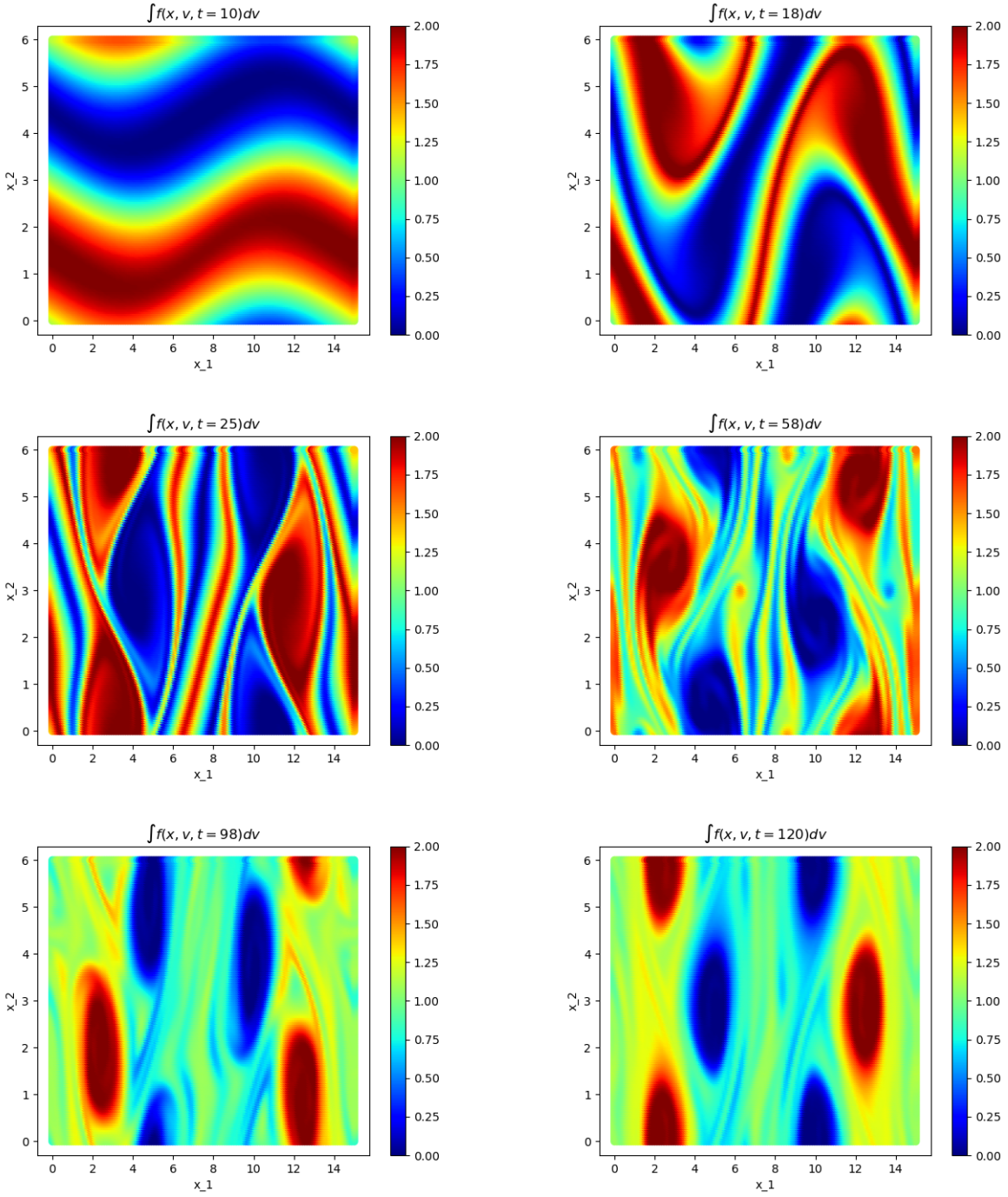

Figure 7: Simulation for time evolution of the density of Vlasov-Poisson system with $\varepsilon = 1/132$. $Nx = 128, Ny = 128, Nvx = 64, Nvy = 64, \Delta t = 0.01$.

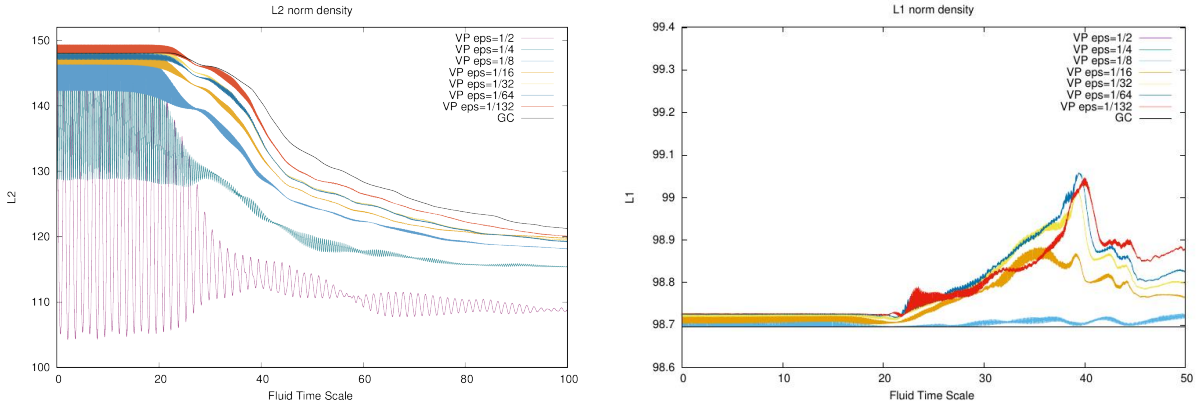

Figure 8: Comparison between the time evolution of theoretically quantities of Vlasov-Poisson system with several values of ε and the guiding center model. $Nx = Ny = 128, Nvx = Nvy = 64, v_{\max} = 8, \Delta t = 0.01$.

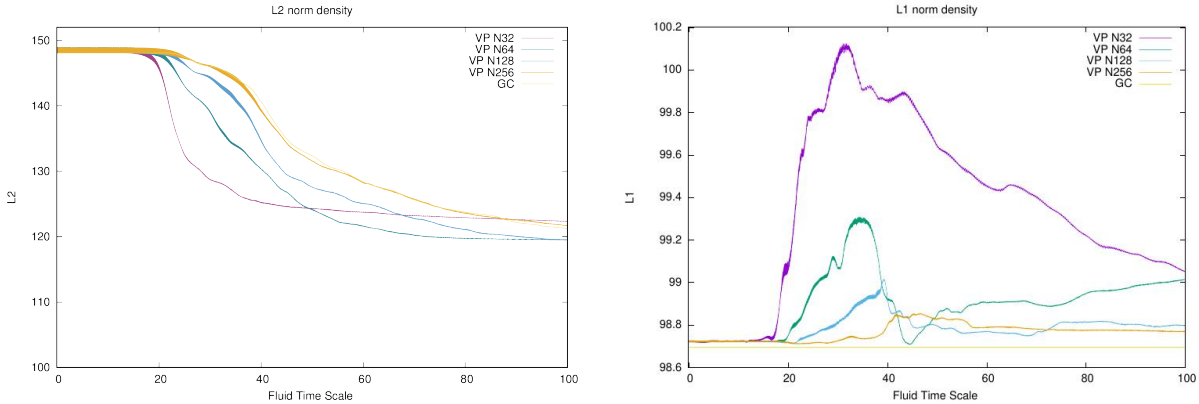

Figure 9: Comparison between the time evolution of theoretically quantities of Vlasov-Poisson system when $\varepsilon = 1/32$ with several values of Nx and the guiding center model with $Nx = 128$. $Nvx = Nvy = 64, v_{\max} = 8, \Delta t = 0.01$.

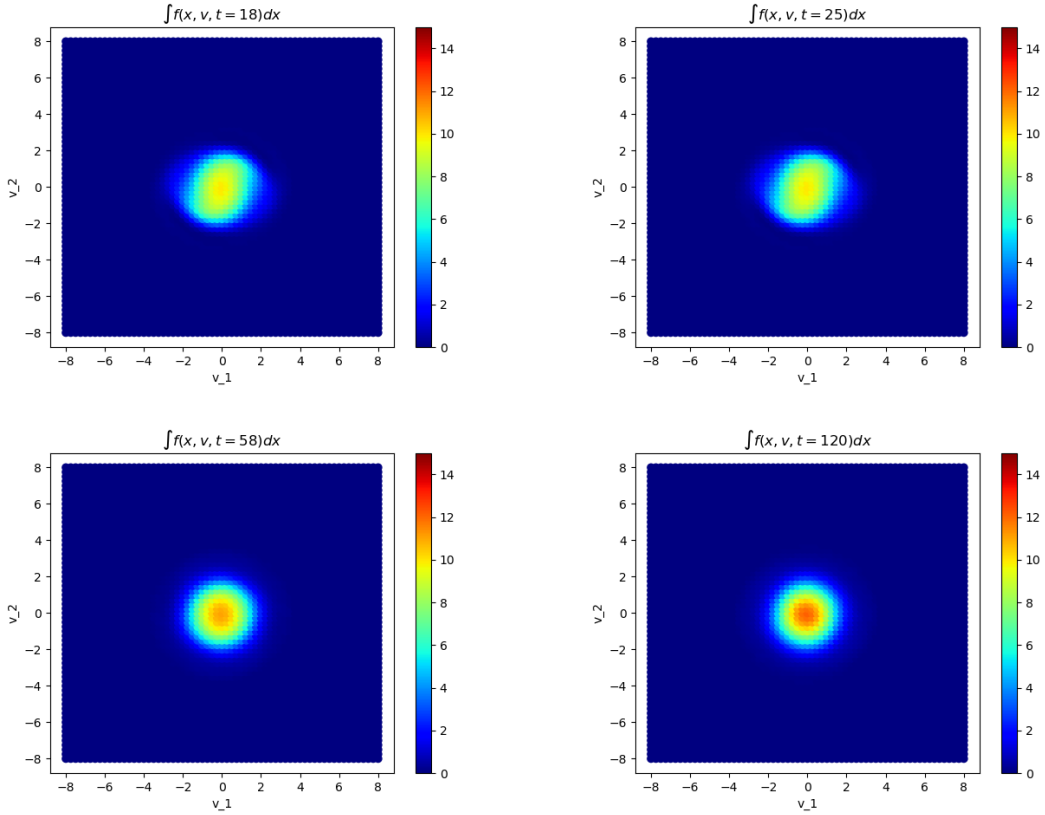

Figure 10: Simulation for time evolution of the kinetic effect of Vlasov-Poisson system with $\varepsilon = 1$. $Nx = 128, Ny = 128, Nvx = 64, Nvy = 64, \Delta t = 0.01$.

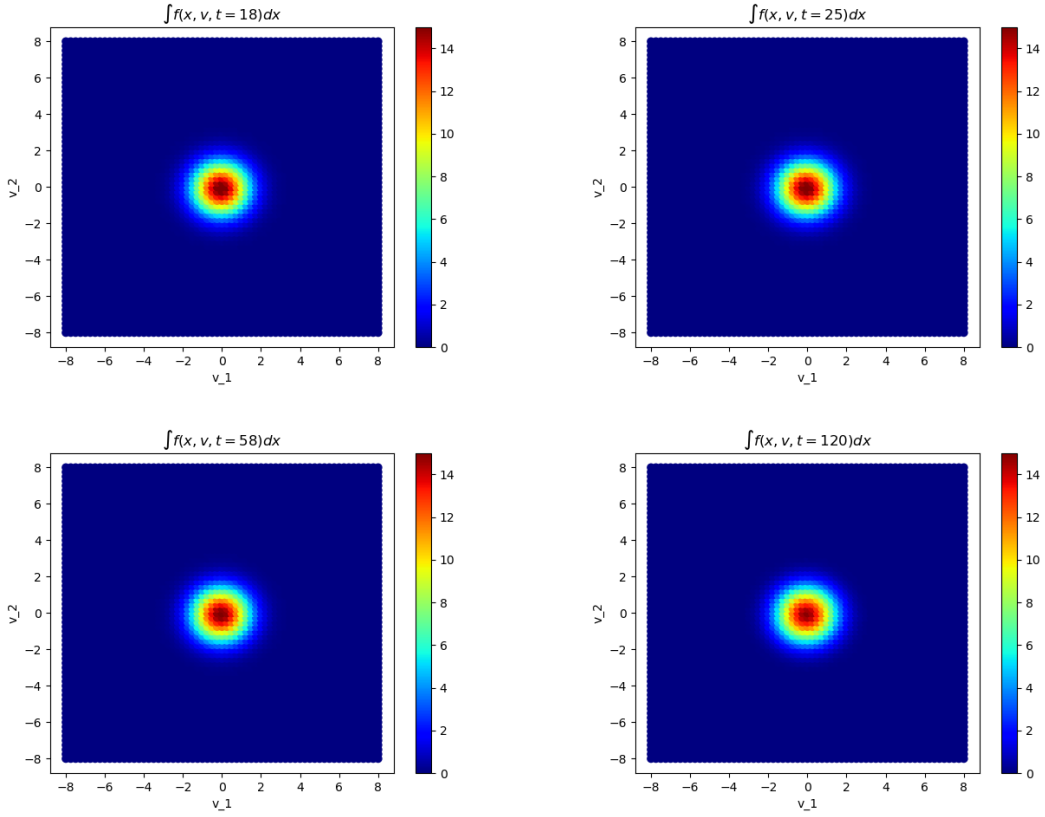

Figure 11: Simulation for time evolution of the kinetic effect of Vlasov-Poisson system with $\varepsilon = 1/32$. $Nx = 128, Ny = 128, Nvx = 64, Nvy = 64, \Delta t = 0.01$.